



UNIVERSITÀ
DEGLI STUDI
DI PADOVA

Head office: Università degli Studi di Padova

Department of Cardiac, Thoracic, Vascular Sciences and Public Health

Ph. D. Course: Translational Specialistic Medicine “G. B. Morgagni”

Curriculum: Endocrine and Metabolic Sciences

XXXVI Cycle

Impaired G-CSF-induced autophagy as a mechanism contributing to diabetic stem cell mobilopathy

Coordinator: Prof. Annalisa Angelini

Supervisor: Prof. Gian Paolo Fadini

Ph.D. STUDENT: Francesco Ivan Amendolagine

Index

ABSTRACT	4
RIASSUNTO	6
1. INTRODUCTION	8
Diabetes mellitus and its complications	8
The role of bone marrow and bone marrow niches in hematopoiesis	10
Hematopoietic stem cells.....	12
The life cycle of neutrophils.....	13
G-CSF in health and disease.....	14
The diabetic stem cell mobilopathy.....	17
The HSPCs role in endothelium dysfunction and CVD in diabetes	18
Molecular mechanisms of diabetic stem cell mobilopathy.....	19
Pharmacological approaches to counteract diabetic stem cells mobilopathy	20
The Autophagosome-Lysosomal System	22
Autophagy in prediabetes and diabetes	24
The role of autophagy in neutrophils.....	25
AIM OF THE WORK	27
2. MATERIALS AND METHODS	28
Mice.....	28
Genotyping	29
Induction of Diabetes	29
Bone Marrow cells and Bone Marrow neutrophils isolation.....	29
<i>In vitro</i> treatments.....	29
<i>In vivo/ex vivo</i> treatments	30
Peripheral blood analysis.....	30
Colony forming unit assay.....	30
Western blotting	30
RNA isolation and quantitative Real-time PCR.....	31
Flow cytometry.....	32
Imaging flow cytometry	32
Sequencing data analysis.....	33
Statistical analysis	36
3. RESULTS	37
Autophagy-related genes are modulated in bone marrow by G-CSF <i>in vivo</i> in mice but not in neutrophils	37
Autophagy is modulated in neutrophils <i>in vivo</i> after G-CSF	37

Autophagy modulation is observable <i>in vitro</i> in BM cells using imaging flow cytometry	38
G-CSF treatment modulates the autophagy flux in mouse neutrophils <i>in vitro</i>	40
G-CSF treatment induces the autophagy flux in mouse neutrophils <i>ex vivo</i>	40
Neutrophils from diabetic mice showed impaired autophagy modulation after G-CSF <i>in vivo</i>	41
Spermidine modulation is not associated to hematopoietic stem cell mobilization	43
Spermidine restores autophagy flux in diabetic mice neutrophils treated with G-CSF.....	44
Hematopoietic stem cell mobilization is not modulated by β -hydroxybutyrate alone	45
G-CSF co-treatment with spermidine or β -hydroxybutyrate partially restore HSPCs mobilization	46
G-CSF modulates autophagy-associated genes in human neutrophils <i>in vivo</i>	48
4. DISCUSSION.....	59
5. BIBLIOGRAPHY	65

ABSTRACT

Diabetes is a chronic disease that affects several organs. Hyperglycemia promotes chronic inflammation and impairs angiogenesis due to the increase of myelopoiesis. In patients with diabetes a condition called stem cell mobilopathy is developed, causing the incapability to mobilize hematopoietic stem and progenitor cells (HSPCs) after Granulocyte-Colony Stimulating Factor (G-CSF) stimulation, a drug used to mobilize HSPCs for Hematopoietic stem cell transplantation (HSCT). Recently autophagy, a cellular recycling system, has emerged as a novel player in HSPCs mobilization after G-CSF treatment. This project aims to investigate whether an alteration of the autophagic pathway in neutrophils, which are the main target of G-CSF mechanism of action, is involved in diabetic stem cell mobilization in a murine streptozotocin diabetic model of type 1 diabetes (T1D STZ). Furthermore we have analyzed bulk and single cell RNAseq public dataset of human neutrophils treated with G-CSF to evaluate the transcriptomic profile of autophagy related genes. Autophagy, and in particular autophagosome formation, was investigated using C57Bl6-TG (GFP-LC3) transgenic mice, looking for GFP-LC3 punctae accumulation in bone marrow neutrophils using the Amnis Imagestream MKII imaging flow cytometry platform. For Western Blot (WB) and qPCR analysis C57Bl6/J wild type mice were used to isolate neutrophils. T1D was induced in 3 months old mice with a single intraperitoneal injection of streptozotocin (STZ) 175mg/kg and used after 4 weeks of subsequent hyperglycemia. HSPCs mobilization was induced using rhG-CSF. To block the autophagic flux, cells were treated *ex vivo* with 80uM chloroquine for one hour. To assess mobilization, we quantified HSPCs in the peripheral blood by flow cytometry and performed a clonogenic colony forming unit (CFU) assay. To induce autophagy or bypass it, diabetic mice were treated with spermidine or β -hydroxybutyrate during G-CSF treatment. We have observed that autophagy-related genes were modulated in unfractionated bone marrow but not in neutrophils, but the results obtained by WB show that ATG5, together with the LC3 lipidated fraction, two important autophagy markers, were upregulated in G-CSF treated mice neutrophils compared to controls. These data were corroborated by the imaging flow cytometry results, in which we could show that *in vivo* G-CSF increases the number of GFP-LC3 *punctae* in GR1⁺ neutrophils of non-diabetic GFP-LC3 mice, confirming the autophagy role in G-CSF mechanism of action. On the other hand, neutrophils from diabetic mice after the treatment with G-CSF did not show any increase in the number of autophagosomes, which supports the hypothesis that autophagy is impaired in diabetes and might be linked to impaired mobilization. Next, we evaluated the effects of spermidine or β -hydroxybutyrate on mobilization in diabetic mice co-treated with G-CSF. By assessing the Lineage⁻ c-kit⁺ Sca1⁺ cells in peripheral blood, which are the murine counterpart of

human CD34⁺ HSPCs, we have found a partial restoration in G-CSF-derived mobilization. Also, the CFU assay, which can detect functionally competent HSPCs, shows that the mobilization by G-CSF in T1D mice seems partially restored after the co-treatment spermidine or β -hydroxybutyrate treatment. Furthermore, by re-analyzing a publicly available bulk and single cell-RNAseq dataset, sorted human neutrophils we showed that autophagy-related genes were modulated after G-CSF treatment. According to our data, G-CSF is ineffective in regulating autophagy in bone marrow neutrophils in diabetic mice. This may contribute to impaired HSPCs mobilization. However, we found that inducing autophagy with spermidine or bypassing it with β -hydroxybutyrate can partially restore mobilization. Finally, bulk RNAseq and single cell RNAseq analysis on human neutrophils showed how autophagy is also modulated by G-CSF in humans, suggesting the translational potential of our research.

RIASSUNTO

Il diabete è una malattia cronica che colpisce diversi organi. L'iperglicemia promuove l'infiammazione cronica e compromette l'angiogenesi a causa dell'aumento della mielopoiesi. Nei pazienti diabetici si sviluppa una condizione chiamata mobilopatia diabetica, che causa l'incapacità di mobilizzare le cellule staminali e progenitrici ematopoietiche (HSPC) dal midollo osseo al flusso sanguigno dopo il trattamento con il granulocyte colony-stimulating factor (G-CSF), un farmaco utilizzato per il trapianto di cellule staminali ematopoietiche. Recentemente l'autofagia, un processo di riciclo cellulare, è emersa come un nuovo attore nella mobilizzazione di queste cellule dopo il trattamento con il G-CSF. Questo progetto mira a investigare se l'autofagia nei neutrofili, che sono il bersaglio diretto del G-CSF, è coinvolta nel difetto di mobilizzazione in un modello murino di diabete di tipo 1 indotto da streptozotocina (T1D STZ). Inoltre, abbiamo analizzato un dataset pubblico di bulk RNAseq e single cell RNAseq di neutrofili umani trattati con G-CSF per valutare il profilo trascrittomico dei geni correlati all'autofagia. L'autofagia, e in particolare la formazione dell'autofagosoma, è stata indagata utilizzando topi transgenici C57Bl6-TG (GFP-LC3), andando a quantificare l'accumulo di *punctae* di GFP-LC3 in neutrofili da midollo osseo utilizzando la piattaforma di imaging flow cytometry Amnis Imagestream MKII. Per l'analisi tramite Western Blot (WB) e qPCR sono stati utilizzati topi C57Bl6/J wild type per isolare i neutrofili. Il diabete di tipo 1 è stato indotto in topi di 3 mesi con una singola iniezione intraperitoneale di streptozotocina (STZ) 175mg/kg e sono stati utilizzati dopo 4 settimane di iperglicemia consecutiva. La mobilizzazione delle cellule staminali ematopoietiche è stata indotta utilizzando rhG-CSF. Per bloccare il flusso autofagico, le cellule sono state trattate *ex vivo* con 80uM di cloroquina per un'ora. Per valutare la mobilizzazione, abbiamo quantificato le cellule staminali circolanti nel sangue periferico mediante citometria a flusso e abbiamo eseguito un test di clonogenico di unità formanti colonie (CFU). Per indurre o bypassare l'autofagia, i topi diabetici sono stati trattati con spermidina o β -idrossibutirrato durante il trattamento con G-CSF. Abbiamo osservato come i geni correlati all'autofagia siano stati modulati nelle cellule di midollo osseo totale ma non nei neutrofili; tuttavia, i risultati ottenuti tramite WB mostrano un aumento di ATG5 e della frazione lipidata di LC3, due importanti marker di autofagia, nei neutrofili di topi trattati con G-CSF rispetto ai controlli. Questi dati sono stati confermati dai risultati ottenuti tramite imaging flow cytometry, in cui abbiamo potuto dimostrare che il G-CSF *ex vivo* aumenta il numero di autofagosomi nei neutrofili di topi GFP-LC3 non diabetici, confermando il ruolo dell'autofagia nel meccanismo d'azione del G-CSF. D'altra parte, i neutrofili dei topi diabetici dopo il trattamento con G-CSF non hanno mostrato alcun aumento del numero di autofagosomi, il che supporta l'ipotesi che l'autofagia sia compromessa nel

diabete e possa essere collegata alla compromessa mobilizzazione. Successivamente, abbiamo valutato gli effetti di spermidina o β -idrossibutirrato sulla mobilizzazione nei topi diabetici co-trattati con G-CSF. Valutando le cellule Lineage⁻ c-kit⁺ Sca1⁺ nel sangue periferico, che sono l'equivalente murino delle cellule staminali e progenitrici ematopoietiche CD34⁺ umane, abbiamo riscontrato una parziale ripresa nella mobilizzazione derivata da G-CSF. Inoltre, il test CFU, che permette di quantificare le cellule staminali ematopoietiche funzionali, mostra che la mobilizzazione tramite G-CSF nei topi T1D sembra parzialmente ripristinata dopo il trattamento con spermidina o β -idrossibutirrato. Inoltre, rianalizzando un dataset pubblico di bulk RNAseq e single cell RNAseq, i neutrofili umani mostrano come i geni correlati all'autofagia siano modulati dopo il trattamento con G-CSF. In conclusione, abbiamo potuto osservare come il G-CSF non è in grado di regolare l'autofagia nei neutrofili del midollo osseo nei topi diabetici, e ciò potrebbe contribuire alla compromessa mobilizzazione. Tuttavia, abbiamo dimostrato che l'induzione dell'autofagia con spermidina o il suo aggiramento con il β -idrossibutirrato può ripristinare parzialmente la mobilizzazione. Infine, con l'analisi di bulk RNAseq e single cell RNAseq su neutrofili umani abbiamo mostrato come anche negli umani l'autofagia viene modulata dal G-CSF, evidenziando le potenzialità traslazionali della ricerca.

1. INTRODUCTION

Diabetes mellitus and its complications

Diabetes mellitus (DM) is a metabolic disease characterized by high blood glucose levels, a condition called hyperglycemia¹. People affected by diabetes were 422 million in 2014 but this number is destined to rise over time². Hyperglycemia is caused either by defects in insulin secretion or action, causing respectively insulin deficiency or resistance and both resulting in glucose control failure. It can be divided into two macro-categories: Type 1 and type 2 diabetes (T1D, T2D). T1D, also known as insulin-dependent diabetes, is mostly developed during childhood, but it can arise at any age³. T1D [Fig 1.1] is the result of the immuno-mediated destruction of pancreatic β cells by CD4 and CD8 T-cells. These cells recognize autoantigens in pancreatic β cells, such as glutamic acid decarboxylase (GAD) or insulin. The onset of T1D is preceded by an asymptomatic period, in which autoantibodies are produced; their detection is commonly used for diagnostic purposes². The β cell destruction could be fast (a few months) or slow (up to 10 years). In both cases, the result is the total impairment of insulin production. The T1D onset causes are still nowadays unknown, but it has been seen that a familiar history of a genetic correlation and viral infection could increase the risk of developing the disease³. T2D [Fig 1.1] is the most common type of diabetes, accounting for more than 90% of patients with diabetes⁴. T2D is characterized by an impairment of insulin responsiveness in peripheral tissue (insulin resistance), which could worsen in an inadequate compensatory insulin production. Known risk for the development of T2D are age, obesity and western- type diet⁵.

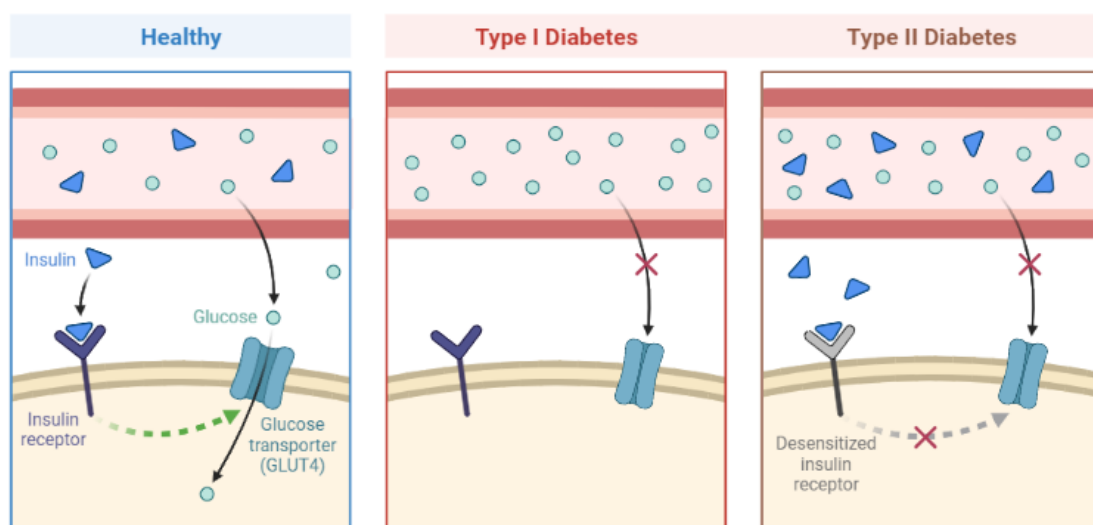


Figure 1.1: Schematic representation of insulin deficiency and insulin resistance in type 1 and type 2 diabetes, respectively. Image created by Huang E. (2022), BioRender.

The higher morbidity and mortality associated with diabetes are due to the onset of vascular complications, which can be divided in high blood pressure, advanced glycation end products (AGEs) formation, ROS production, myelopoiesis, proinflammatory gene expression, and cytokine release, inducing a state of chronic inflammation⁶. Diabetes is also associated with impaired angiogenesis, which leads to micro and macroangiopathy⁷ [Fig. 1.2]:

- Because of microangiopathy, new frail and immature blood vessel are generated, and combined with high blood pressure causes diabetic retinopathy due to the continuous blood vessels rupture, provoking hemorrhages in the retina and causing retinal detachment and glaucoma⁸.
- Wound healing is delayed due to the abnormal revascularization that impairs the normal blood flow to the extremities, and in some serious cases amputation is necessary⁹.
- In kidneys, due to the high blood pressure in small blood vessels, microangiopathy, and high glucose exposure lead to nephropathy, characterized by abnormal glomerular dimension and kidney overwork¹⁰.
- Hemorrhages in blood vessels within atherosclerotic plaques are more frequent, exacerbating atherosclerosis complications and increasing the risk of ischemia and stroke¹¹.
- The vasa nervorum rarefaction in axons induces demyelination and nutrient shortage, impairing the correct tissue innervations and causing diabetic neuropathy¹².

The bone marrow (BM) is notably affected by diabetic neuropathy, leading to severe complications including abnormal myelopoiesis and impaired hematopoiesis¹³.

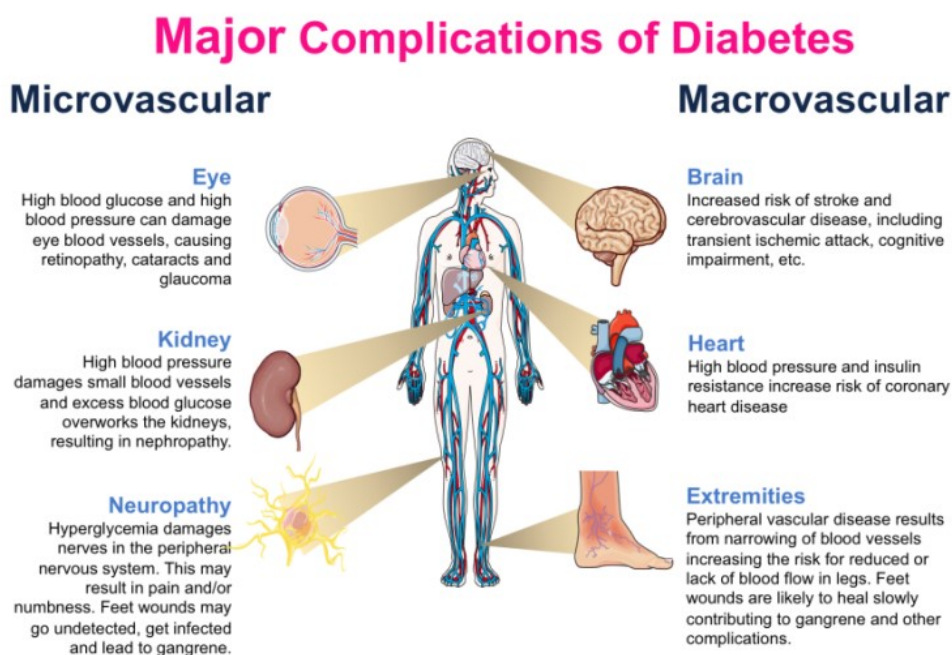


Figure 1.2: Overview of the principal diabetic micro and macrovascular complications: the high glucose environment impairs angiogenesis and causes micro and macroangiopathy¹⁴.

The role of bone marrow and bone marrow niches in hematopoiesis

BM is the anatomical site of hematopoiesis. It is primarily situated within the long bones, the cranial vault and the iliac crests¹⁵. This spongy tissue has a specialized vasculature composed of rare arterioles that enter through the bone and creates a dense network of sinusoids within the trabecular spaces¹⁶. Due to the particular vascularization, the BM is considered a hypoxic tissue, with nutrients and oxygen shortage¹⁷.

Macroscopically, two distinct categories of bone marrow can be distinguished: red bone marrow, serving as the site of true hematopoiesis, and yellow bone marrow, functioning as a repository for adipose tissue¹⁵. In humans, the red bone marrow is the prevalent until approximately the age of 7 years, while a gradual replacement by yellow bone marrow occurs during aging. It is known that adults typically have a similar distribution of both bone marrow types, each occupying fifty percent of the overall volume of the bone cavity¹⁸. The BM encompasses different cells from multiple lineages, such as hematopoietic cells, sympathetic nerve cells, stromal cells, osteogenic cells and endothelial cells. Stromal cells produce the bone marrow extracellular matrix (ECM), a non-cellular tridimensional network composed of proteoglycans, collagens, fibronectin, elastin, laminin glycosaminoglycan, osteocalcin and periostin¹⁹ that supports BM internal structure. ECM is also a source of growth factors and proteases²⁰. The heterogenic bone marrow cell population, combined with the hypoxic environment, the ECM, and the particular microvascular network constitutes the bone marrow microenvironment (BMM)²¹, in which the niches reside and enable hematopoietic stem cells (HSCs) to engage in self-renewal, proliferation and differentiation²². Stromal niches are localized near the endosteum (endosteal niches) and the vascular sinusoids (vascular niches)²³ [Fig.1.3]. Within endosteal niches are localized the younger HSCs with a great self-renewal capacity compared with the HSCs in central marrow, which are present also progenitor cells²⁴. The increasing or decreasing in the number of osteoblasts in the endosteal niches leads to HSCs expansion or depletion¹⁸. Osteolineage cells are responsible for the HSCs retainment and mobilization, by producing surface molecules that anchor the cells, or growth factors that allow mobilization²⁵. The vascular niches are localized near the BM sinusoids, in communication with endothelial cells²⁶. In addition, in vascular niches, there is an abundance in CXCL-12 abundant reticular (CAR) cells, that are involved in HSC retention, and Nestin⁺ cells, localized near sympathetic nerves and enriched in β_3 -adrenergic receptor to follow the noradrenergic signaling modulation from the sympathetic nervous system (SNS)²⁷.

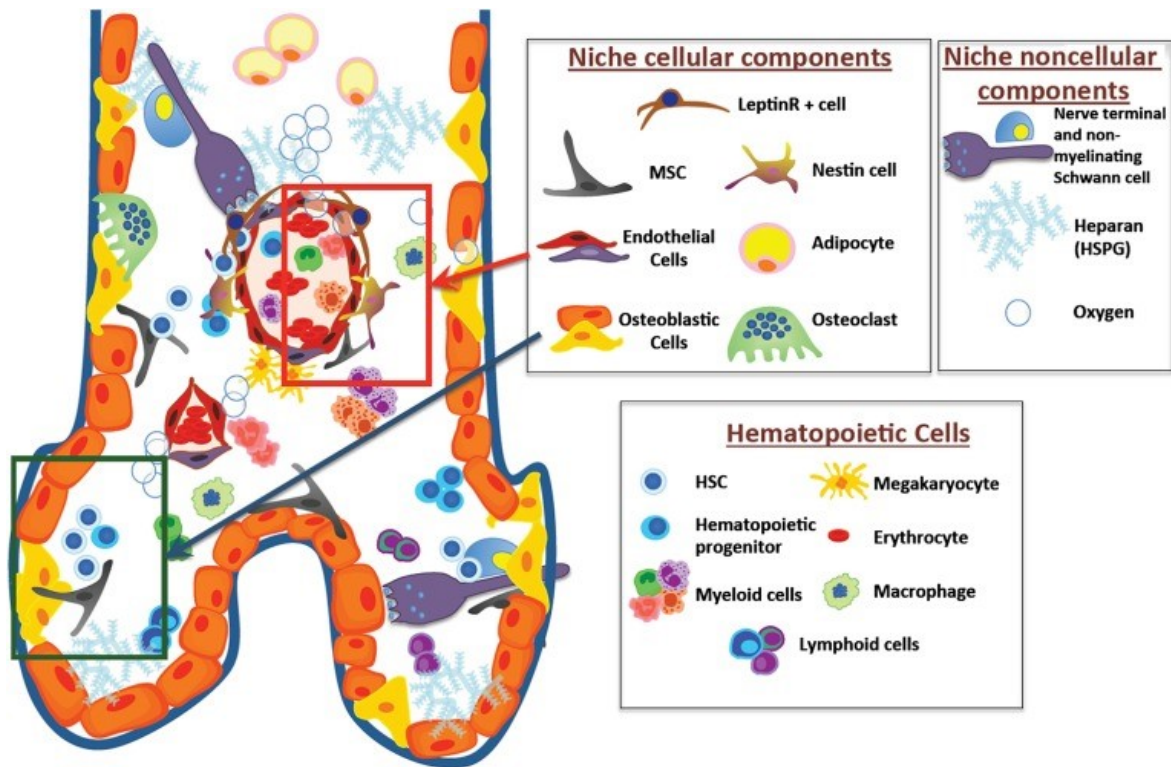


Figure 1.3: Representation of bone marrow cell population and microenvironment with endosteal(green box) and vascular(red box) stem cell niche localization²³.

Hematopoietic stem cells

All the mature hematopoietic cells in the blood derived from multipotent stem cells called hematopoietic stem cells (HSCs), which postnatally are mainly located within the BM, although rare HSCs can be found circulating in peripheral blood (PB)²⁸. HSCs differentiation allow the continuous replenishment of leucocytes, erythrocytes and platelets through a series of lineage restriction steps, in which lose their self-renewal capacity to become myeloid or lymphoid mature cells [Fig. 1.4].

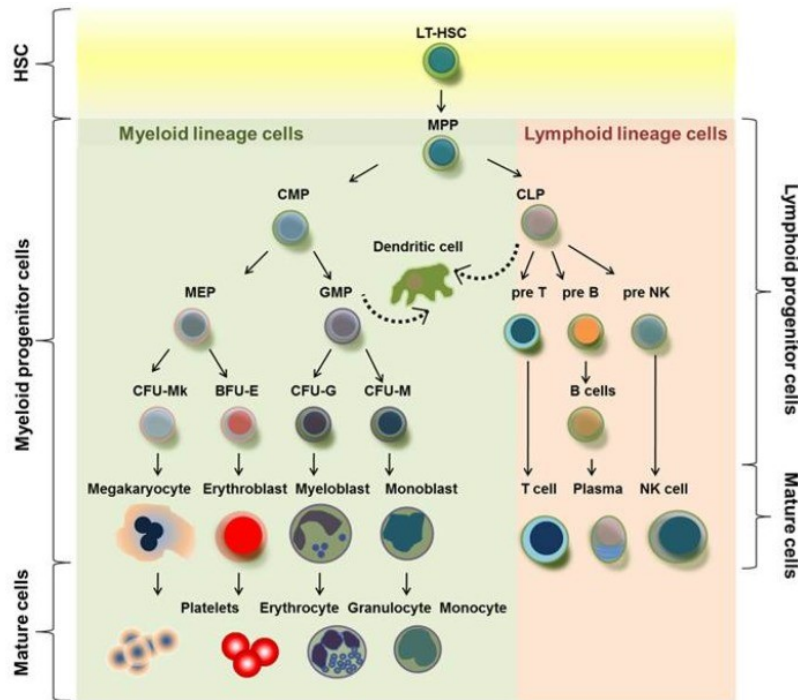


Figure 1.4: Representation of hematopoiesis in adult bone marrow. Through different cytokines and growth factors, HSCs could differentiate in myeloid or lymphoid lineage cells.²⁸

The adhesion of HSCs to the stroma of the BM is tightly regulated by several integrins and adhesion molecules; in particular L-selectin (also known as CD62L) expressed on HSCs surface, binds its receptor P-selectin glycoprotein ligand-1 (PSGL) on the extracellular matrix²⁹.

C-kit (CD117) is the receptor for stem cell factor (SCF or kit ligand) and is involved in hematopoiesis and stem cell maintenance³⁰. CD44 is a cell-surface glycoprotein expressed by HSCs and binds hyaluronic acid in ECM³¹. $\alpha 4\beta 1$ Integrin (VLA-4) expressed by HSCs interacts with vascular cell adhesion molecule-1 (VCAM-1) in stromal cells³². Similarly, C-X-C chemokine receptor type 4 (CXCR4) expressed by HSCs binds the C-X-C motif chemokine ligand 12 (CXCL12), also known as stromal cell-derived factor-1 α (SDF-1 α) expressed by stromal cells by creating a gradient: more CXCL12 means more anchoring, *viceversa*, a reduction in CXCL12

content means an improvement in mobilization³³. Also the hypoxic environment within BM and stromal niches is a retainment factor: quiescent HSCs requires a low O₂ environment, and during differentiation migrate to more oxygenated compartments of the BM³⁴.

HSCs are normally localized in BM stromal niches, but under stress conditions, such as myelosuppressive regimens or granulocyte-colony stimulating factor (G-CSF) treatment, CD34⁺ hematopoietic stem and progenitor cells (HSPCs) can migrate from the BM to the PB. In particular, the HSCs egression after G-CSF treatment is exploited hematopoietic stem cell transplantation (HSCT)³⁵.

The life cycle of neutrophils

Neutrophils, also known as polymorphonuclear cells (PMNs), are the most abundant white blood cells in humans accounting for 60%-70% of circulating leukocytes. Neutrophils are involved in innate immunity as the first barrier against pathogens, as they can be rapidly recruited at the infection site and can adopt several effector functions: phagocytosis, oxidative burst and cytokine release³⁶. In addition these cells can adopt a peculiar mechanism to entrap and kill pathogens: they can extrude their nuclear chromatin forming a sticky mech decorated with granular enzymes and cytokines that have been termed Neutrophil Extracellular Trap (NETs)³⁶. Ultimately, after the release of NETs, neutrophils die by NETosis. The most distinguishable characteristics of neutrophils are the lobulated nucleus and the cytoplasm enriched in granules that contain several antimicrobial enzymes, matrix metalloproteases and elastase. Physiological granulopoiesis is regulated by G-CSF signaling which induces progenitor cell differentiation³⁷. As for hematopoiesis in general, granulopoiesis is believed to be a hierarchical process where hematopoietic stem cells (HSCs), differentiated into Common myeloid progenitors (CMP) followed by Granulocyte-macrophage precursors (GMPs), myeloblasts, promyelocytes, myelocytes metamyelocytes, band cells and finally neutrophils, which are finally released into the circulation [Fig.1.5].

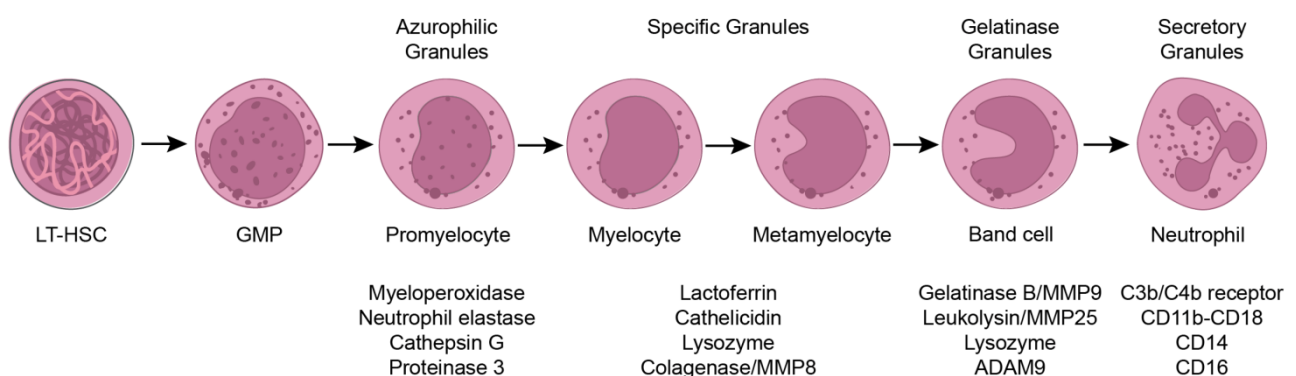


Figure 1.5: *Neutrophil development in the bone marrow. Hematopoietic stem cells give rise to mature neutrophils via several intermedial stages. Granule content changes among various stages of differentiation*³⁸.

In absence of inflammatory triggers, neutrophils return to the BM and are cleared by phagocytosis from BM macrophages (BMM Φ)³⁹; alternatively, they will undergo apoptosis in peripheral tissues within 24/48 hours³⁶. The estimated neutrophil half-life in the bloodstream is 6-12 hours in mice⁴⁰ and 8-10 hours in humans⁴¹. Due to their short lifespan neutrophil production and release is continuous: every day more than 10^{10} neutrophil are produced in humans⁴². During an inflammatory process, neutrophils can reach the target sites by an initial low-affinity interaction with the endothelium termed tethering and rolling, mediated via P-selectin/PSGL-1 crosstalk⁴³. This interaction is strengthened by the activation of neutrophils by chemokines and the interaction with integrins such as CD18 or LFA-1, resulting in the firm adhesion to the endothelium⁴³. Following adhesion, neutrophils transmigrate between endothelial cells (diapedesis) and penetrate the basement membrane to reach the site of infection site⁴³. Besides their antimicrobial activity, several evidence show that neutrophils are essential for hematopoiesis, HSCs mobilization and niches homeostasis⁴². During acute inflammation, neutrophils stimulate hematopoietic stem/progenitor cells (HSPCs) proliferation and expansion⁴⁴. Recently, it has emerged that neutrophils drive sinusoidal regeneration by producing tumor necrosis factor α (TNF α), that stimulates endothelial cells to regenerate blood vessels after hematopoietic stem cell transplantation (HSCT)⁴⁵. Finally, G-CSF administration is associated with an increased granulopoiesis and HSCs mobilization⁴⁶, suggesting that neutrophil role in hematopoiesis is relevant.

G-CSF in health and disease

HSPCs can reach the peripheral circulation to produce tissue-resident innate immune cells during inflammation⁴⁷. This process is called mobilization. The SNS is involved in BM niche function, and HSPCs mobilization is mediated by catecholaminergic neurotransmitters⁴⁸. During infections, when leukocyte proliferation and HSPCs egression are necessary, SNS releases catecholamines, such as norepinephrine, which are recognized by β_3 -adrenergic receptors in endothelial and stromal cells. Hematopoietic growth factors such as the Granulocyte colony-stimulating factor (G-CSF) and Granulocyte-Macrophages colony-stimulating factor (GM-CSF), are produced by endothelial and stromal cells⁴⁹. Among growth factors, G-CSF stands out as one of the most interesting, both due to its physiological significance and its application as a therapeutic agent. G-CSF is a ≈ 20 kDa glycoprotein belonging to the colony-stimulating factor (CSF) family and is mainly produced from fibroblasts, endothelial cells, stromal cells, and neuronal cells⁵⁰. During infections endothelial cells

sense pathogen-associated molecular patterns (PAMPs) and produce G-CSF. The binding with G-CSF receptor (G-CSFR), expressed predominantly by neutrophils and HSPCs, promotes the differentiation toward the granulocytic lineage and the neutrophil release in the bloodstream⁵¹. Moreover, the G-CSF binding with its receptors induces G-CSFR phosphorylation, which activates the Janus kinase/signal transducer and activator of transcription (JAK/STAT) pathway that promotes phospho STAT3 (pSTAT3) migration in the nucleus. STAT3 is a key player in the regulation of pluripotent cell maintenance⁵², and it has emerged as crucial for G-CSF mediated differentiation⁵³. In parallel, JAK2 recruits Lck/Yes-related novel protein tyrosine kinase (Lyn) and its coupling with Phosphoinositide-3 kinase (PI3K) promotes mitogenesis⁵⁴[Fig.1.6].

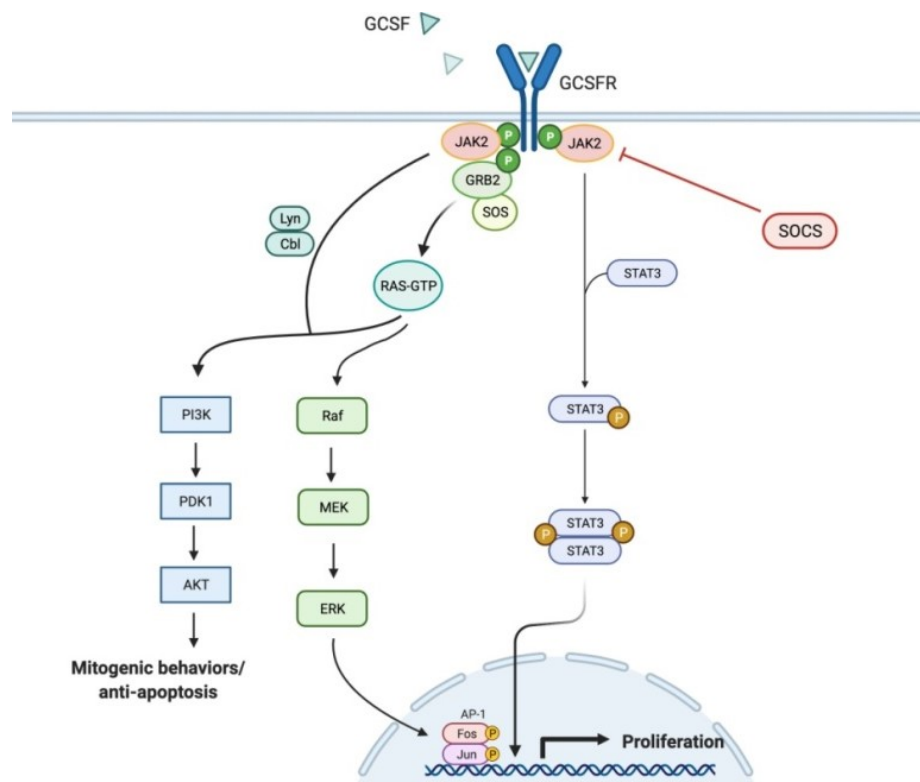


Figure 1.6: G-CSF interaction with its receptor and signal pathways activation⁵³.

G-CSF also reprograms the BM microenvironment: under the control of adrenergic signals from the sympathetic nervous system (SNS)⁵⁵, there is the CXCL12⁺ osteoblasts depletion, resulting in a severe reduction in CXCL12 abundance, also exacerbated by its downregulation in stromal cells. CD169⁺ BMMΦ are also suppressed by G-CSF. This cytokine stimulates the release of neutrophil proteases such as neutrophil elastase (ELANE) and metalloproteases such as MMP-9 that are involved in extracellular matrix degradation and disruption of the interactions between adhesion molecules and their receptors that retains the HSPCs in stromal niches [Fig. 1.7], resulting in both neutrophils and HSCs egress from the BM to the bloodstream.

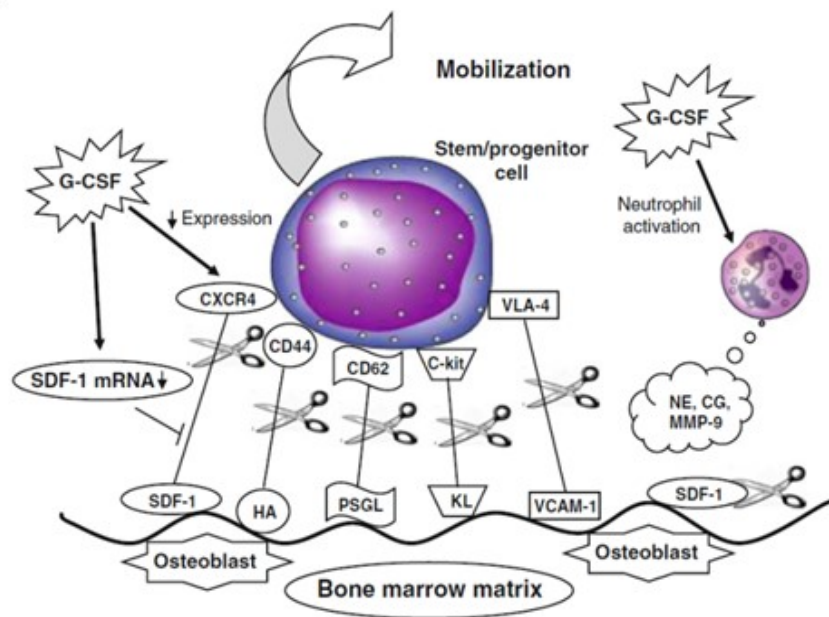


Figure 1.7: Schematic representation of the mobilizing effects of G-CSF on stromal niches and neutrophil protease release⁵⁶

It has been observed how the autophagy pathway is required both in HSPCs and neutrophils for mobilization and their survival after G-CSF stimulus, but the reason is still poorly understood⁵⁷. Both abnormal up or downregulation of G-CSF is associated with several detrimental effects: the lack of G-CSF in murine models results in severe neutropenia, associated with a low response to *lysteria monocytogenes* infection, reduced granulopoiesis and a delayed monocyte increase in the blood⁵⁸. On the other hand, an excess in autocrine G-CSF production in tumor cells implicated in cancer growth, tumor angiogenesis, and tumor microenvironment maintenance⁵⁹.

G-CSF treatment induces CD34⁺ HSPCs mobilization⁶⁰ and that could be collected by leukapheresis from peripheral blood to allow both allogeneic and autologous HSCT⁶¹. G-CSF is commonly used for HSCs collection for transplantation, because its safety, due to reduced risk of Graft versus Host disease (GVHD)⁶² in allogeneic transplants and because it is cheaper compared to the bone marrow transplant or the umbilical cord blood⁶³. Furthermore, G-CSF treatment has reduced antibiotic use and shortened the hospitalization periods⁶⁴. Some patients fail to reach a threshold level of CD34⁺ HSCs (e.g. >20/ μ L) to collect a minimum number of HSCs (e.g. >2 \times 10⁶/kg) needed to consistently achieve safe engraftment. This patients has been termed "poor mobilizer"⁶⁵. Several factors are responsible for a poor response to G-CSF: age, underlying hematologic disease, BM infiltration, chemotherapy, radiotherapy and diabetes⁶⁶.

The diabetic stem cell mobilopathy

During DM (both type 1 and 2), the BM microenvironment is extensively remodeled: diabetic neuropathy causes the pauperization of the sympathetic innervation in BM; sympathetic innervation is required for HSCs, therefore defective BM innervation leads to poor mobilization⁶⁷. The hematopoietic fraction is reduced because of the adipocytic differentiation of HSCs, resulting in fat accumulation⁶⁸. Microangiopathy causes the small blood vessels impairment to bring nutrients and oxygen within the BM, resulting in hypoperfusion and depletion of HSCs⁶⁹. The excess of reactive oxygen species (ROS) caused by fat accumulation, hypoperfusion, and high glucose environment increases the inflammation and aging of HSCs. The chronic low-grade inflammation causes a dramatic myelopoiesis, and immature myeloid cells produce in turn proinflammatory cytokines that exacerbate the complications, resulting in a reduced number of circulating HSPCs after G-CSF stimulation. The incapability of the diabetic BM to mobilize HSPCs from the BM to the bloodstream after G-CSF treatment⁷⁰ both in murine models⁶⁶ and patients with diabetes⁷¹ is called diabetic mobilopathy¹³. The lack of HSPCs in peripheral blood leads to macrovascular complications such as cardiovascular disease (CVD), atherosclerosis⁷², impaired wound healing that could lead to ulcers⁷³ and multiorgan complications [Fig1.8].

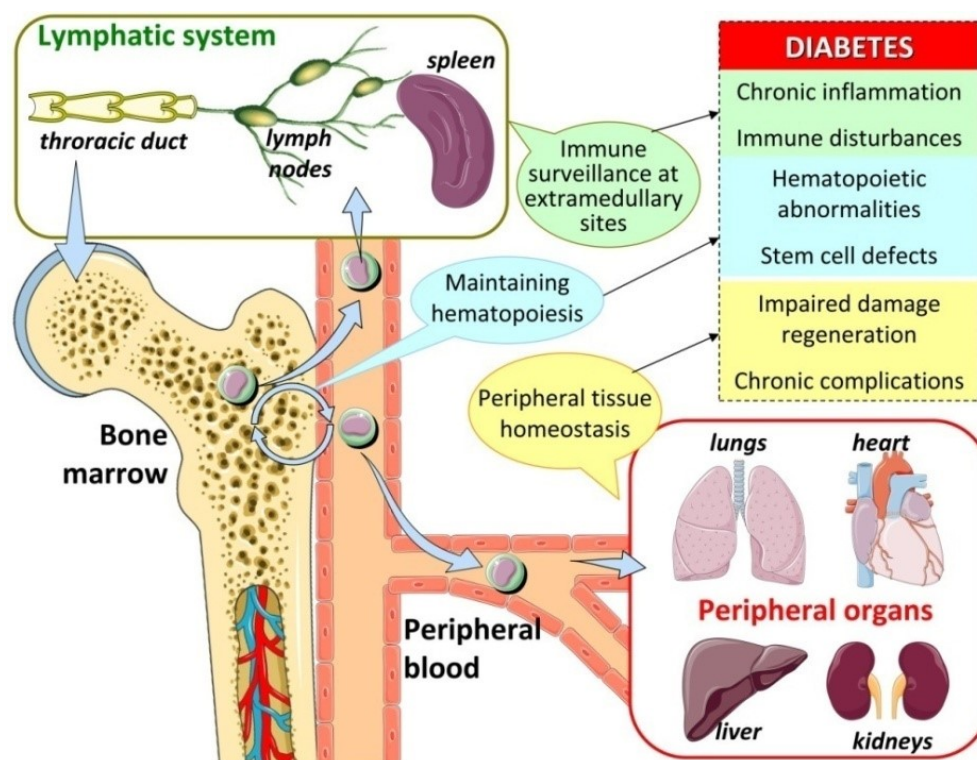


Figure 1.8: Schematic representation of bone marrow Hematopoietic stem cells in health and diabetes: the cartoons identifies the normal path of HSCs and in the box are represented the consequences of the impaired function caused by diabetes⁷⁴.

The HSPCs role in endothelium dysfunction and CVD in diabetes

The endothelium is defined as a monolayer of endothelial cells that covers the inner surface of blood and lymphatic vessels⁷⁵. Endothelial cells form a semi-permeable membrane that allows communication between blood vessels and surrounding tissues⁷⁶. These cells produce several mediators involved in blood vessel plasticity and leukocyte trafficking. The endothelial tissue is one of the major players in inflammation and angiogenesis regulation and is also known to promote vasodilatation and fibrinolysis [Fig 1.9]⁷⁷.

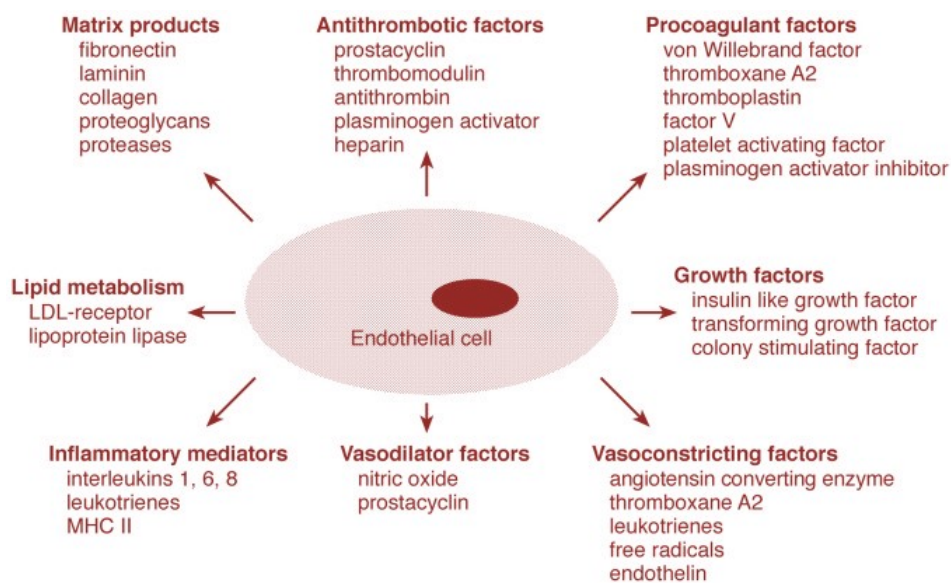


Fig 1.9: Schematic representation of endothelial cells function: Their role is involved in several mechanisms, which contributes to vascular homeostasis⁷⁷.

Diabetes (both type 1 and type 2) and obesity cause metabolic disorders that lead to the onset of CVD risk, due to endothelial dysfunction: both hyperglycemia and lipotoxicity cause increased ROS production, reduction NO release, and systemic inflammation impairs angiogenesis and vascular repairing, accelerating the atherosclerotic plaques formation^{71,72,78}. Recently, it has also been identified diabetes as a high-risk condition in SARS-CoV-2 outcome, due to multi-organ damage, chronic inflammation, and endothelial dysfunction^{79,80}.

Among the circulating HSPCs produced by the BM, two population with potential pro-angiogenic properties has been described:

- myeloid angiogenic cells, also known as circulating angiogenic cells (CACs) are hematopoietic cells with a paracrine activity that could stimulate angiogenesis by producing pro-angiogenic factors such as vascular endothelial growth factor (VEGF)
- endothelial colony forming cells (ECFCs), a particular type of cultured cells derived from peripheral blood mononuclear cells (PBMCs) or umbilical cord blood grown under endothelial cell culture condition that exhibit angiogenic properties, by repairing damaged endothelium and forming new blood vessel⁸¹.

In a model of hind-limb ischemia in diabetic rats model it has been demonstrated that impaired recovery is associated with a reduced mobilization of circulating progenitors, suggesting the link between BM HSPCs release and endothelial dysfunction⁸². Clinical data suggest the correlation between the reduction of circulating CD34⁺ HSPCs during diabetes and an increased risk in atherosclerosis and CVD, making the HSPCs quantification a biomarker for CVD risk estimation⁸³.

Mobilopathy is developed during diabetes⁷⁰, inhibiting the mobilizing effects of G-CSF, both in human patients and diabetic mice models, which fail to mobilize HSPCs and endothelial progenitors. By treating diabetic mice with the SGLT2 inhibitor Dapagliflozin results in a better recovery in wound healing and re-endothelialization after carotid injury, and the response to G-CSF is also replenished⁸⁴. Altogether, this evidence highlights the functional crosstalk between BM HSPCs trafficking and maintenance of endothelial functions.

Molecular mechanisms of diabetic stem cell mobilopathy

In diabetes, the BM features an excess in CD169⁺ BMMΦ that produces Oncostatin M (OSM)⁸⁵. OSM is a cytokine that belongs to the interleukin-6 (IL-6) cytokine family, and it plays a role in immune regulation and inflammation⁸⁶. OSM binds to the receptor complex composed of two subunits: the OSM receptor (OSMR) and the gp130 subunit, which is shared with other IL-6 family cytokines. OSM interacts with stromal mesenchymal stem cells (MSC) inducing the release of CXCL12⁸⁷. OSM signal transduction is activated in stromal cells via a non-mitochondrial function of p66Shc to induce CXCL12 production retaining HSPCs in BM niches⁸⁷. In diabetes, hyperglycemia trigger myelopoiesis, expanding the pool of BMMΦ, which in turn increase the total amount of OSM, counteracting HSCs mobilization [Fig 1.10]. Patients living with diabetes suffer from autonomic neuropathy, characterized by SNS fibers pauperization and dysfunction in several organs, including the BM. Diabetic autonomic neuropathy of the BM is also mediated by p66Shc, and it is associated with a reduction of sirtuin 1 (SIRT1) expression, leading to a poor mobilization⁶⁷.

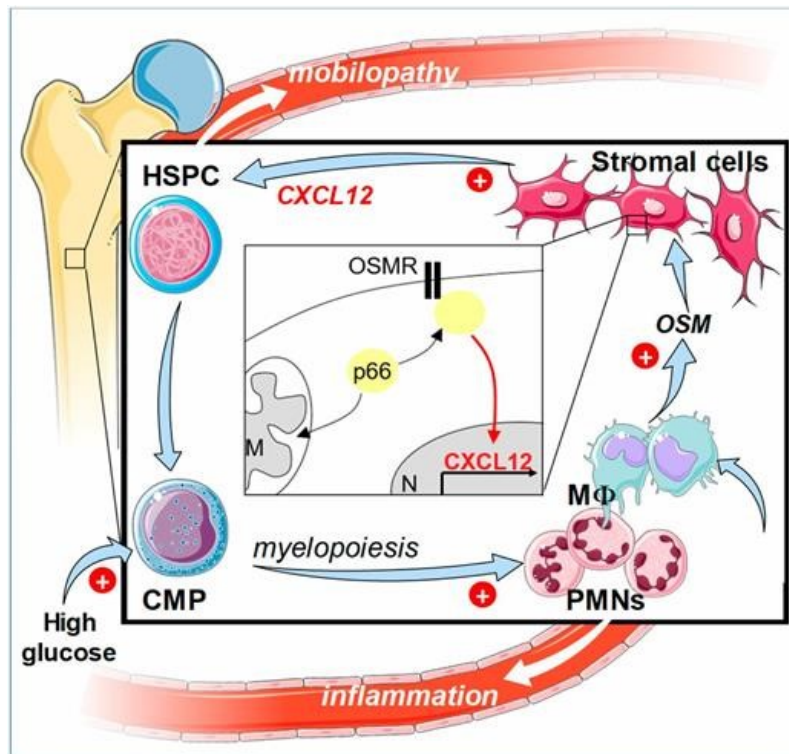


Figure 1.10: Mobilopathy detrimental loop caused by the combination of high glucose environment, chronic inflammation, and Oncostatin M overproduction, which induce stromal cells to produce the retention factor CXCL12⁸⁷.

Pharmacological approaches to counteract diabetic stem cells mobilopathy

The discovery of diabetic stem cells mobilopathy, prompted the efforts to find a pharmacological strategy to restore BM functions, with potential cardiovascular benefit for patients with diabetes⁸⁸. Desipramine, a noradrenaline reuptake inhibitor used as antidepressant, partially restores mobilization, improving the BM adrenergic tone and ameliorating the diabetic neuropathy detrimental effects, both in mice⁸⁹ and patients with multiple myeloma⁹⁰. In diabetic mice, desipramine partially restores mobilization of LKS cells, probably by improving the output of the residual SNS²³. Glucose control with insulin could partially restore HSPCs mobilization in diabetic rats, resulting in a better recovery from hindlimb ischemia⁸². Inhibitors of the renal sodium/glucose cotransporter 2 (SGLT2i) such as dapagliflozin has been investigated for both their ability to reduce hyperglycemia and to improve cardiovascular outcomes⁹¹. Studies in mice showed that Dapagliflozin reduced myelopoiesis-derived CD169⁺ BMMΦ. This reduction results in a restored mobilization after G-CSF and improved endothelial wound healing capacity⁸⁴. Diabetes is associated with chronic low-grade inflammation, which leads to micro and macrovascular complications⁵. CD169⁺ BMMΦ produce an abnormal amount of OSM that is involved in mobilopathy³⁸. By inhibiting OSM using neutralizing antibodies there is a partial restoration in G-

CSF mobilization⁸⁵. Plerixafor, also known as AMD3100, is a CXCR4 antagonist clinically used alone or in combination with G-CSF to obtain more HSCs compared with G-CSF alone⁹². Diabetic mice and patients with diabetes can mobilize HSCs with Plerixafor treatment⁹³, but surprisingly during a phase IIa, randomized, double-blind, placebo-controlled trial, it has been observed a worsening in recovery in ischemic wound healing in patients with diabetes, maybe due to the egression of non-functional HSPCs, or due to increased inflammatory cells output from the BM⁹⁴. The examples mentioned above show us that diabetic mobilopathy involves several molecular and cellular mechanism in the BM, intimately intertwined. Due to this complexity is difficult to find a unified treatment, suggesting that more studies, and possibly combined pharmacological treatment, will be necessary to tackle this diabetic complication.

The Autophagosome-Lysosomal System

The autophagosome-lysosomal system is a well-conserved catabolic system, used for maintaining cellular and metabolic homeostasis. It is crucial for the removal of cytosolic components, misfolded or aggregated proteins, to clear damaged organelles, and as a defense mechanism by degrading intracellular pathogens⁹⁵. Along with the ubiquitin-proteasome system, it is the main mechanism of molecule recycling and is ubiquitously expressed in each cell of the organism, with differences in its activity between cell types⁹⁶. Autophagy is mainly activated during reduced nutrient availability, and is essential to recycle amino acids, growth factors, energy, oxygen and is also essential for embryonal development⁹⁷. Three different forms of autophagy have been described: macroautophagy, chaperone-mediated autophagy and microautophagy [Fig 1.11].

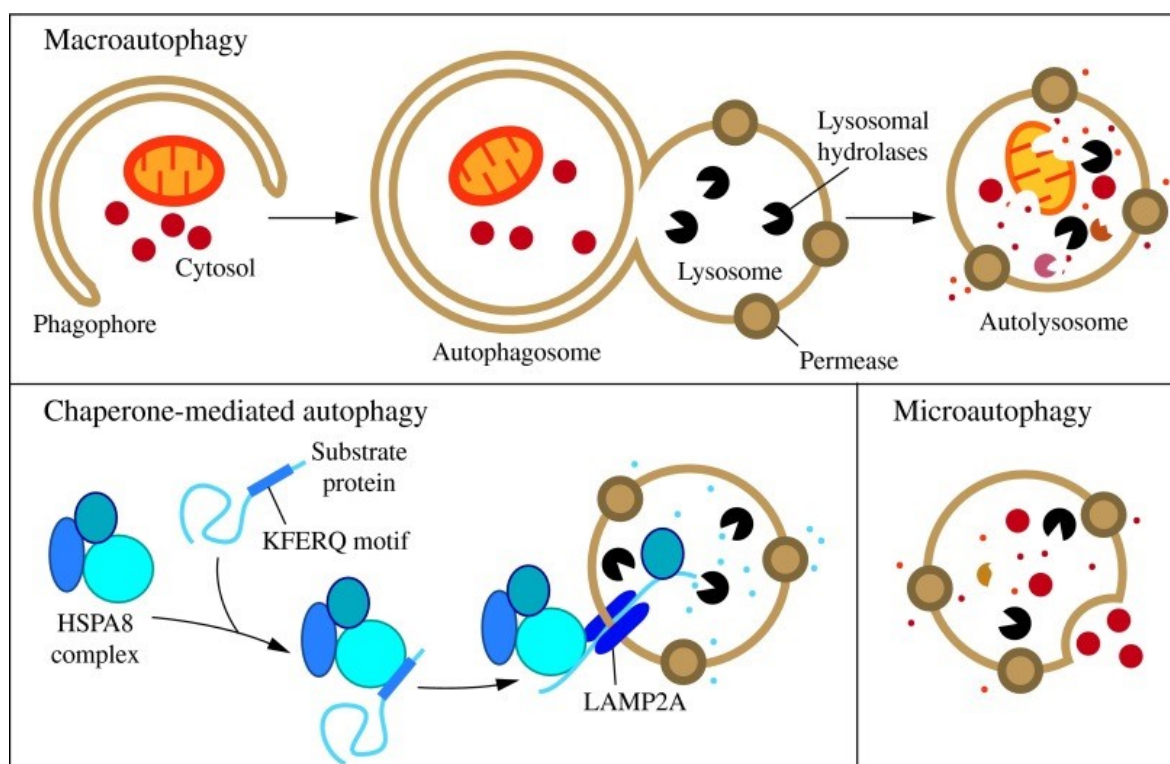


Figure 1.11: Schematic representation of the principal features of the three principal kinds of autophagy⁹⁸.

Chaperone-mediated autophagy uses the intracellular heat shock cognate chaperone of 70 kDa, (HSC70) to bind soluble cytosolic proteins containing a specific aminoacidic motif (KFERQ) and to shuttle them directly to the lysosomal membrane, after its recognition by the lysosomal membrane receptor LAMP-2A⁹⁹. In microautophagy cytosolic components to be degraded are invaginated by the lysosome itself¹⁰⁰. Macroautophagy (hereafter simply called autophagy) is the most-described type of autophagy, characterized by the formation of the autolysosome, a specific double membrane organelle involved in degradation and recycling¹⁰¹. Due to the continuous cycle of degradation and

recycling of its molecular components, autophagy is considered a “flux”; therefore the analysis of autophagy requires several tools to induce or block its components to assess whether autophagy is deregulated¹⁰². Several upstream regulations can activate autophagy, but five principal steps are necessary for autolysosome formation: induction, nucleation and elongation, maturation, fusion, and finally degradation¹⁰³. Induction, in which the autophagy inhibitor mechanistic target of rapamycin (MTORC1) dissociates from the Unc51-like-1/2(ULK1/2) - autophagy related 13 (ATG13) - focal adhesion kinase family-interacting protein of 200 kDa (FIP200) complex. The activation of ULK1 activates the phosphorylation of BECLIN1 and induces the phosphatidylinositol-3-phosphate generation. The activated nucleation induced by BECLIN1 allows the elongation, in which there is the phagophore generation by ATG5-ATG12 complex, and maturation, in which the microtubule-associated protein 1 light chain 3 (LC3) is conjugated by ATG3 with phosphatidylethanolamine (PE) forming LC3II. LC3II interacts with the cargo protein sequestosome1 (SQSTM1, also known as p62) completing the autophagosome. The lysosome fusion is mediated by Soluble N-ethylmaleimide-sensitive factor attachment protein receptor (SNARE) proteins, generating the autolysosome and finally degradation by the lysosomal enzymes. [Fig 1.12]⁹¹.

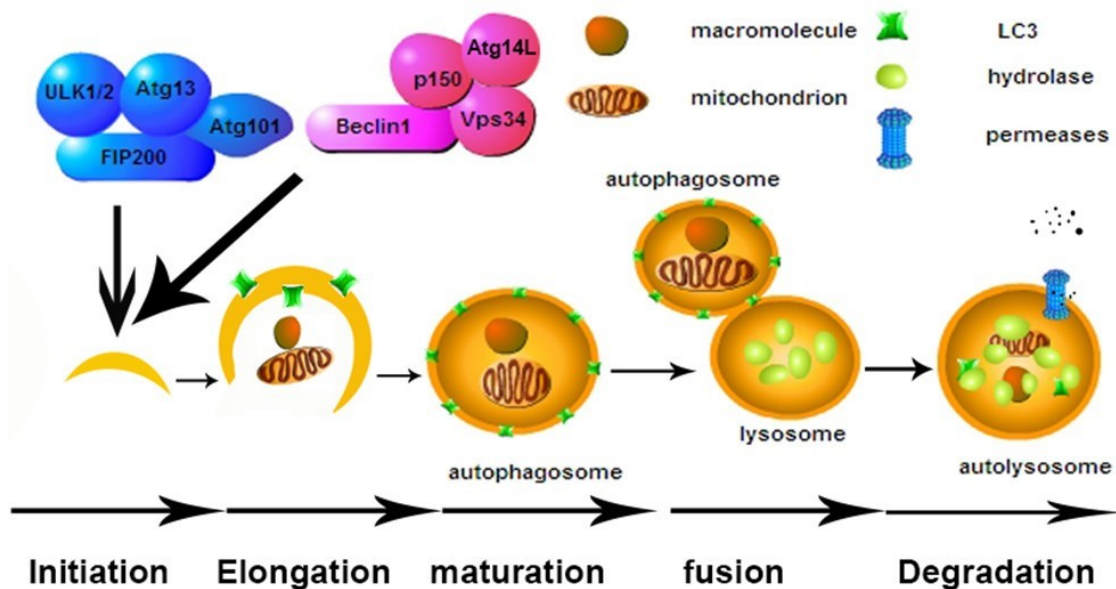


Figure 1.12: Schematic representation of the steps involved in autophagy-mediated degradation of organelles or macromolecules, from the phagophore initiation to the complete autolysosome formation.⁹⁸

Autophagy in prediabetes and diabetes

In pancreatic β cells, autophagy is important for the organization and function of pancreatic islets; it has been hypothesized how the autophagy impairment could lead to detrimental effects in β cell homeostasis and insulin production¹⁰⁵. For instance, knocking out ATG7 in β cells leads to structural defective islets and reduced insulin secretion in mice¹⁰⁶. It has also been suggested that the stimulation of autophagy in the prediabetes could prevent the onset of T1D¹⁰⁷. The continuous exposure to high glucose impairs autophagy in renal cells, resulting in damaged organelles and protein accumulation, leading to diabetic nephropathy¹⁰⁸. In addition, excess ROS production due to hyperglycemia deregulates autophagy in Schwann cells causing apoptosis, resulting in axon demyelination and peripheral neuropathy¹⁰⁹. HSCs show an upregulation of autophagy compared with mature hematopoietic cells, which is believed to be essential for self-renewal and differentiation⁹⁵. Furthermore, autophagy can control oxidative metabolism by removing active mitochondria (mitophagy) in HSCs, contributing to stemness maintenance. During aging, old HSCs fails to activate autophagy, increasing OXPHOS metabolism and resulting in replication stress and impaired engraftment in HSC¹¹⁰. In addition, autophagy contributes to cytotoxic drug resistance during chemotherapy¹¹¹. Because of its capacity to help successful engraftment, it has been supposed that autophagy could be a valid therapeutic target for GVHD prevention and successful engraftment¹¹². Several studies have confirmed that the autophagy impairment in HSCs results in hematopoietic abnormalities: in *Vav-Atg7^{-/-}* mice, where autophagy is blunted in hematopoietic cells, it has been observed aberrant mitochondria accumulation in HSCs, an increased level of ROS, multilineage cytopenia, severe myeloproliferation and BM failure¹¹³. Similarly, *Vav-Atg5^{-/-}* mice, which lacked the *Atg5* gene in hematopoietic cells, showed an accumulation of aberrant mitochondria, increased level of ROS in addition to anemia, severe lymphopenia and impaired BM reconstitution after transplantation¹¹⁴. In humans, CD34⁺ cells from patients with acquired aplastic anemia (AA) have a lower autophagic activity compared with healthy controls¹¹⁵.

The role of autophagy in neutrophils

Autophagy is involved in both differentiation and in bactericidal activity of neutrophils¹¹⁶ [Fig 1. 13].

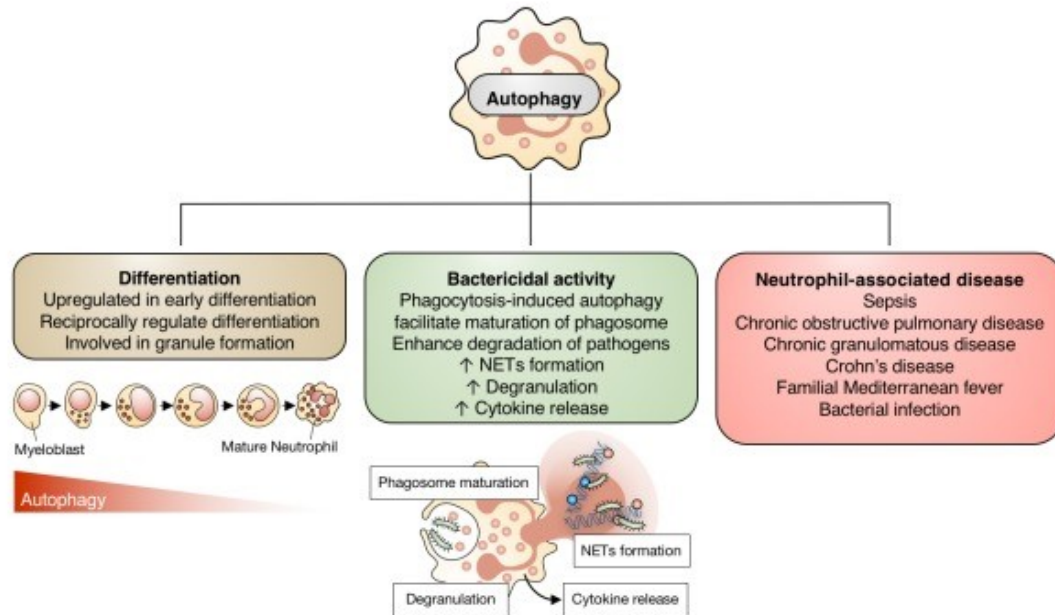


Figure 1.13: The role of autophagy in regulating neutrophils differentiation and effector functions. Its involvement is crucial for differentiation and bactericidal activity. The autophagy lack is associated with several diseases¹¹⁶.

During neutrophil generation, termed granulopoiesis, autophagy regulates the maturation of myeloid lineage cells¹¹⁷. Autophagy is upregulated during the myeloblasts, promyelocytes, and myelocytes steps of differentiation but is downregulated during the late stages of metamyelocytes and band cells^{118,119}. In granulopoiesis, there is a metabolic shift from glycolysis to oxidative phosphorylation and it has been evidenced how the lipid droplets are degraded by autophagy (lipophagy) to provide free fatty acids to generate ATP¹¹⁹. The deletion of *Atg5* or *Atg7* in early granulocytic lineages resulted in a defective differentiation into promyelocytes, due to a lack of ATP necessary for differentiation. During infections, a specific form of macroautophagy can be used by neutrophils for pathogen removal, that has been called xenophagy¹²⁰, in which bacteria are recognized and destroyed by the neutrophils' autophagosome. It has also been observed how autophagy is involved in ROS production during the oxidative burst and during degranulation; indeed the deletion of *Atg5* or *Atg7* results in impaired degranulation¹¹⁶. The role of autophagy of neutrophils in cancer is divergent depending on the type of cancer. For example, in hepatocellular carcinoma, autophagy upregulation in neutrophils maintains mitochondrial function and neutrophils survival within the tumor microenvironment, which produce pro-metastatic MMP-9 and OSM,

exacerbating tumor growth and metastasis¹²¹. On the other hand in acute myelocytic leukemia (AML), correcting the defective autophagy functioning allows normal granulocytic differentiation, reducing the risk of cancer cell formation¹²². The autophagic machinery has been also associated with NETosis: in non-surviving septic patient, neutrophils were showing both autophagy impairment and reduction of NETs formation, compared with surviving patients¹²³. Induction of autophagy in a mouse model of lethal sepsis can rescue NETs and increasing survival¹²³.

In diabetes, it has been observed the impaired autophagic activity: it has been shown how, in T1D rats, the neutrophils' lifespan is shortened because of the impaired autophagy process derived by the mTOR overactivation, and a reduced ROS production, which is known to inhibit mTOR, leading to apoptosis¹²⁴.

AIM OF THE WORK

Among the diabetes complications, diabetic stem cell mobilopathy is one of the most insidious⁷⁰. Despite increasing research efforts, the mechanisms underlying this complication are still poorly understood. Neutrophils are believed to be one of main target of G-CSF and it has been reported that autophagy is required for G-CSF mobilization of HSPC⁵⁷.

This project aims to understand if diabetic stem cells mobilopathy is linked to a deregulation of autophagy in neutrophils is impaired during diabetes. Moreover, we want to investigate whether a pharmacological induction of autophagy can restore, at least in part, mobilization in diabetic mice.

2. MATERIALS AND METHODS

Mice

All the procedures were approved by the local ethics committee and the Italian Ministry of Health. National and international guidelines for the use and care of laboratory animals were followed. Mice were housed in the animal facility of the Venetian Institute of Molecular Medicine (VIMM), where they were kept in constant 12-h dark–light cycles and given access to food and water ad libitum. C57BL/6J wild-type (Wt) mice were purchased from The Jackson Laboratory and established as a colony since 2001. C57BL/6Jtg GFP-LC3 mice were generated by Dr. Noboru Mizushima [Fig 2.1]¹²⁵ and obtained by Prof. Paolo Bonaldo (University of Padova) upon approval from Dr. Mizushima (Graduate School and Faculty of Medicine, University of Tokyo, Japan). GFP-LC3 mice were established as a colony since 2019. This mouse model is commonly used for autophagy studies: the fusion protein produced is normally localized in the whole cytoplasm, but once that autophagy is induced, the forming autophagosomes forms GFP-LC3 aggregates called *punctae*. By quantifying the *punctae* with a fluorescence microscope or imaging flow cytometry is possible to investigate the autophagy flux.

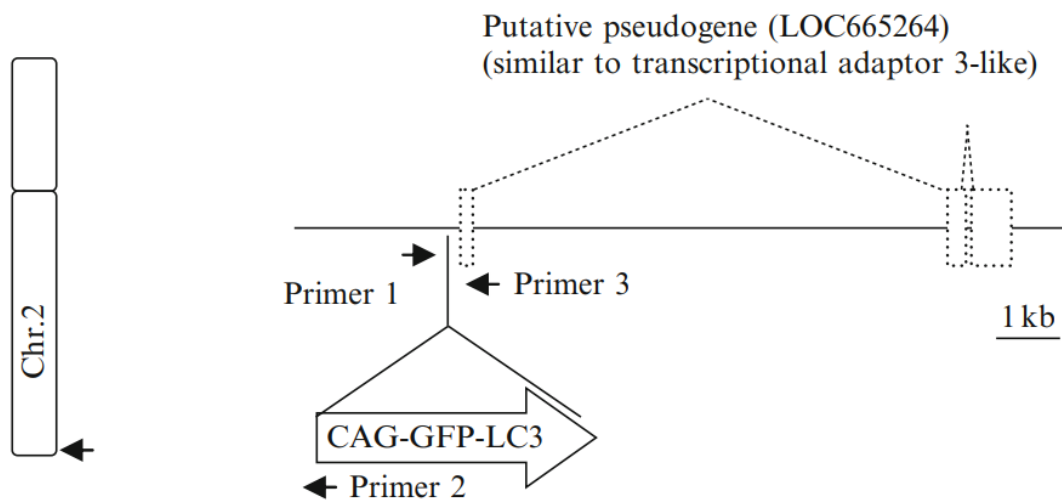


Figure 2.1: GFP-LC3 construct scheme. GFP-LC3 construct is localized in the mouse chromosome 2 distal portion. It doesn't interfere with the expression of other genes and the resulting fusion protein has no steric hindrance problems¹²⁶.

Genotyping

Genomic DNA (gDNA) from ears' fragments was extracted by digesting the sample for 1 hour at 56°C in 50 µL of lysis buffer (proteinase K 20 ng/mL in Tris HCl 1M pH 7.5) followed by 5 minutes at 99°C using the primer list in table 2.1.

Primer 1	5-ATAACTTGCTGGCCTTTCCACT-3
Primer 2	5-CGGGCCATTTACCGTAAGTTAT-3
Primer 3	5-GCAGCTCATTGCTGTTCTCAA-3

Table 2.1: Genotyping primer list

Samples were amplified using the C1000™ Thermal Cycler (Bio-Rad Laboratories, Milano, Italy) according to the protocol¹²⁷.

Induction of Diabetes

3- to 6- month-old mice were used for all the experiments. Type 1-like diabetes was induced by a single intraperitoneal injection of 175 mg/kg streptozotocin (STZ) (Cayman, Cat. No. 13104), in 100 mmol/L, pH 4, Na-citrate buffer¹²⁸. Blood glucose was measured using a point-of-care device (FreeStyle; Abbott). Diabetes onset was confirmed for blood glucose ≥ 300 mg/dL 48 h after STZ injection, but only mice with persistent hyperglycemia in the subsequent 4 weeks were used.

Bone Marrow cells and Bone Marrow neutrophils isolation

BM cells were isolated by flushing femurs and tibiae of 2- to 6- month-old mice with ice-cold PBS through a 40 µmol/L cell strainer. Neutrophils were purified using the Neutrophil Isolation Kit (MiltenyiBiotec, Cat. No. 130-097-658) according to the manufacturer's instruction. 2×10^6 unfractionated Bone Marrow cells or purified neutrophils were cultured in RPMI 1640 (Corning, Cat. No. 15-041-CV) with 10% FBS, L-Glutamine, and penicillin/streptomycin (Gibco) or lysed for western blotting and RNA extraction.

In vitro treatments

Whole flushed bone marrow cells or isolated neutrophils were cultured in six wells plate (Corning) in complete RPMI medium previously described with hr-G-CSF 100ng/ml, in the presence or absence of chloroquine 80uM (Merk, Cat. No. C6628-50G) for 4 hours. After the treatment cells were centrifuged and fixed with 4% PFA and stained for flow cytometry. Alternatively, were centrifuged and lysed for western blotting.

In vivo/ex vivo treatments

HSPC mobilization was induced by injecting animals subcutaneously with 200 ug/kg/day human recombinant granulocyte colony-stimulating factor (hr-G-CSF, Amgen, Cat. No. A027772096) for 4 consecutive days. Spermidine (Merck, Cat. No. S2626-1G) was added to the drinking water at 3mM for 1 week. Ketone supplement (Keto BHB Salts Supplement; Zenwise Health, Wilmington, DE) was added to the drinking water at 5 gr/kg/day for 2 weeks. Mice were sacrificed the day after the last G-CSF injection. Alternatively, mice were sacrificed 1 hour from the last G-CSF injection and flushed Bone Marrow cells or isolated neutrophils were cultured in FACS tubes for 1 hour in presence absence of chloroquine 80uM (Merk, Cat. No. C6628-50G) in complete RPMI medium.

Peripheral blood analysis

Blood ketones were measured using a point-of-care device (Menarini diagnostics) at specific time points. Total White Blood Cells (WBC) count was performed using the CELL-DYN Emerald Hematology Analyzer (Abbott) on fresh EDTA-treated mouse blood. Spermidine level was assessed in plasma-EDTA samples by enzyme-linked immunosorbent assay (ELISA) according to the manufacturer's instructions (Abxexa, Cat. No. abx585001)

Colony forming unit assay

Mouse fresh EDTA-treated blood was collected and after Red Blood Cell (RBC) lysis, 15×10^4 WBC were plated in 24-well plates containing 0.5 mL MethoCult (Voden, Cat. No. GF M3434) supplemented with 1% penicillin/streptomycin. Images were acquired with CYTELL cell imaging system (GE Healthcare, Buckinghamshire, UK). Colony formation was scored after 10 days of culture.

Western blotting

1×10^6 purified neutrophils were lysed using RIPA buffer prepared as follows: 150 mM NaCl pH 7.5, 50 mM Tris HCl, 1% Sodium Deoxycholate, 0.1% SDS, 1 mM EDTA, 1% TritonX-100, 1:100 Phosphatase inhibitors cocktail II and III (Merk, Cat. No. P5726/P0044) and 1:50 Complete® Protease inhibitor (Roche, Cat. No. 05-892-791-001). Protein concentration was determined using Pierce BCA protein assay (Thermo Scientific, Cat. No. 23227). 30µg of proteins were loaded on NuPAGE 12% Bis-Tris gel (Invitrogen, Cat No. NP0342BOX) and transferred to nitrocellulose membrane. Membranes were blocked with 5% milk or 5% BSA in TBS-T (1M Tris HCl pH 7.4, 5M NaCl, 0.1% Tween 20) and then incubated with primary antibodies mouse anti-rabbit-LC3 (1:1000, Merk, Cat. No. L7543), mouse anti-rabbit-ATG5 (1:1000, cell signaling Cat. No. 12994S)

and anti-mouse β -ACTIN (1:10.000, Abcam, Cat. No. ab6276) as loading control. Immunolabeled proteins were finally detected by using appropriate HRP-conjugated secondary antibodies (Jackson Immuno Research) at the dilution 1:1000, 1:2000, and 1:10.000, respectively. Finally, immunoreactive bands were revealed using enhanced chemiluminescence (ECL) detection (Advansta, Cat. No. K-12042).

RNA isolation and quantitative Real-time PCR

RNA was isolated from whole bone marrow cells or purified neutrophils using Qiazol® Lysis Reagent (Qiagen, Cat. No. 79306) according to the manufacturer's instructions and quantified with a Nanodrop 2000 spectrophotometer (Thermo Fisher Scientific, Waltham, MA, USA). cDNA was synthesized with the SensiFast cDNA Synthesis Kit (Bioline, Cat. No. BIO65054). Quantitative real-time PCR was performed using the SensiFAST™ SYBR® Lo-ROX Kit (BiolineCat. No. BIO-94050) via a QuantStudio 5 Real-Time PCR System (Thermo Fisher Scientific, MA, USA) using the primer list in Table 2.3. Relative expression was calculated using the Δ Ct method against beta actin. reference target and shown as fold change relative to the controls.

Gene	Symbol	Sequence 5'- 3'
Microtubule-associated protein 1A/1B-light chain 3	lc3	Forward primer: CACTGCTCTGTCTTGTGTAGGTTG
		Reverse primer: TCGTTGTGCCTTTATTAGTGCATC
Autophagyrelated 5	atg5	Forward primer: TGTGCTTCGAGATGTGTGGTT
		Reverse primer: GTCAAATAGCTGACTCTTGGCAA
Autophagyrelated 7	atg7	Forward primer: GTTCGCCCCCTTTAATAGTGC
		Reverse primer: TGAACTCCAACGTCAAGCGG
B-actin	β act	Forward primer: CTGGCTCCTAGCACCATGAAGAT
		Reverse primer: GGTGGACAGTGAGGCCAGGAT

Table 2.2: qPCR primer list

Flow cytometry

200 µl of freshly collected EDTA-treated peripheral blood was incubated with 4ul Pacific blue α -mouse Lineage ab, 1ul, FITC α -mouse ab c-kit, sca-1 ab for 10 minutes, then RBC was lysed, and after centrifugation WBC was resuspended in PBS. Data were acquired with a FACSCanto (BD Biosciences) cytometer and analysed using FlowJo software (BD Biosciences). The list of antibodies is provided in Table 2.3.

Antigen	Clone	Company	Catalog	RRID
Lineage Cocktail (CD3, Ly-6G/C, CD11b, CD45R, TER-119) Pacific Blue	17 [°] 2, RB6- 8C5, Ra3- 6B2, Ter-119, M1/70	BioLegend	133306	AB_11126978
Isotype control	Rat IgG2a K	BioLegend	133306	AB_11126978
Rat anti-mouse CD117 (c-kit) FITC	2B8	eBioscience	11- 1171-85	AB_465187
Rat anti-mouse Ly-6A/E (Sca-1) PE	D7	eBioscience	12- 5981-83	AB_466087
Rat anti-mouse Ly-6G/C (Gr-1) PE	RB6-8C5	eBioscience	108408	AB_313373

Table 2.3: flow cytometry and imaging flow cytometry antibody list.

Imaging flow cytometry

Single-cell suspensions of BM were obtained by flushing the bone cavity of femurs and tibiae with ice-cold PBS through a 40-µm cell strainer. Red blood cells were lysed with ACK buffer. After centrifugation, 2×10^6 cells were stained with 1 ul PE α -mouse Gr-1 Ab (eBiosciences, Cat. No. in table 2.3) for 10 minutes and then fixed with 4% PFA for 15 minutes and resuspended in PBS. In each experiment, 50.000 events for each sample were acquired using a 6-channel Amnis Image StreamMkII (Cytek biosciences) imaging flow cytometer equipped with 405 nm, 488 nm, and 642 nm lasers. Single color compensation controls were also acquired. The integrated software INSPIRE (Cytek Biosciences) was used for data collection. The following acquisition settings were applied: brightfield on, 488 nm laser on at a power of 200 mW, low-speed fluidics, magnification at

60×, core size of 7 μm, numerical aperture of 0.9, DOF of 2.5 μm. GFP fluorochrome was read at the intensity band of 505-560 nm, and PE fluorochrome was read at the intensity band of 560-595 nm. During the *in vitro* experiment, in which only isolated neutrophils were present, only GFP-positive cells were acquired. During the *ex vivo* experiment, both PE and GFP positive cells were acquired, in order to analyze an enriched population in neutrophils. Images were analyzed with IDEAS 6.3 (Image Data Exploration and Analysis Software). Single color controls were used to calculate the spectral crosstalk matrix that was applied to each of the files for spectral compensations in the detection channels. The resulting compensated data files were analyzed using image-based algorithms available in the IDEAS statistical analysis software package. Single cells were separated from debris and doublets using a bivariate plot of aspect ratio vs area of the BF image. Next, cells in best focus were identified using Gradient RMS feature of the BF image. This was followed by gating on positive events for PE and LC3. Finally, Spot Count values were calculated from the positive cells to identify the number of GFP-LC3 *punctae* within cells.

Sequencing data analysis

Briefly, unprocessed raw read bulk RNA-seq files were downloaded from the EBI repository (accession number E-MTAB-11190)¹²⁹. A total of 35 samples were selected for reanalysis, including neutrophils isolated from by immuno-magnetic selection from the peripheral blood of 18 untreated and 17 GCSF-treated healthy donors¹²⁹. Raw reads were assessed for quality using the fast QC tool, and adapter sequences and low-quality reads were trimmed using Trimmomatic sliding window method (window size=4bp, average quality requested=20). Trimmed data were again assessed using fast QC, and good quality sequencing data was verified. Trimmed reads were aligned to the reference genome (GRCh38/hg38) using the HISAT2 tool with default parameters. Aligned reads were filtered using the Samtools suite, only retaining alignments with a minimum MAPQ quality score of 20. Aligned counts were processed using the feature Counts tool with default parameters, obtaining the final raw count matrix. Differentially expressed genes were evaluated using the DESeq2 tool, removing genes with less than 10 overall aligned reads. Normalized reads were obtained from the raw count matrix using the DESeq2 tool and used as input for the GSEA desktop utility. GCSF-treated samples were compared with untreated ones, and the enrichment was calculated for Reactome terms. The heatmaps and the enrichment plots were generated by the GSEA suite using default parameters. For single-cell RNA sequencing data analysis, the barcode and 10X-derived gene and feature matrix files were downloaded from the EBI repository (accession number E-MTAB-11188). A total of 6 samples were selected for reanalysis, including neutrophils isolated by immuno-magnetic selection from the peripheral blood of 2

untreated and 4 G-CSF-treated healthy donors¹²⁹. The Seurat package (<https://satijalab.org/seurat/>) was then used to perform all downstream analyses. First, each sample was loaded in the Seurat space, and from each of them, cells expressing fewer than 300 unique genes and genes expressed in fewer than three cells from the non-normalized UMI count matrix of each sample were removed. Raw count matrices of all samples were then combined in a single Seurat object (36601 genes and 56680 cells) with the use of the merge function. A cell/gene quality control was then performed. We jointly examined the distribution of the count depth (number of counts per barcode) of the number of genes per barcode and of the fraction of counts from mitochondrial genes per barcode. Cells with a total number of detected molecules <500, cells with a percentage of reads that map to the mitochondrial genes greater than 10, and cells with a number of detected genes > 4,000 were discarded. The final raw count matrix was composed of 23728 genes and 52439 cells. The sc transform normalization (SCTransform function) while adjusting for the mitochondrial mapping percentage and the cell cycle scores computed with the CellCycle Scoring function. Data were then scaled with ScaleData, and the top 1,000 variable features were selected with the 'vst' method of the Find Variable Features function. A shared nearest neighbor graph was constructed using the Find Neighbors function taking as input the first 50 principal components, computed with the RunPCA function. Cell clusters were defined using a resolution of 0.2, were calculated with the FindCluster function and were visualized in two dimensions using UMAP. Expression scores for single genes or immature/mature neutrophils gene signatures were plotted on the UMAP graph using respectively the FeaturePlot and the AddModuleScore/FeaturePlot functions from the Seurat package. The immature/mature gene dataset used is showed in table 2.4¹³⁰. To obtain pseudotime trajectory, the full Seurat object was converted to a CDS object using the SeuratDisk package, and trajectory calculation was obtained using the monocle3 package with default parameters, maintaining the clustering and neighbor information from the original Seurat object. Root nodes were selected as the ones closer to most of the control samples-derived cells, while the end trajectory node was automatically selected by the monocle3 tool.

Immature neutrophils	
Gene name	-Fold increase
Azurocidin 1 (cationic antimicrobial protein 37)	292
Neutrophilelastase 2	291. 4
Bactericidal/permeability-increasing protein	243. 4
Lipocalin 2	241. 1
Myeloperoxidase	231. 9
Cathepsin G	177. 2
Matrix metalloproteinase 8 (neutrophil collagenase)	163. 3
Defensin, α 4 (corticostatin)	162. 1
Neutrophil-specific defensin, α 3	84. 7
Cathelicidin antimicrobial peptide	24. 9
Cytochrome <i>b</i> -245, β -polypeptide	7. 42
Mature neutrophils	
Gene name	-Fold increase
Alkaline phosphatase	172. 7
Interleukin-8 receptor β	76. 2
Receptor for Fc fragment of IgG, low affinity IIIb (CD16)	65. 4
Semaphorin 3C	62. 9
Putative human chemokine receptor	42. 6
Mitochondrial superoxide dismutase 2	42. 3
Receptor for Fc fragment of IgG, low affinity IIIa (CD16)	42. 1
Interleukin-8	42. 1
Sialyl transferase	40. 6
Interleukin-8 receptor α	36. 2
Receptor for Fc fragment of IgG, low affinity IIa (CD32)	31
G-CSF 3 receptor	11. 2
Neutrophil acyloxyacyl hydrolase	5. 03

Table 2.4: Relative expression levels of neutrophil-specific genes in immature versus mature neutrophils used for single cell gene signature. Data retrieved by Martinelli et al¹³⁰.

Statistical analysis

Data are reported as the mean \pm SE for continuous variables. All analyses were performed using GraphPad Prism software. Comparison of data between two or more groups was performed using a two-tailed unpaired Student's t-test or two-way ANOVA (with post hoc Bonferroni correction) with Sidak multiple comparison test, respectively. Statistical significance was set at * $p < 0.05$. GraphPad Prism 9.0 (GraphPad Software, La Jolla, CA) or JMP[®] Pro 17.0.0 (JMP Statistical Discovery LLC, NC, USA) were used for data analysis. The number of biological replicates is reported in the figure legends or shown as individual data points in the figures.

3. RESULTS

Autophagy-related genes are modulated in bone marrow by G-CSF *in vivo* in mice but not in neutrophils

To address whether autophagy is modulated by G-CSF *in vivo*, we have analyzed the expression of *Lc3*, *Atg5* and *Atg7*, which are some of the most relevant genes involved in the autophagolysosome formation¹²⁰, that have been previously shown to be modulated by G-CSF in humans and mice⁵⁷. By performing qPCR on unfractionated BM of wild type mice treated with 200 µg/kg of rh-G-CSF for 4 days [Fig. 3.1 A], we found that G-CSF induces the genes upregulation of *Lc3* (1.26±0.00 fold vs Ctrl, *p<0.05), *Atg5* (1.43±0.02 fold vs Ctrl, **p<0.01) and *Atg7* (1.73±0.09 fold vs Ctrl, *p<0.05) [Fig 3.1A]. The upregulation observed is likely due to the heterogeneous bone marrow population, which includes other leukocytes besides neutrophils, such as macrophages¹³¹, lymphocytes¹³² and HSCs⁵⁷, suggesting that the G-CSF treatment may modulate autophagy in other cell types. However, when we analyzed neutrophils isolated from mice treated with G-CSF we did not observe any modulation gene expression [Fig 3.1 B].

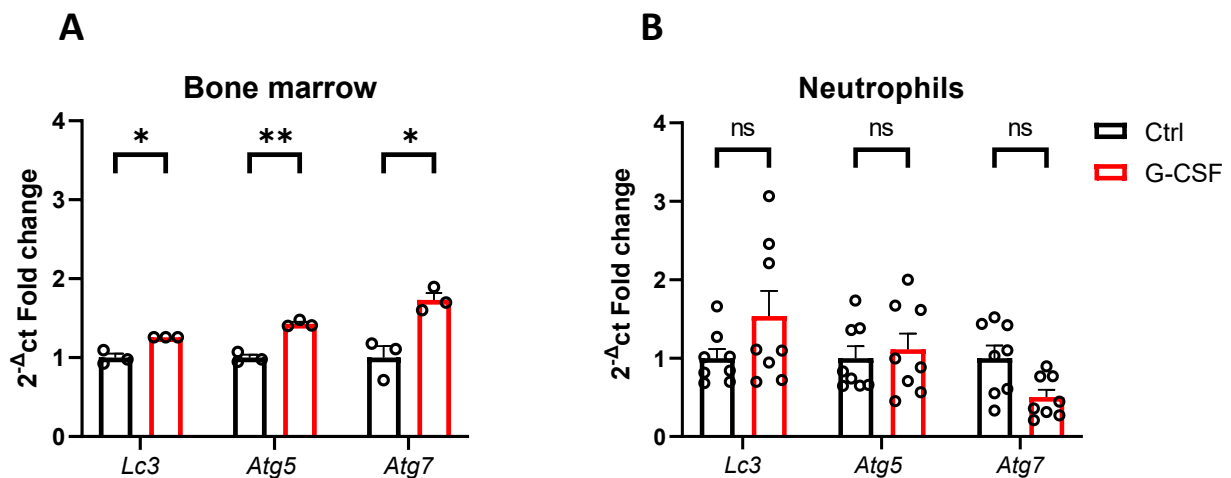


Fig. 3.1: Autophagy related genes are modulated in unfractionated bone marrow but not in purified neutrophils. *A*: qPCR analysis on unfractionated BM; $n=3$. *B*: qPCR analysis isolated neutrophils. Δct was calculated by comparing the ct of the target gene against the housekeeping ($mActb$); $n \geq 8$. Results were normalized for their own control. Statistical test: multiple t -test with Holm-sidak multiple comparison test, * $p < 0.05$, ** $p < 0.01$.

Autophagy is modulated in neutrophils *in vivo* after G-CSF

Transcriptomic changes might not correlated with protein modulation due to post-transcriptional events that may modify the translation efficiency, such as feedback mechanisms, post-

transcriptional modifications, or mRNA degradation¹³³⁻¹³⁵. Therefore, we sought to evaluate the modulation of protein expression in response to G-CSF. Western blot revealed the presence of the 14 kDa lipidated isoform of LC3 (LC3II) in neutrophils treated with G-CSF, which is suggestive of autophagy modulation [1.85 ± 0.22 fold vs untreated $*p < 0.05$, Fig 3.2 A, B]. Accordingly, ATG5 was also upregulated by G-CSF [4.35 ± 0.55 fold vs untreated $**p < 0.01$, Fig 3.2 A, C]. Due to the lack of an autophagy inhibitor in this experiment, we cannot assess whether LC3II accumulation is the results of an activation of autophagy or an engulfment due to G-CSF treatment. However, ATG5 upregulation is normally associated with autophagy induction¹³⁶.

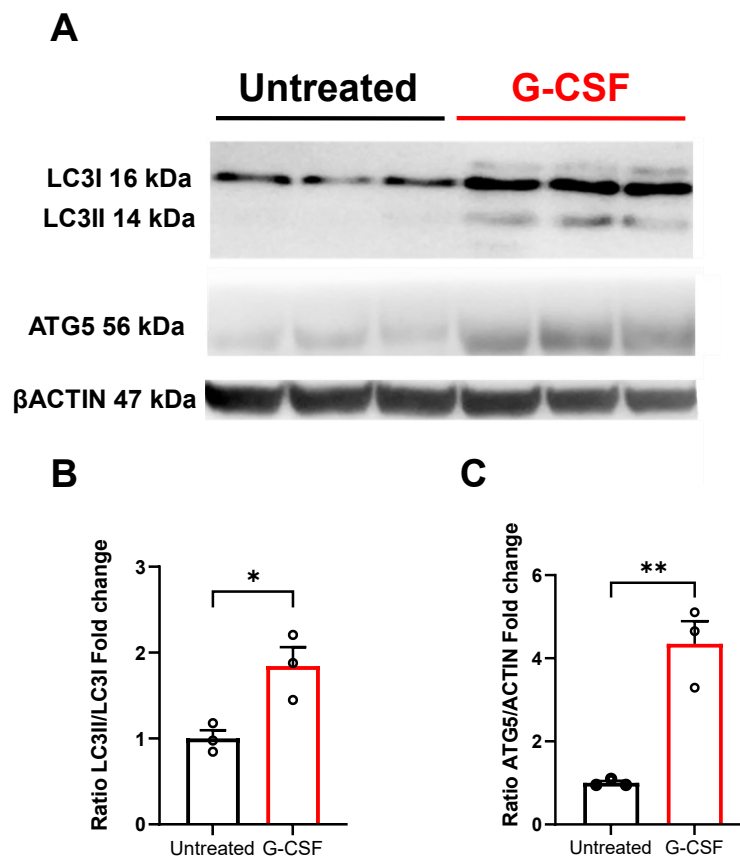


Fig. 3.2 Autophagy is modulated by G-CSF. Western blot representative images and densitometry analysis. **A:** LC3II was normalized to LC3I; $n=3$. **B:** ATG5 was normalized to β ACTIN; $n=3$. Statistical test: unpaired t -test. $*p < 0.05$, $**p < 0.01$.

Autophagy modulation is observable *in vitro* in BM cells using imaging flow cytometry

We aimed to confirm that the modulation of LC3 and ATG5 was the results of autophagy induction, rather than engulfment. To do this we, take advantage of the GFP-LC3 mouse model¹²⁶ as a tool to investigate the autophagy flux using imaging flow cytometry. To validate whether imaging flow cytometry was a suitable technique for evaluating the autophagic flux, we have performed some preliminary assays. Serum deprivation and starvation are known inducer of autophagy both *in vitro*

and *in vivo*¹³⁷. Thus, unfractionated BM cells were subjected *in vitro* to serum starvation for 4 hours, while autophagy was blocked by adding 80 μ M chloroquine (CQ) during the serum deprivation [Fig. 3.3 A]. CQ inhibits the lysosome fusion with the autophagosome by altering the acidic environment of lysosomes, resulting in autophagosomes accumulation [3.3 B, C]¹³⁸.

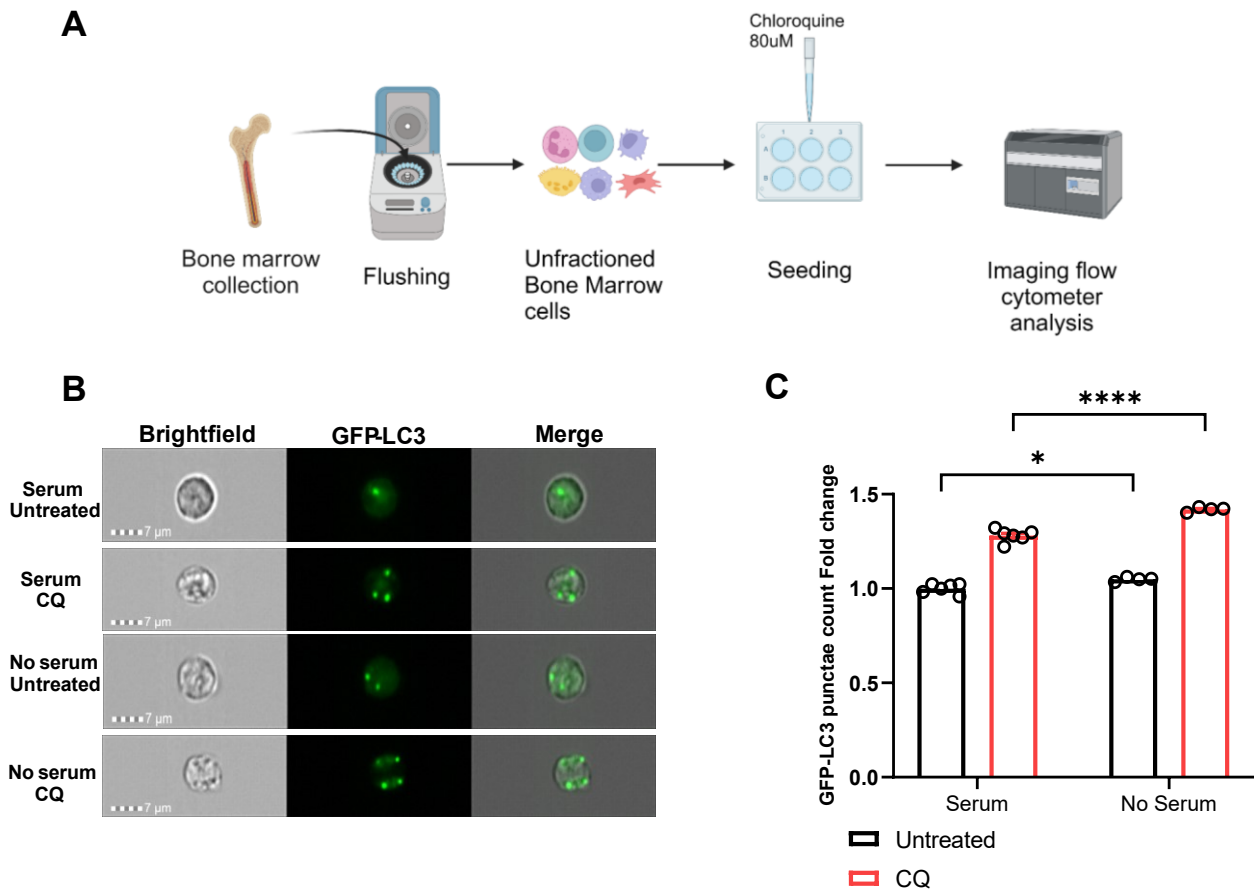


Fig. 3.3: GFP-LC3 punctae modulation in BM cells in vitro. *A: experimental design B: representative images showing the accumulation of GFP-LC3 punctae in BM cells. C: The mean of GFP-LC3 punctae counted: each condition was normalized for serum untreated condition; $n \geq 4$. Statistical test: two-way ANOVA with sidak multiple comparison test. $*p < 0.05$ **** $p < 0.0001$.*

Imaging flow cytometry revealed that serum starvation induced a modest but significant increase in the number of GFP-LC3 *punctae* within cells, which represents the autophagosomes (1.05 ± 0.01 fold vs serum untreated, $*p < 0.05$)¹²⁶. CQ co-treatment, by block the autophagic flux resulted in a further accumulation of autophagosomes. As expected, also control cells treated with CQ have an increased punctae accumulation compared to basal due to autophagy inhibition, but the effect is lesser compared with the G-CSF co-treated cells (1.42 ± 0.01 fold vs 1.281 ± 0.03 serum CQ, **** $p < 0.0001$).

G-CSF treatment modulates the autophagy flux in mouse neutrophils *in vitro*

Next, we aimed to understand whether autophagy is induced by G-CSF. Isolated neutrophils from GFP-LC3 mice were treated *in vitro* with 100ng/ml for 4 hours while autophagy was blocked by adding 80 μ M CQ during the treatment. G-CSF increased the number of GFP-LC3 *punctae* (1.42 \pm 0.01 fold vs Ctrl untreated, **** p <0.0001), while CQ in combination with G-CSF resulted in a higher number of punctae compared to the control CQ treated cells (1.79 \pm 0.04 fold vs 1.59 \pm 0.03 Ctrl CQ, *** p <0.001) [Fig 3.4 B, C]. This last evidence strongly support that G-CSF can induce autophagy in neutrophils *in vitro*.

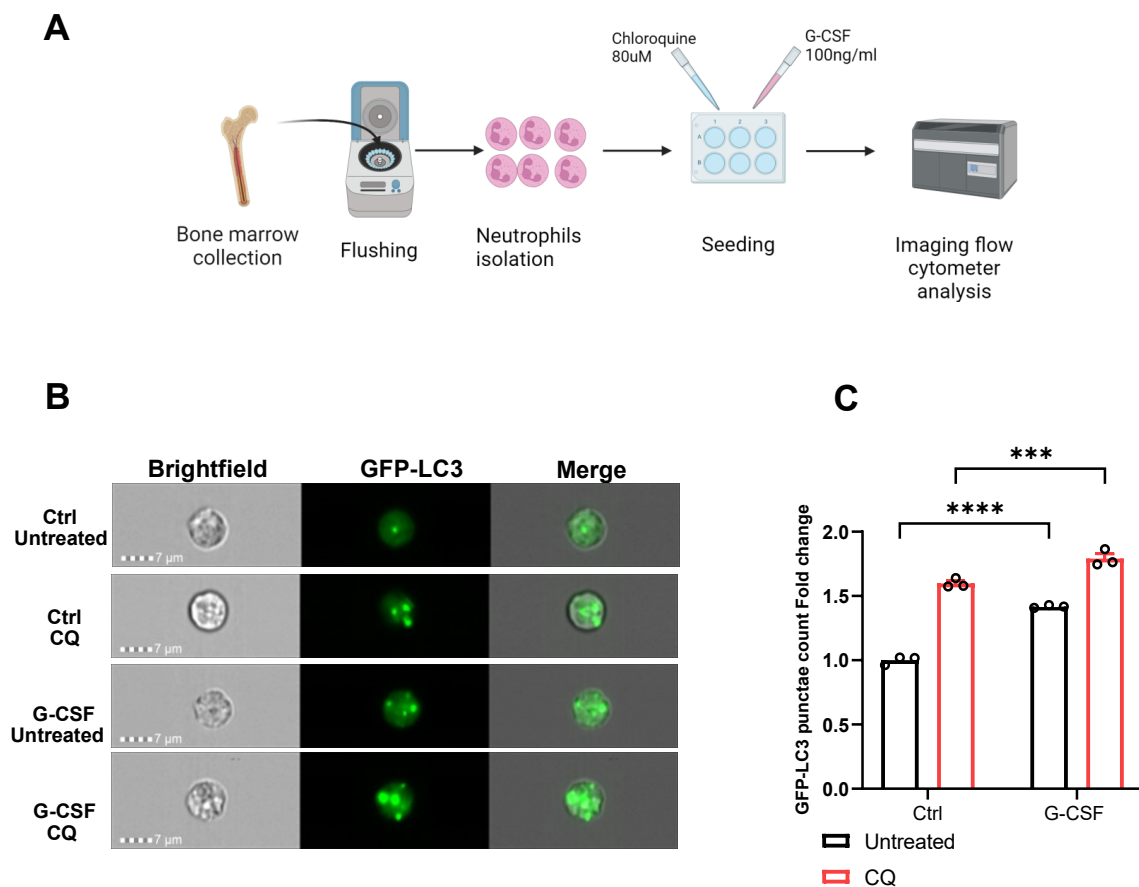


Fig. 3.4: Autophagy is modulated *in vitro* after G-CSF treatment. *A*: experimental design. *B*: representative images showing that in G-CSF treated neutrophils the number of visualized autophagosomes are increased compared with Ctrl untreated condition. *C*: the mean of GFP-LC3 punctae count results: each condition was normalized for control untreated condition; $n=3$. Statistical test: Two way ANOVA with Sidak multiple comparisons test. *** p <0.001, **** p <0.0001

G-CSF treatment induces the autophagy flux in mouse neutrophils *ex vivo*

With the purpose to understand whether G-CSF can activate autophagy *in vivo*. Blocking autophagy *in vivo* in neutrophils is challenging, thus we opted to use *ex vivo* approach. Mice were treated 4

days with G-CSF 200 $\mu\text{g}/\text{kg}/\text{die}$ and sacrificed 1 hour after the last injection. Freshly isolated bone marrow cells were incubated for 1 hour with 80 μM chloroquine, before staining with Gr-1 antibody and fixed in 4% PFA. By analyzing Gr-1^{bright} cells, which represent *bona fide* mature neutrophils¹³⁹, we found that chloroquine was sufficient to block autophagy *ex vivo* in control neutrophils and to clearly appreciate the effects of G-CSF [Fig 3.5]. Similarly to the *in vitro* experiment, we can observe the lesser effect of chloroquine in control neutrophils compared with the G-CSF treated cells. These results confirm that G-CSF can induce autophagy in neutrophils *ex vivo*.

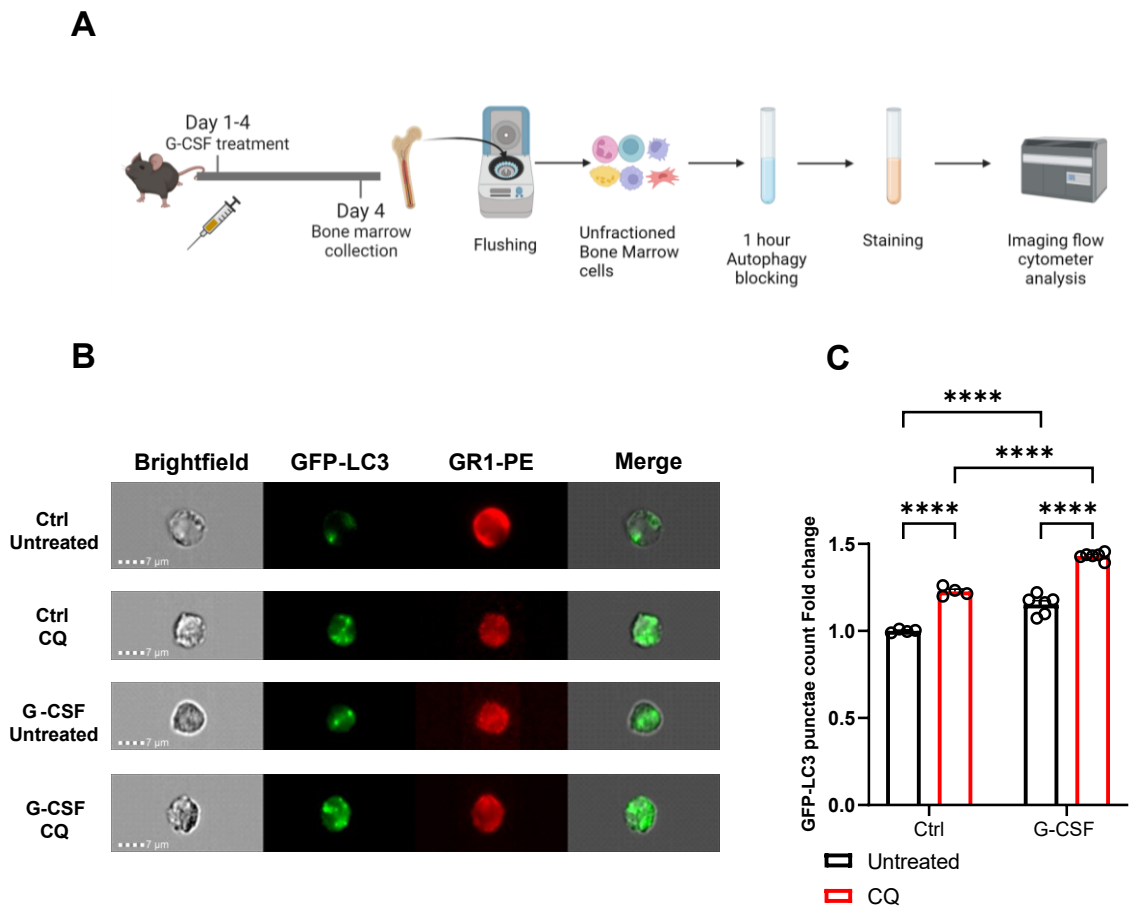


Fig. 3.5: Autophagy is induced in neutrophils *ex vivo* after G-CSF. *A*: experimental design *B*: imaging flow cytometry representative images showing the G-CSF derived GFP-LC3 punctae modulation; scale bar = 7 μm . *C*: mean GFP-LC3 punctae. Results were normalized to the control basal condition; $n \geq 4$. Statistical test: Two-way ANOVA with Sidak multiple comparisons test, **** $p < 0.0001$.

Neutrophils from diabetic mice showed impaired autophagy modulation after G-CSF *in vivo*

Autophagy is studied as an important player in the pathophysiology of diabetes and its complications¹⁰⁵, however the role of autophagy in diabetic stem cell mobilopathy was never

investigated. Thus, we used the model of streptozotocin-induced T1D (T1D STZ) in mice, which we have previously show to recapitulate the mobilopathy phenotype of patients with diabetes⁸⁵.

To trigger bone marrow dysfunction and diabetic mobilopathy, T1D STZ mice were exposed to hyperglycemia for 4 weeks. Using the afore-mentioned protocol, we could show that in diabetic mice autophagy modulation is completely defective in neutrophils [Fig 3.6 A, B], and it is associated with a complete unresponsiveness toward mobilization, assessed by the quantification of LKS cells (Lin⁻, C-kit⁺, Sca1⁺ cells), which identifies HSPCs circulating in peripheral blood [Fig 3.6 C, D]. Interestingly both impaired autophagy and defective mobilization share a similar on/off fashion.

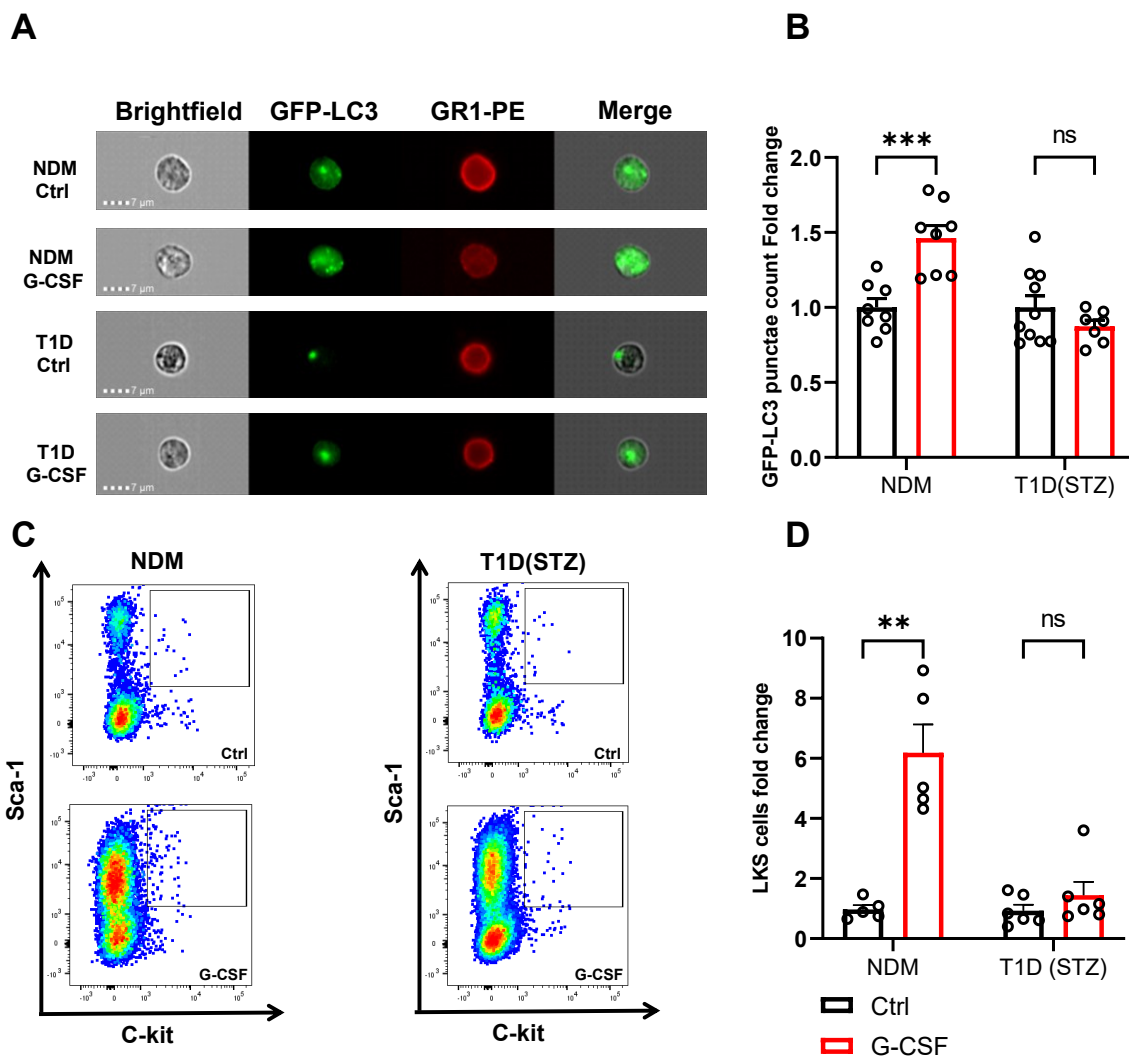


Fig. 3.6: Autophagy modulation and mobilization are impaired in T1D mice. *A*: imaging flow cytometry representative images. T1D mice did not show a modulation of GFP-LC3 punctae in response to G-CSF; scale bar = 7 μ m. *B*: the mean of GFP-LC3 punctae count results. Data were normalized to their respective control condition; $n \geq 5$. *C*: flow cytometer representative images showing the gating strategy of LKS cells. *D*: flow cytometer results showing the fold change of LKS

cells; $n \geq 5$. Data were normalized to their respective control condition. Statistical test: multiple *t*-test with Holm-sidak multiple comparison test $**p < 0.01$, $***p < 0.001$.

These findings support our hypothesis that the induction of autophagy by G-CSF in neutrophils might be deregulated in diabetes and that could have a role in jeopardizing hematopoietic stem cell mobilization. Once assessed the correlation between autophagy in neutrophils and mobilization, we aimed to devise pharmacological strategies to revert autophagy deregulation and possibly restore mobilization: spermidine and β -hydroxybutyrate.

Spermidine modulation is not associated to hematopoietic stem cell mobilization

Spermidine (Sp) is a polyamine commonly used as food supplement¹⁴⁰, and its role as a positive regulator of autophagy is well known¹⁴¹. To evaluate if endogenous spermidine is modulated during mobilization, we quantified plasma spermidine in diabetic and diabetic mice, both treated with G-CSF. As shown in Fig. 3.7 A, plasma spermidine concentration is not affected neither by diabetes nor G-CSF treatment. Next, we treated non-diabetic wild-type mice with 3 mM spermidine in the drinking water for 1 week. Despite a significant raise in plasma spermidine concentration, [Fig 3.7 B], HSPCs mobilization was not affected as shown by CFU assay on peripheral blood, which allows the quantification of competent HPSCs in blood [Fig 3.7 C, D].

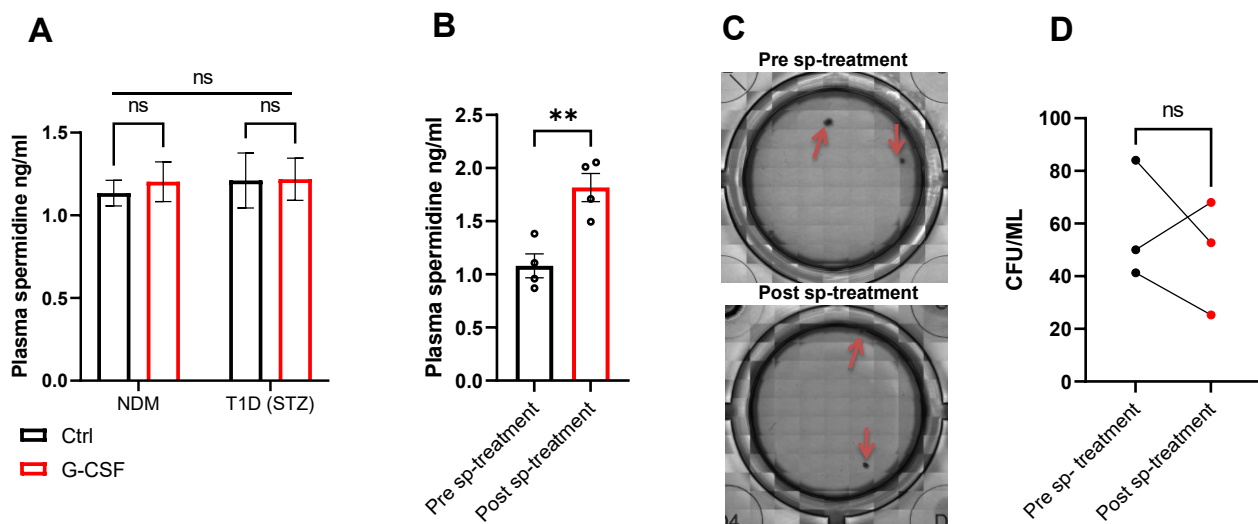


Fig. 3.7: spermidine is not modulated during hematopoietic stem cell mobilization. **A:** plasma spermidine is not modulated by the presence of diabetes or G-CSF treatment; $n=10$. Statistical test: Two-way ANOVA with Sidak multiple comparisons test **B:** Plasma spermidine quantification after spermine supplementation in the drinking water; $n=4$. Statistical test: unpaired *t* test. $**p < 0.01$. **C:** CFU assay representative images. **D:** Total number of colonies pre vs post spermidine treatment shows that modulation is not affected by spermidine; $n=3$. Statistical test: unpaired *t*-test with Holm-sidak multiple comparison test $**p < 0.01$.

Spermidine restores autophagy flux in diabetic mice neutrophils treated with G-CSF

Once established that spermidine *per-se* has no effect in mobilization-competent mice, we evaluated the effects of spermidine in diabetic mice in modulating autophagy and hematopoietic stem cell mobilization. Our hypothesis is this pharmacological activation could restore autophagy in diabetes. Thus, an *ex vivo* experiment on isolated bone marrow neutrophils from GFP-LC3 mice co-treated with G-CSF and spermidine. T1D STZ mice were treated with Spermidine 3mM in drinking water for one week. In parallel G-CSF 200 ug/kg was injected during the last 4 days. Mice were sacrificed and bone marrow cells were processed for the previously described *ex vivo* analysis using imaging flow cytometry [Fig 3.8 A, B].

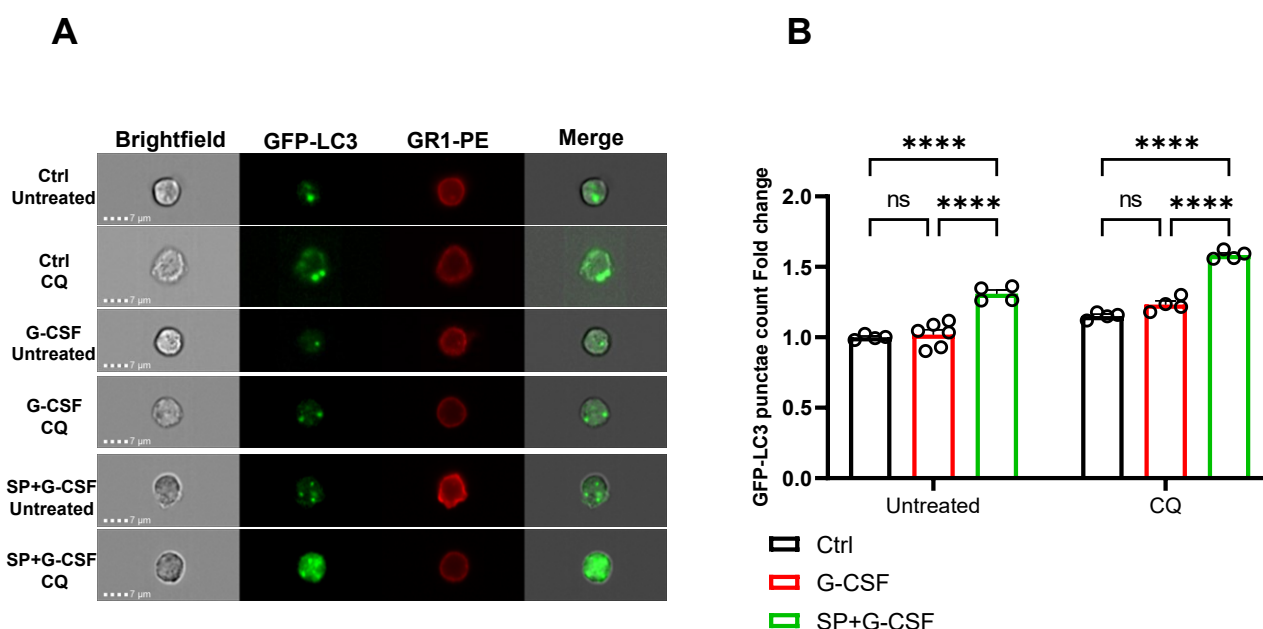


Fig. 3.8: Autophagy modulation is restored after spermidine treatment in T1D mice. *A*: imaging flow cytometry representative images; scale bar = 7 μ m. T1D co-treated with spermidine and G-CSF shows an enhanced modulation in GFP-LC3 punctae. *B*: average GFP-LC3 punctae quantification; $n \geq 4$. Data were normalized to Ctrl untreated. Statistical test: Ordinary Two-way ANOVA with Sidak multiple comparisons test. **** $p < 0.0001$.

Diabetic GFP-LC3 mice were treated with 3 mM spermidine for 1 week before receiving G-CSF. Bone marrow cells were stained with Gr-1 and autophagy assessed through imaging flow cytometry. Surprisingly, the combination of spermidine with G-CSF was sufficient in restoring autophagy flux in neutrophils from T1D STZ mice. The pattern is similar to what has been observed in non-diabetic mice, characterized by the accumulation of *punctae* after G-CSF, which was further increased by chloroquine treatment. Neutrophils from mice that have not received spermidine co-cultured with chloroquine, exhibited a mild upward trend in punctae number compared to the

baseline. This was due the autophagy inhibitor effect and had a similar pattern to previous imaging flow cytometry experiments.

Hematopoietic stem cell mobilization is not modulated by β -hydroxybutyrate alone

β -hydroxybutyrate belong to the ketone bodies family and it is the results of ketogenesis and it is used during glucose shortage as a secondary source of energy¹⁴². Autophagy is induced during nutrient deprivation and neutrophils uses lipophagy to recover energetic intermediates¹¹⁹. Therefore, because autophagy is impaired in diabetic mice, we aimed to test whether β -hydroxybutyrate could restore mobilization after G-CSF treatment, by mimicking an autophagy activation. We have at first assessed whether the supplementation of this ketone body was sufficient alone to induce mobilization: β -hydroxybutyrate was added in drinking water for 2 weeks at the concentration of 5gr/kg/die as previously described⁸⁴ and blood ketones level was monitored during the treatment. In non-diabetic mice, blood ketones showed a modest increase at the end of the 2 weeks, which did not reach statistical significance. However, in T1D mice blood ketones increase after the first week of treatment to return at basal level at the end of the treatment [Fig 3.9 A]. This could be due to rapid clearance of blood ketones through their metabolism. In non-diabetic mice, β -hydroxybutyrate supplementation was not associated with increased HSPCs mobilization, assessed by the quantification of competent HPSCs after β -hydroxybutyrate treatment through CFU assay [Fig. 3.9 B, C].

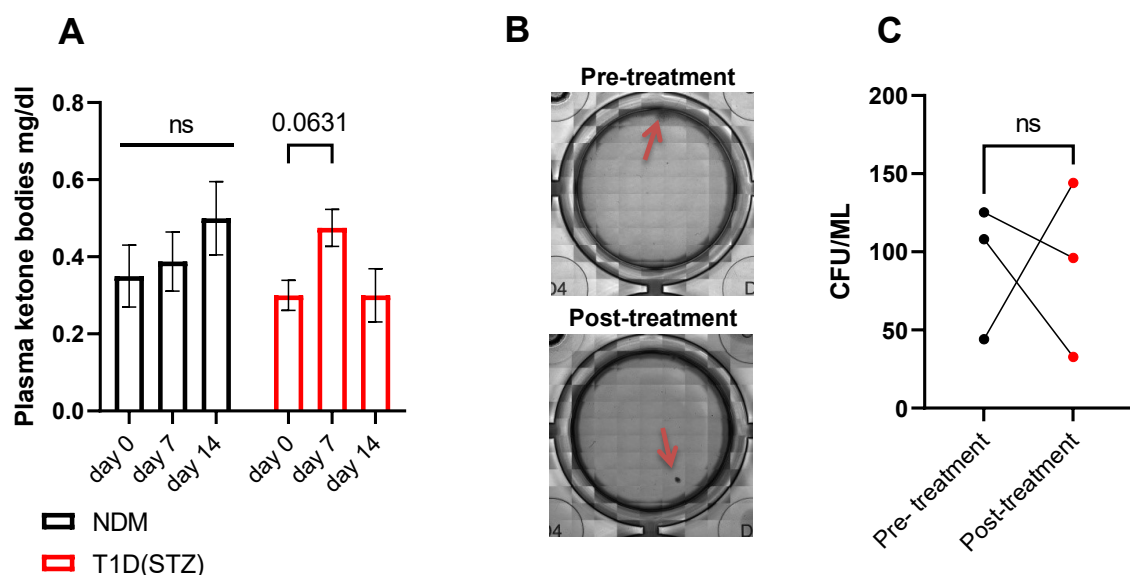


Fig. 3.9: β -hydroxybutyrate alone is not sufficient to induce mobilization. **A:** Blood ketone bodies accumulation differences from non-diabetic and T1D mice. Statistical test: ordinary two-way ANOVA with Turkey multiple comparison test; $n=10$. **B:** CFU assay representative images. **C:**

CFU assay analysis, $n=3$. Total number of colonies was compared from baseline to the post treatment. Statistical test: unpaired t -test.

G-CSF co-treatment with spermidine or β -hydroxybutyrate partially restore HSPCs mobilization

Once confirmed that the two drugs cannot modulate mobilization alone, our efforts were focused on mobilization combined with G-CSF in diabetic mice. To do this, LKS cells were quantified by flow cytometry [Fig 3.10].

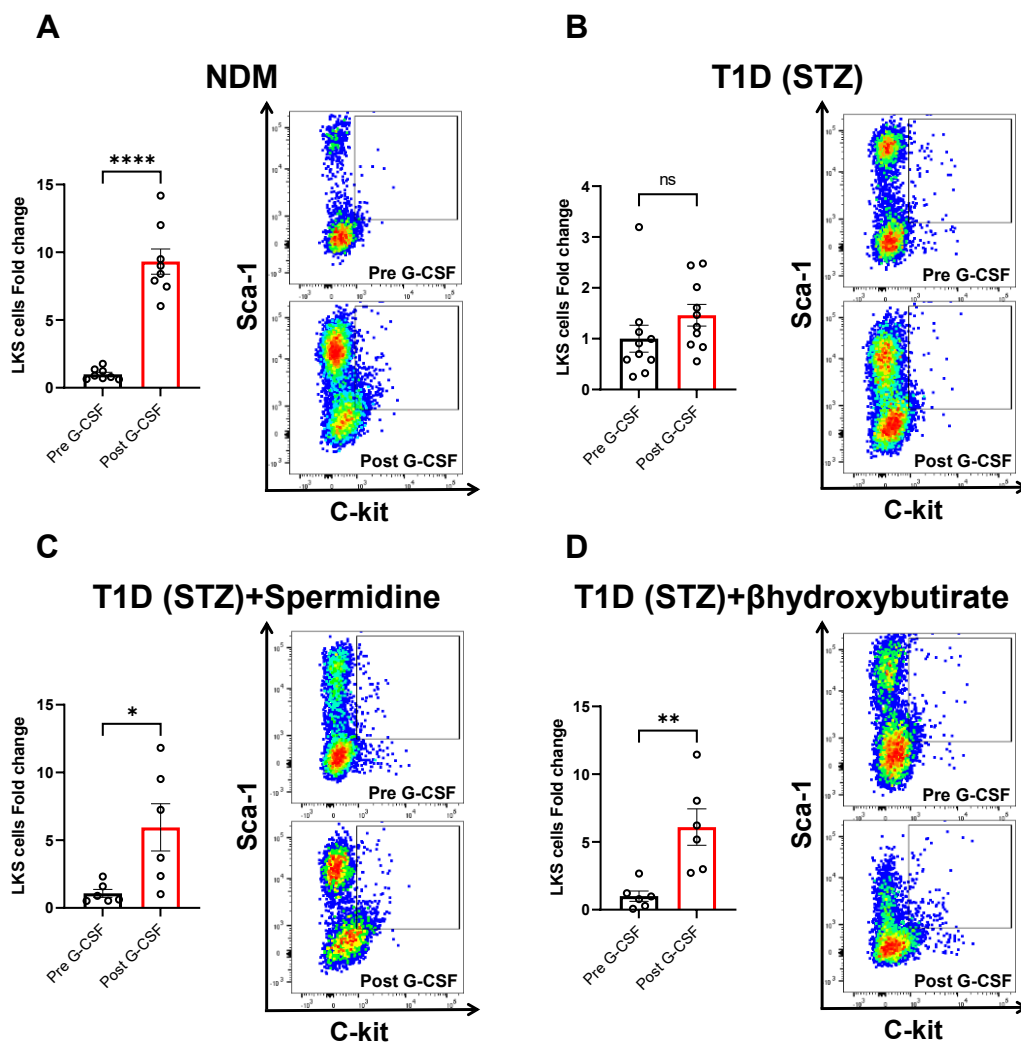


Fig. 3.10: Spermidine and β hydroxybutyrate partially restores mobilization. Each letter identifies a different condition and corresponding graphs and gating plot showing LKS cells pre and post treatment; $n \geq 6$. Statistical test: unpaired t -test. * $p < 0.05$, ** $p < 0.01$, **** $p < 0.0001$.

The effect of G-CSF in non-diabetic mice increases the number of circulating LKS (9.31 ± 0.93 fold vs Pre G-CSF, **** $p < 0.0001$) in peripheral blood while no modulation was observed in diabetic mice as expected. Both pharmacological treatments were able to partially restore mobilization (spermidine treatment: 5.95 ± 1.74 fold vs Pre G-CSF, * $p < 0.05$; β -hydroxybutyrate treatment: 6.10 ± 1.35 fold vs Pre G-CSF, ** $p < 0.01$). This suggests that the co-treatment of sp+G-CSF or β hydroxybutyrate+G-CSF was able to induce mobilization despite the diabetic phenotype.

Obtained this evidence we investigated if the circulating HSPCs mobilized in peripheral blood after G-CSF treatment were functional and able to proliferate. Thus, peripheral blood was collected for the Colony Forming Unit assay to strengthen the flow cytometry data [Fig 3.11].

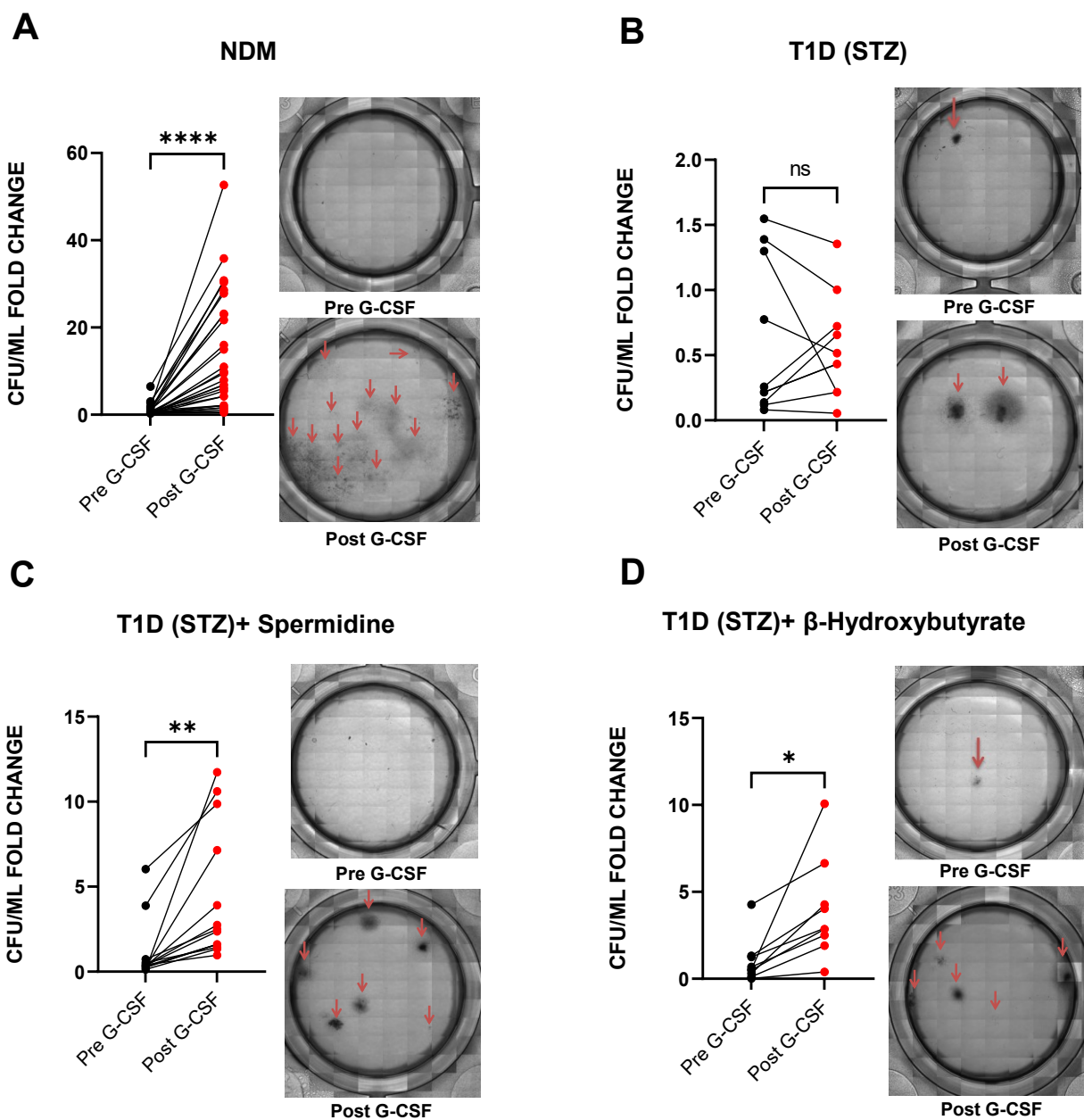


Fig. 3.11: Spermidine and β hydroxybutyrate partially restores mobilization. Each letter identifies a different condition and shows graphs and representative images showing colony forming unit pre and post treatment; $n \geq 8$. Statistical test: unpaired t-test. * $p < 0.05$, ** $p < 0.01$, **** $p < 0.0001$.

10 days after the blood seeding, we were able to see if the blood is enriched in functional HSPC by counting the colonies growth number. As expected, in non-diabetic mice the number of competent HSPCs in peripheral blood increases up to 10 fold (12.97 ± 2.42 fold vs Pre G-CSF, **** $p < 0.0001$), T1D (STZ) mice that received only G-CSF confirms the mobilization impairment and spermidine and β -hydroxybutyrate were able to partially restore the CFU amount (spermidine: 4.24 ± 1.03 fold vs Pre G-CSF, ** $p < 0.01$; β -hydroxybutyrate 3.95 ± 0.96 fold vs Pre G-CSF, * $p < 0.05$). The results obtained were exciting and corroborates our hypothesis: by giving an autophagy inducer like spermidine or an intermediate energy substrate such as β -hydroxybutyrate to diabetic mice is possible to partially replenish mobilization of functional HSPCs in peripheral blood.

G-CSF modulates autophagy-associated genes in human neutrophils *in vivo*

To understand the transcriptional modulation induced by G-CSF on human neutrophils, we retrieved available bulk- and sc-RNAseq dataset of peripheral blood neutrophils from patients treated with G-CSF ($n=18$ G-CSF patients vs $n=17$ control patients)¹²⁹. Among the numerous pathways that were regulated by G-CSF, we investigated whether autophagy was modulated in neutrophils. Firstly, we performed a Gene Set Enrichment Analysis (GSEA) on bulk RNAseq data, which can identify relevant pathways differentially modulated among experimental groups. The enrichment scoreplot for autophagy showed that treatment with G-CSF was positively correlated with the upregulation of genes associated with autophagy in neutrophils. Indeed, the Normalized Enrichment Score (NES) was = 1.65 ($p=0.01$) [Fig 3.12].

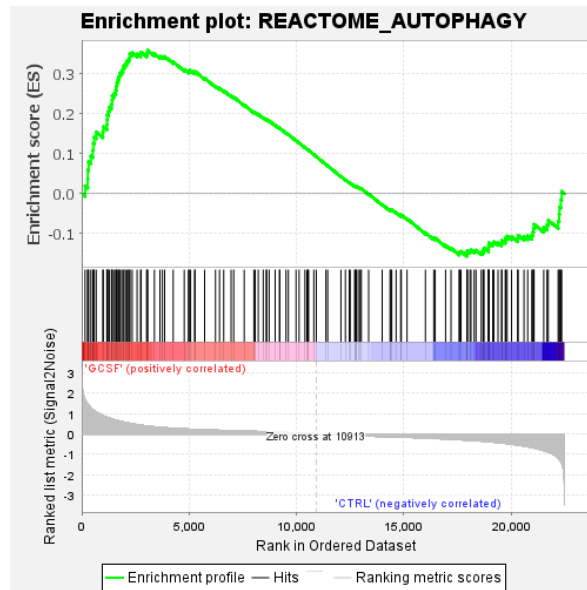


Fig. 3.12: GSEA enrichment plot related to the *REACTOME_AUTOPHAGY* signature (Number signature: *R-HSA-9612973*) in control neutrophils versus *G-CSF* treated neutrophils. NES (NORMALIZED ENRICHMENT SCORE) = 1.65 $p=0.01$.

Accordingly, hierarchical clustering of GSEA expression data of the autophagy reactome, found several genes modulated by *G-CSF*, including the upregulation of genes canonically associated with the activation of the autophagy such as *Atg7* and *Atg10*, which are involved in LC3 cleavage and conjugation with phosphatidylethanolamine⁹⁶ [Fig 3.13 A, B]. Despite a general upregulation of several genes within the autophagy reactome, we found that some genes were not modulated or are instead downregulated, such as *Ulk1*, which is important for the autophagy induction, and *Map1lc3b* (hereafter simply called *Lc3*) involved in the autophagosome formation. We have hypothesized that the induction of autophagy requires a continuous recycling and reuse of some of its components, and transcriptional upregulation of the gene might not be correlate with the activity of such proteins¹⁰² [Fig 3.13 B].

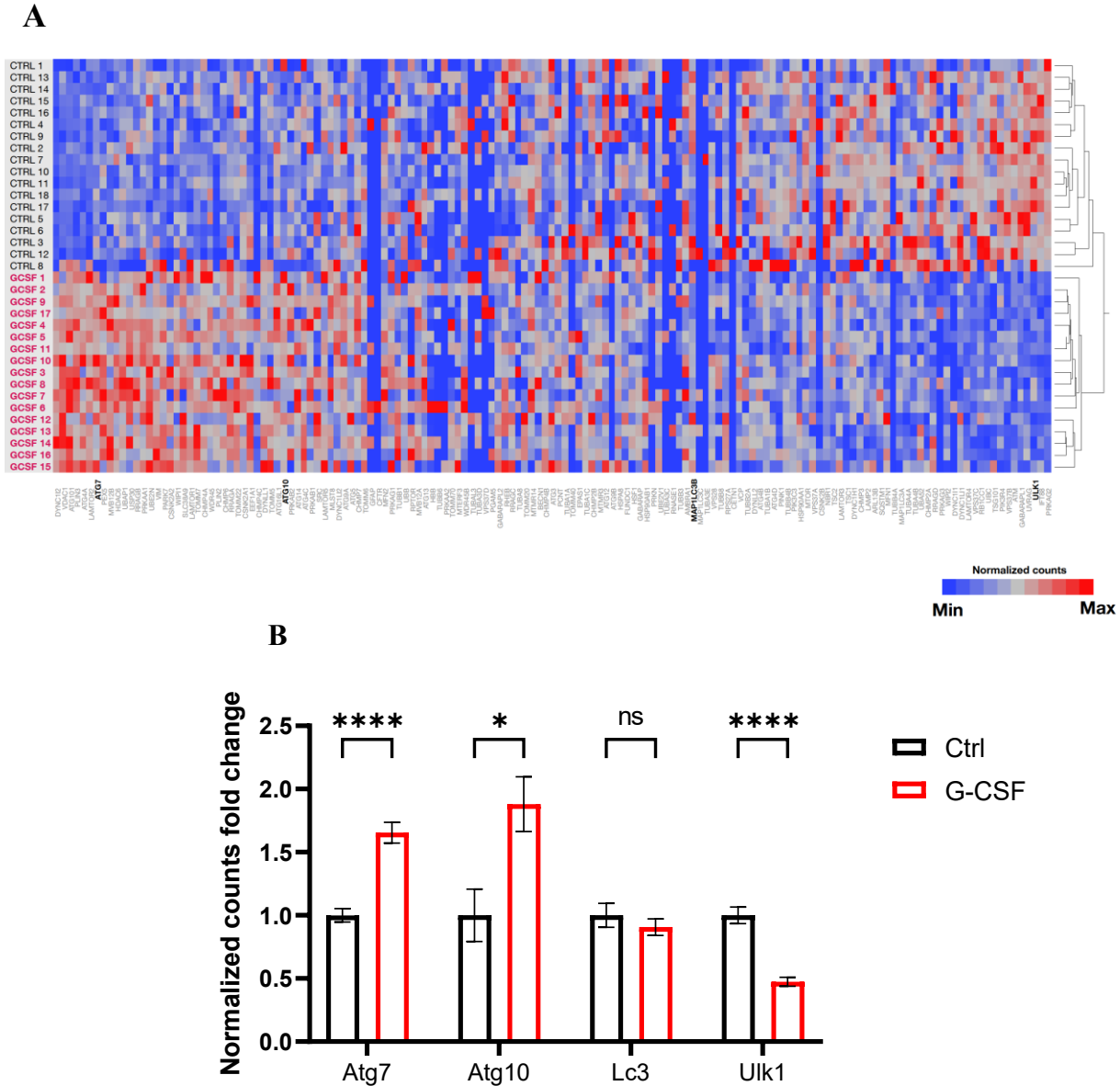
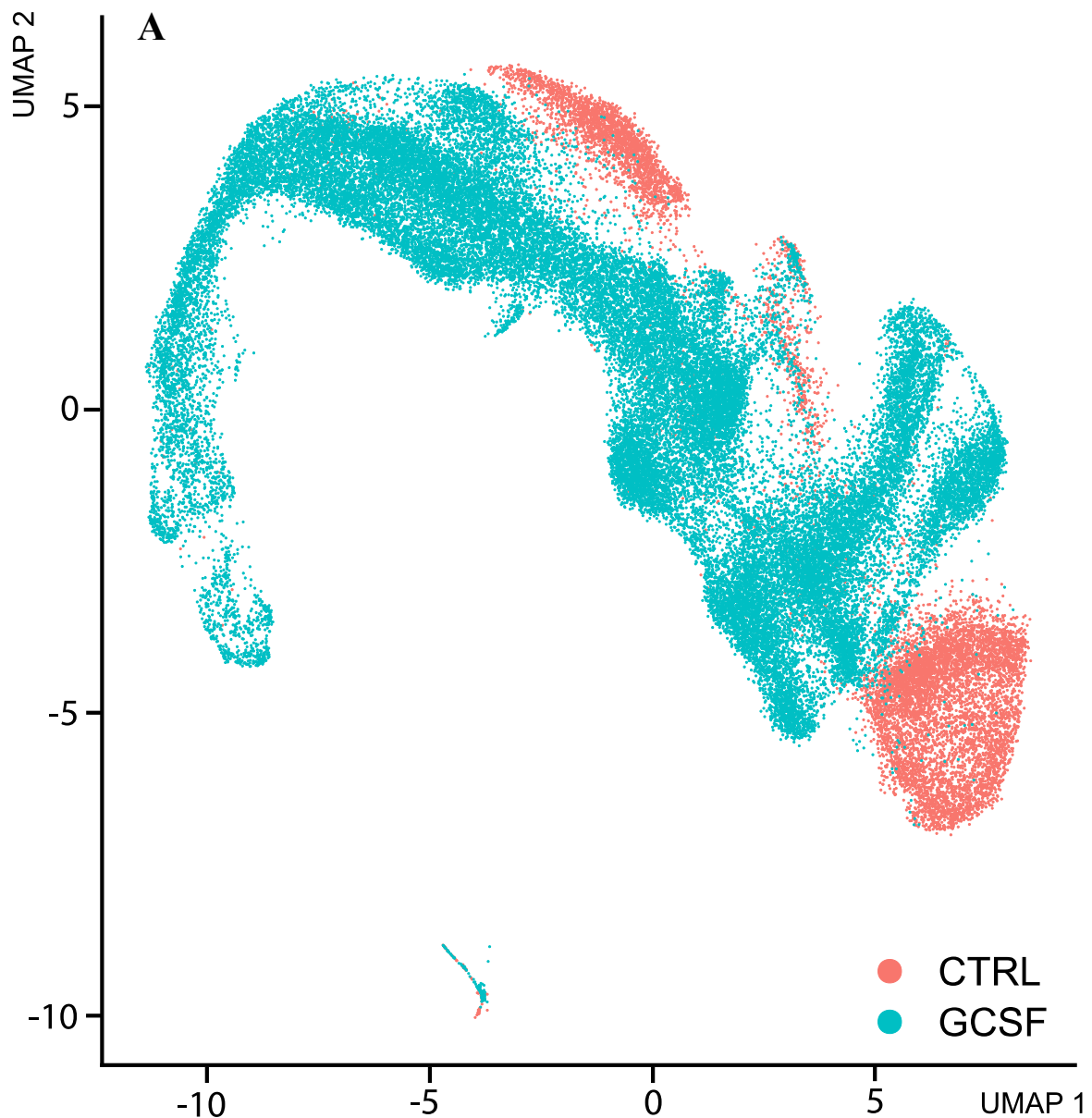


Fig. 3.13: G-CSF modulates the autophagy reactome in human neutrophils. *A*: heatmap plot of normalized gene expression of the REACTOME_AUTOPHAGY signature of untreated (Ctrl) versus G-CSF treated neutrophils displays the minimum value and red the maximum for each gene). *B*: Normalized reads count fold change of some autophagy related genes. Control $n=18$, G-CSF $n=17$. Statistical test: multiple t -test with Holm-Sidak multiple comparisons test. $*p<0.05$, $****p<0.0001$.

Single cells RNA sequencing (Sc-RNAseq) expanded our knowledge cellular identities and transcriptional programs within a heterogenous population as it allows to quantify gene expression of a single cell within a complex matrix or a sorted population, and it is possible to cluster them according to their transcriptomic profile. This is particularly important during a pharmacological treatment as we can appreciate whether the drug has similar effects among all the cells that we analyze. By employing a dimensionality reduction approach via the algorithm UMAP (Unifold

Manifold Approximation and Projection) we can generate graphs showing single cell distribution according to their transcriptomic profile¹²⁹. As expected, G-CSF treatment (N=4) resulted in transcriptional changes yielding separate clusters from neutrophils of control subjects (N=2) [Fig 3.14 A]. To have further insight about the transcriptional effects on neutrophils responding to G-CSF, we used a trajectory analysis model to trace a path among the cells projecting a trajectory based on the quantitative transcriptional divergence, which is referred as pseudotime, from a common starting point¹⁴³. We have manually set the root nodes within the clusters of neutrophils from control subjects. From these root nodes, the pseudotime graph reveal us that from control groups (1-2) the trajectories both converge towards the point 3 [Fig. 3.14 B], suggesting a common differentiation pattern after G-CSF treatment.



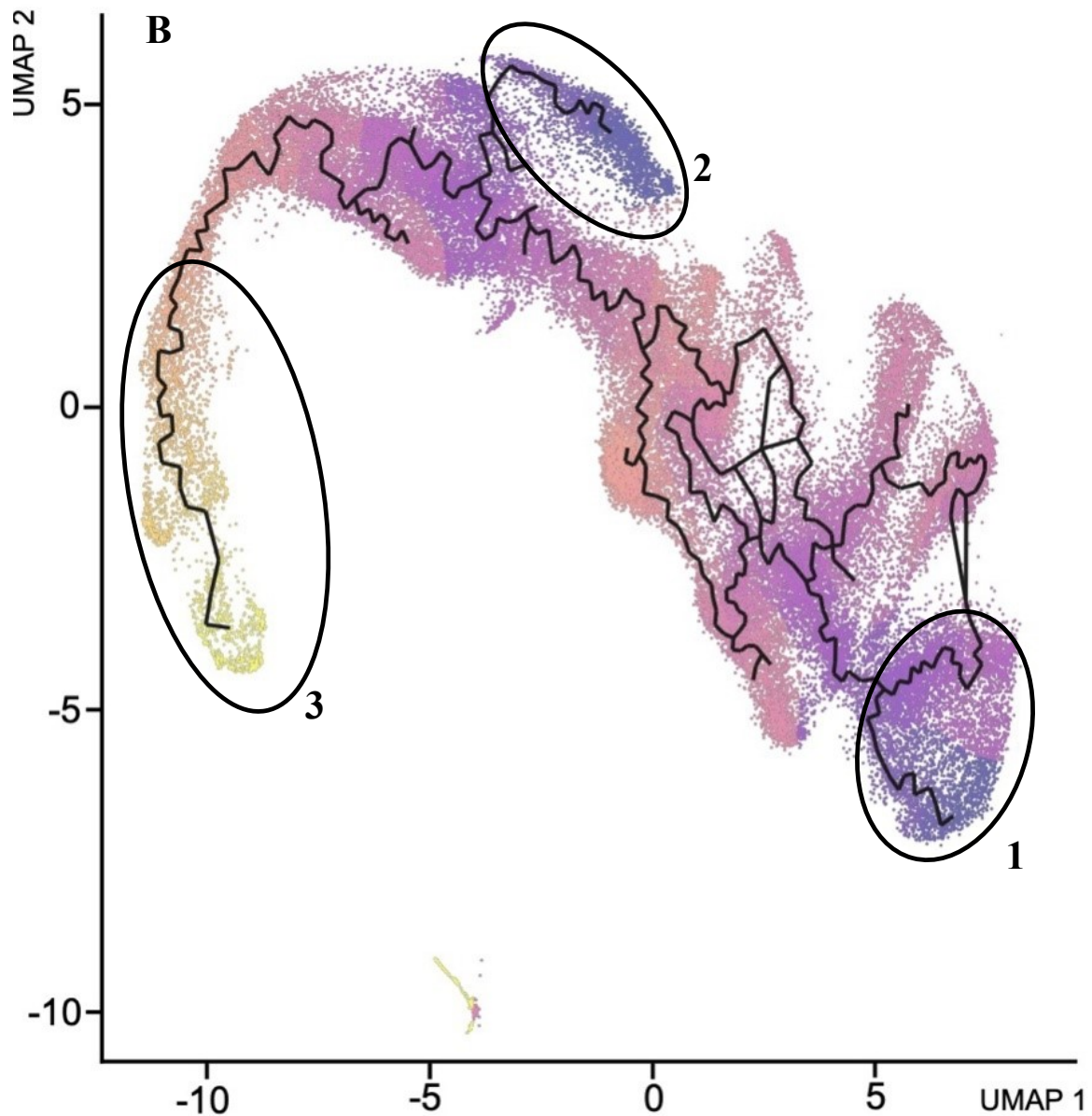
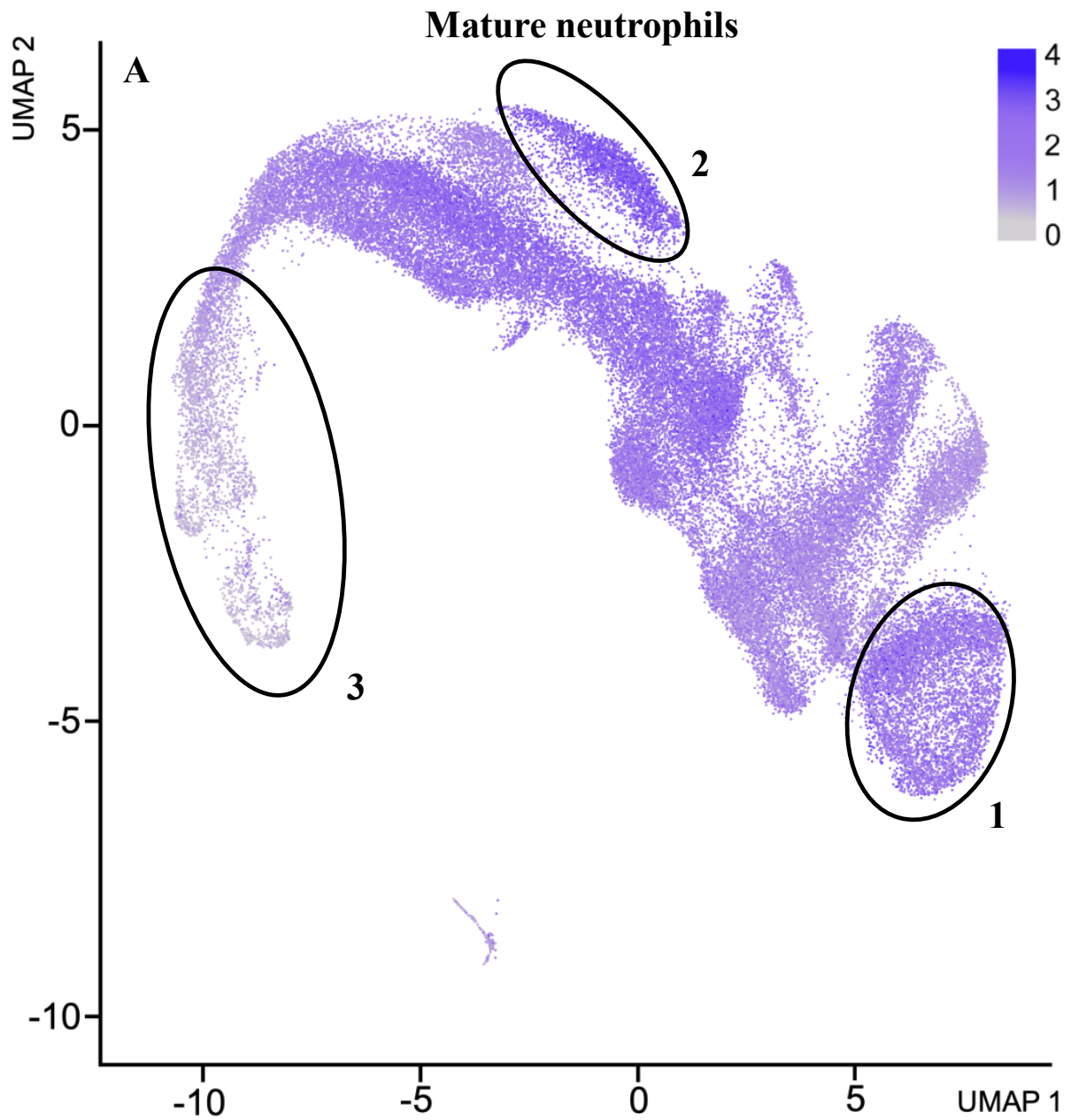


Fig. 3.14: UMAP dimensionality reduction plots for sorted neutrophils samples displaying that G-CSF treatment modifies neutrophils' single cell distribution. **A:** Single cell distribution according to their transcriptomic profile. **B:** single cells transcriptomic divergences visualized by pseudotime graph. Point 1 and 2 represents control clusters chosen as root nodes. Point 3 represents the cluster with the most transcriptomic differences from the root nodes. Ctrl N=2, G-CSF N=4.

Next, we aim to understand the transcriptional identity of the population represented in the subcluster 3 present at the convergence of pseudotime path. It is known that G-CSF activates granulopoiesis, leading to an increased number of immature neutrophils in the peripheral

circulation¹⁴⁴. Thus, using a transcriptomic signature of immature neutrophils¹³⁰, we checked whether we can discriminate for the presence of neutrophils at different maturation stages [Fig. 3.15 A, B].



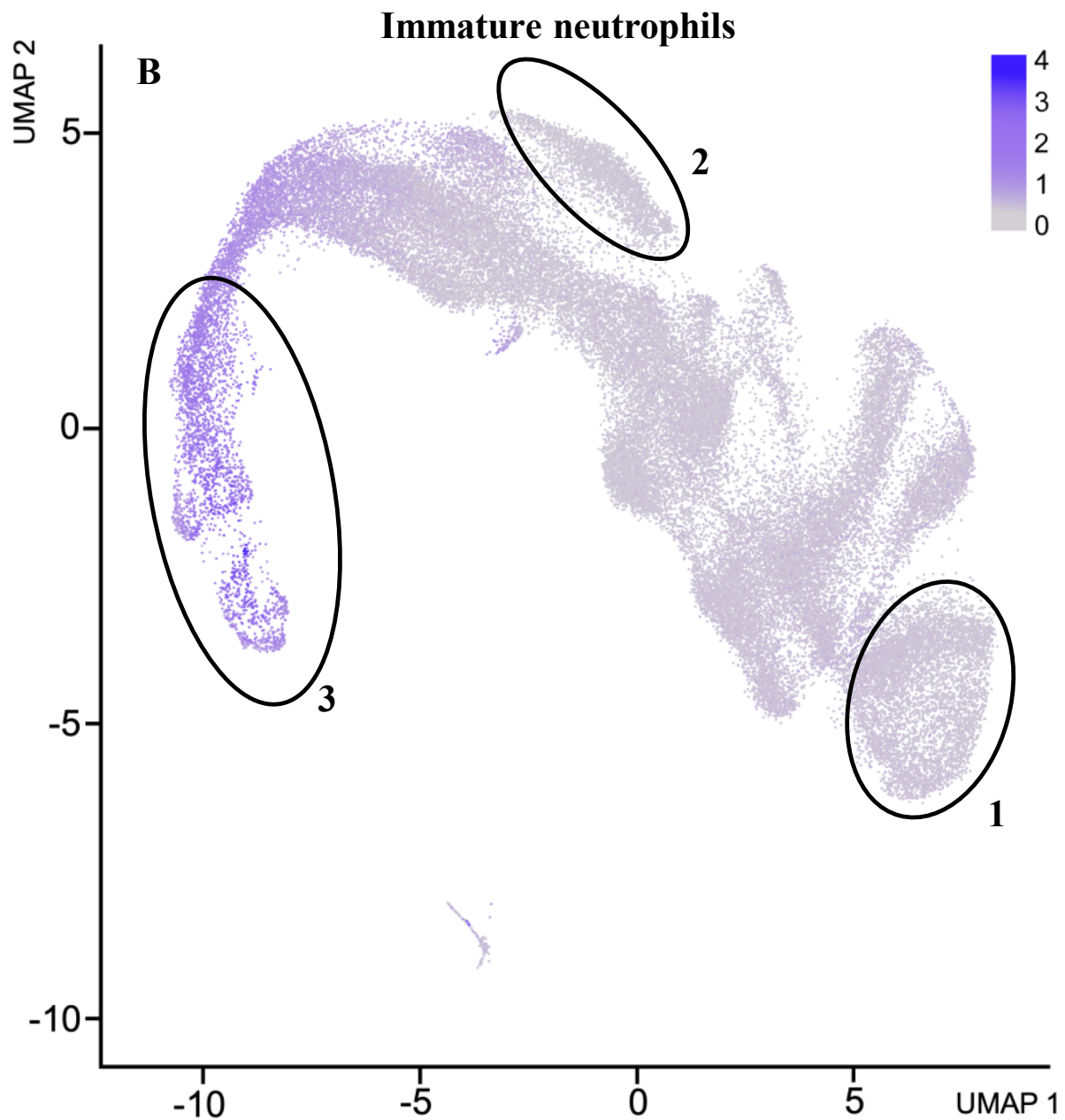
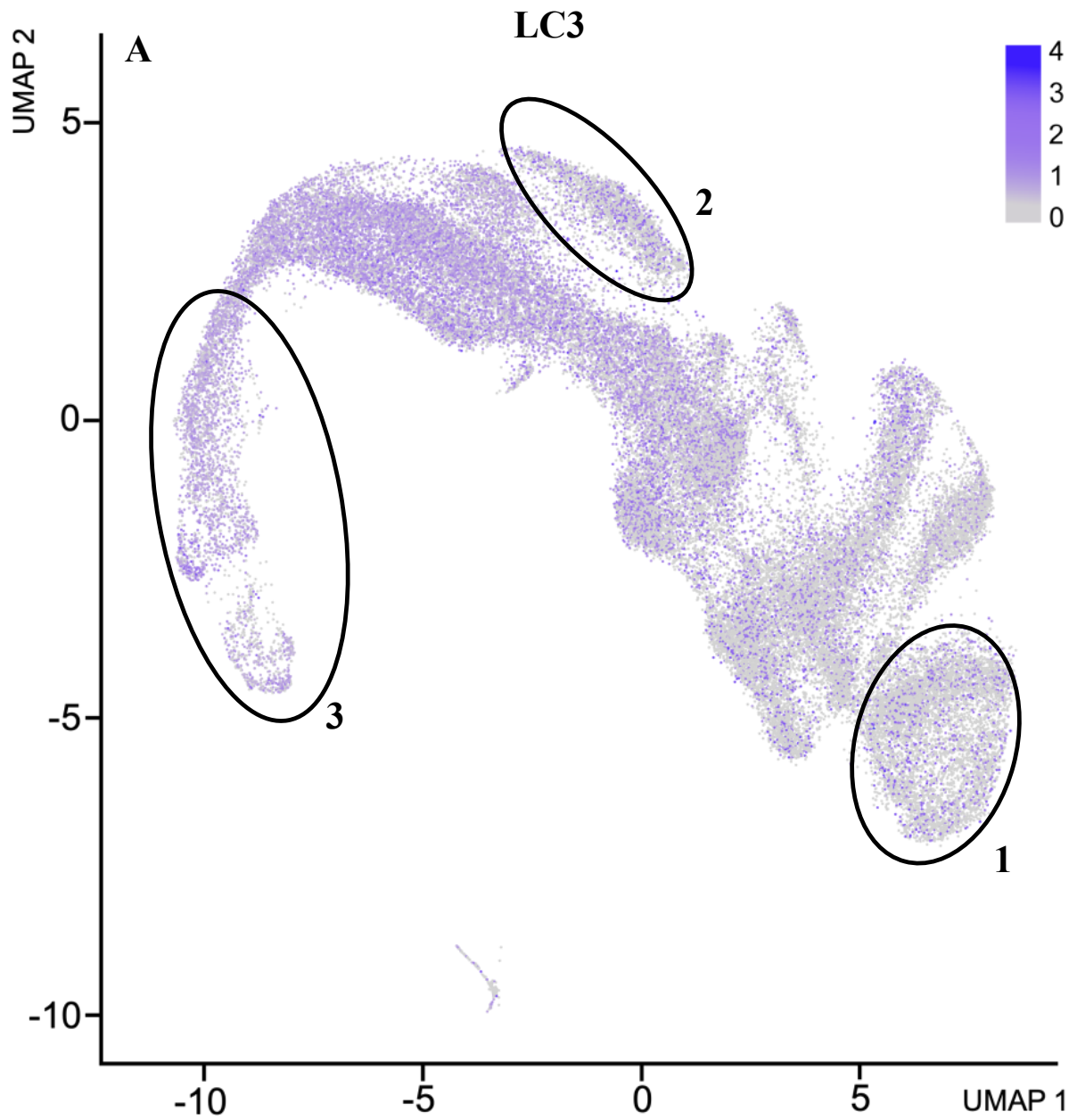
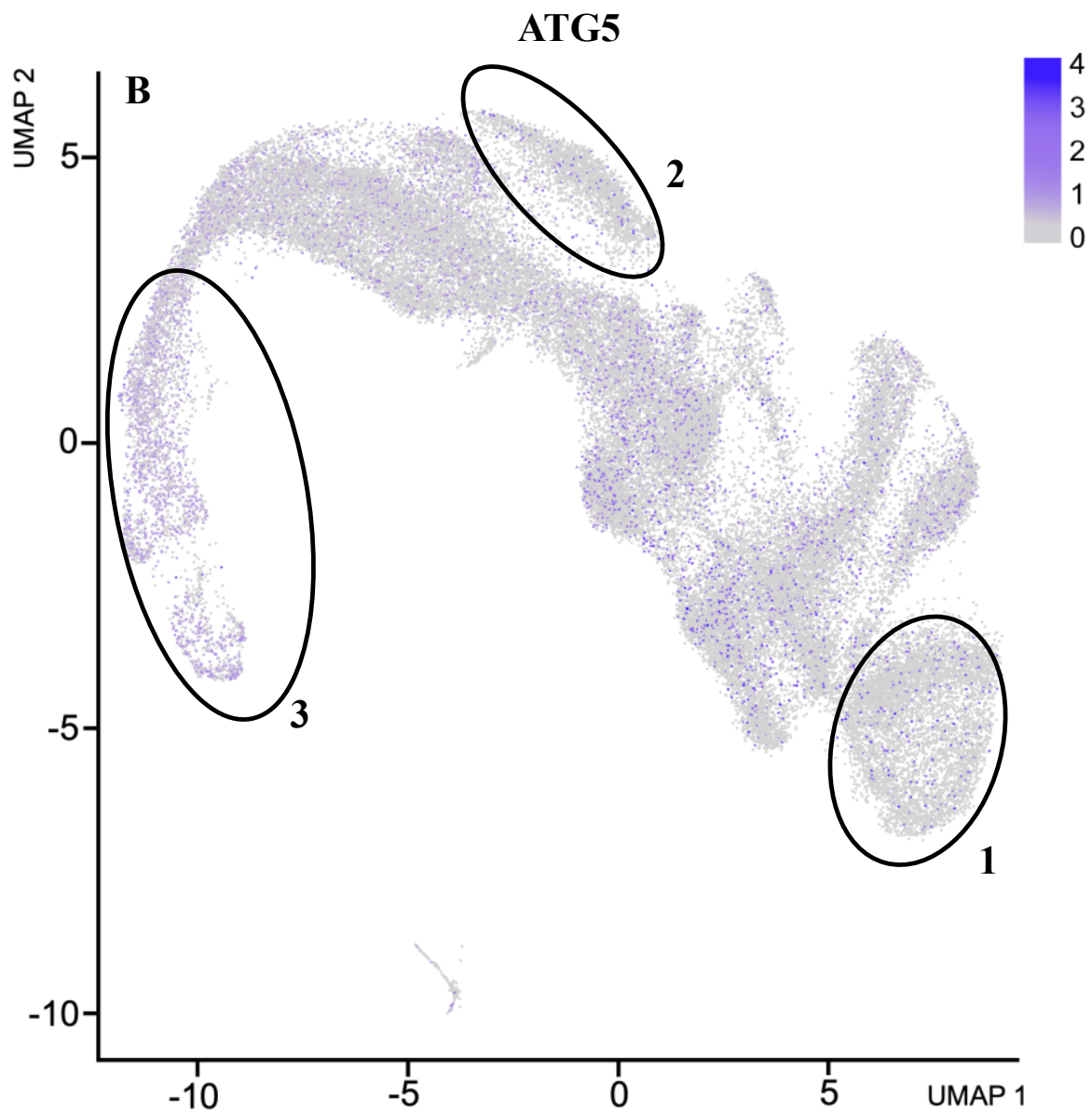


Fig. 3.15: UMAP dimensionality reduction plots showing that mature and immature transcriptomic profile diverges from control clusters to G-CSF treated clusters. Figure A shows upregulated genes in mature neutrophils, figure B shows upregulated genes in immature neutrophils. The G-CSF cluster 3 can be identified as immature neutrophils.

Using this approach, we found that cells in cluster 3 can be deemed as immature neutrophils according to their transcriptomic profile, while most of the other cells belonging to the control group and in the G-CSF group shared more similarity with a mature phenotype [Fig 3.15 A, B].

Neutrophil differentiation requires the critical modulation of metabolism that switch from glycolysis to lipolysis, that is regulated by autophagy¹¹⁹. Therefore we wanted to asses if the gene expression of *Lc3*, *Atg5* and *Atg7*, which are widely used to evaluate the autophagy modulation^{57,111,118}, were upregulated and in which clusters [Fig 3.16 A, B, C].





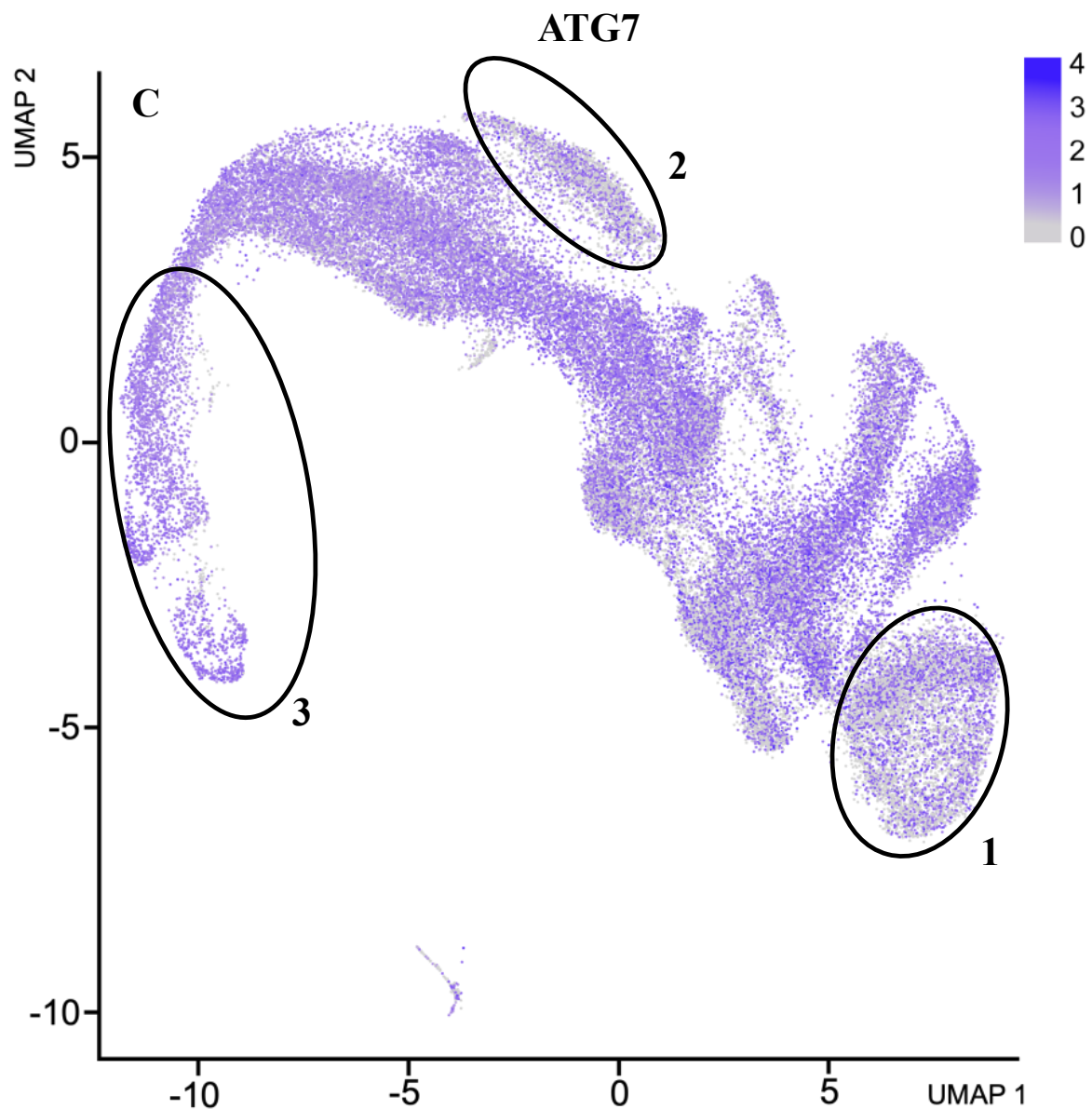


Fig. 3.16: UMAP dimensionality reduction plots for sorted neutrophils showing Autophagy related genes transcriptomic differences. A/B: Both Lc3 and Atg5 are more expressed in immature neutrophils. C: Atg7 is expressed widely in G-CSF treated population compared with control clusters.

Once plotted it was clear that these genes were upregulated in G-CSF treated clusters, but in particular the cluster previously identified as immature neutrophils, was mostly affected compared to the root nodes, suggesting that autophagy upregulation among neutrophil differentiation process is more evident during the early stages of differentiation, according to the literature^{116,118}. Moreover the gene expression of these three genes presents some differences: while Atg5 and Lc3 are clearly

upregulated in immature neutrophils rather than mature neutrophils, due to the downregulation of autophagy in late stages of neutrophil differentiation¹¹⁹, Atg7 is also expressed within all the G-CSF treated clusters, probably due to its role in non-autophagic processes, in particular is known to repress Caspase 9, inhibiting apoptosis¹⁴⁵. These evidences corroborate previous findings which showed that autophagy in neutrophils was modulated after G-CSF in humans⁵⁷.

4. DISCUSSION

Diabetic stem cell mobilopathy results in a low response to G-CSF, leading to an impaired release of CD34⁺ cells that could contribute to maintaining endothelial homeostasis and preventing ischemic injuries¹³. The mechanisms underlying diabetic mobilopathy, however, are still poorly investigated and understood. With this research project, we aimed to address the role of macroautophagy, a highly conserved mechanism for cellular homeostasis and survival, in the onset of diabetic stem cell mobilopathy. It is known that BM remodeling in response to G-CSF leads to an elevated energy request from endothelial and granulocytes to cope with the increased proliferation of hematopoietic progenitors and neutrophils¹⁴⁶, thus we hypothesized that BM cells should require autophagy to deal with increased proliferative stress⁵⁷.

We have shown for the first time that in diabetic mice suffer from mobilopathy is linked to impaired autophagy modulation in neutrophils. These findings highlight the critical role of autophagy in the G-CSF mechanism of action. We have also shown that restoring autophagy with spermidine or supplying β -hydroxybutyrate can effectively restore mobilization in diabetic mice.

By assessing the modulation of autophagy-related genes in mice after G-CSF treatment, we have observed a diverging response of unfractionated BM population compared to neutrophils. While unfractionated bone marrow showed a response to G-CSF that was suggestive of induction of autophagy, we were not able to observe any modulation in bone marrow isolated neutrophils, in contrast with the literature findings⁵⁷. This experiment, and the existing literature, provide us two different hints: the first one is that G-CSF-derived autophagy modulation could affect other cell types besides neutrophils, such as hematopoietic stem cells⁵⁷, Tcells¹³², and macrophages¹³¹, explaining the autophagy-related genes upregulation in total bone marrow mRNA; the second one is that we may not be able to see any differences in isolated neutrophils due to the known low transcriptomic activity of these cells¹⁴⁷. For example, Wong and colleagues have demonstrated how intron retention is widely used during granulopoiesis to reduce the mRNA content, especially in mature neutrophils¹⁴⁸, suggesting that neutrophils tightly regulates mRNA amount during their differentiation. We concluded that a more sensitive approach, such as scRNAseq, possibly couple with ATAC-seq, could be more useful to evaluate the transcriptomic activity in neutrophils. However, the western blot analysis confirms that ATG5 and LC3 were significantly upregulated after G-CSF. It should be noted that the absence of modulation in transcriptomic profile does not necessarily mean the absence in protein modulation^{135,149–151}. Furthermore, during autophagic flux, these two proteins are continuously recycled and reused: in particular ATG4 deconjugates LC3

from PE, resulting in LC3 recycling¹⁵²⁻¹⁵⁴, and also the ATG5-ATG12 complex is detached from the late autophagosome to being reused^{155,156}, therefore transcript upregulation could be not required for the maintenance of autophagy.

While this experiment presents some limitations because the lacking of a strategy to block the autophagy flux¹⁰², the results were robust and consistent and prompted us to investigate further if autophagy was upregulated in response to G-CSF.

We chose to assess autophagy flux by imaging flow cytometry for its capability to couple flow cytometric analysis on a single cell level with the capability to capture high-resolution images and perform statistical analysis. Furthermore, the instrument is particularly suited to quantify LC3 punctae using the GFP-LC3 mouse model¹⁵⁷.

G-CSF promotes neutrophils expansion¹⁴⁴, and autophagy is necessary for mature neutrophil differentiation¹¹⁸, as evidenced by GFP-LC3 *punctae* increasing both *in vitro* and *ex vivo* in G-CSF treated neutrophils. Using chloroquine, a drug that inhibits autophagy by acting on lysosome pH¹⁵⁷, we have observed a further increase in GFP-LC3 punctae both in control and G-CSF-treated mouse neutrophils, confirming that G-CSF do increase autophagy in neutrophils. However, we observed an increase in the number of punctae in control neutrophils after chloroquine treatment confirm previous literature observations⁵⁷ and suggesting that autophagy might be active also in mature neutrophils, despite being post mitotic cells with a low metabolic rate¹⁵⁸.

It has been recently shown that neutrophils from T1D rats show impaired autophagy in response to inflammatory activation¹²⁴. The authors proposed that impaired autophagy was due, at least in part, to glucose overload due to hyperglycemia, which induced overactivation of mTOR and the subsequent autophagy inhibition¹²⁴. Stemming from the observation that autophagy is activated in neutrophils after G-CSF, we wondered if unresponsiveness to G-CSF in diabetic mice was due to an impaired autophagy induction in neutrophils. Our imaging flow cytometry results strongly showed an impaired modulation of autophagy in T1D STZ mice neutrophils after G-CSF treatment. The autophagy defect in neutrophils of diabetic mice raises questions about the importance of this catabolic pathway in G-CSF mechanism of action. During their differentiation, neutrophil progenitors, in particular myeloblasts and myelocytes, preferentially use oxidative phosphorylation for their differentiation. Free fatty acids generated through lipophagy are subsequently processed through mitochondrial β /oxidation to support TCA cycle and subsequent OXPHOS¹¹⁹. Given the metabolic constrain imposed by the harsh diabetic environment we still don't know if the defect of autophagy after G-CSF is linked to a potential defect of lipophagy, or in lipid droplets

accumulation. Nevertheless, diabetes is known to trigger myelopoiesis leading to an exaggerated production of neutrophils and inflammatory monocytes⁷². The role of autophagy and lipophagy in this context is still unknown.

To attempt to restore impaired autophagy in diabetic mice neutrophils we opted for using spermidine, a polyamine that induces autophagy by inhibiting mTOR and the acetyltransferase EP300, two of the major inhibitors of the autophagy pathway^{140,141}. The spermidine choice was supported by literature evidences that show spermidine as safe in humans and mice, both in pathological and non-pathological condition^{159–161}. We have decided to not induce autophagy through fasting in diabetic mice due to the potential detrimental effect of starvation on a frail phenotype such as the streptozotocin-induced diabetic mice. Furthermore, this approach could be difficult to translate into humans, as the extent of starvation need to activate autophagy could be too extreme. After the treatment, increased levels of spermidine were detectable in plasma, confirming the bioavailability of the molecule, as recently evidenced¹⁶². While spermidine alone was not effective in triggering mobilization, suggesting that autophagy induction could be necessary but not sufficient, the combination of G-CSF and spermidine was also able to replenish autophagy in neutrophils from diabetic mice and a partial mobilization, without reducing blood glucose levels. Besides the striking evidence of autophagy induction in neutrophils, spermidine is also known to reduce inflammation by reducing IL-1 β ^{163,164}. Furthermore, spermidine upregulates SIRT1/PGC1 α pathway, an important regulator of mitochondrial biogenesis¹⁶⁵. We know that SIRT1 is deregulated in the bone marrow of diabetic mice⁶⁷, we could speculate that spermidine could synergistically act on autophagy modulation, chronic inflammation reduction and mitochondrial homeostasis. We will further investigate the spermidine role in G-CSF induced mobilization in the upcoming experiments.

In T1D, glucose metabolism of both insulin-dependent and independent tissues is severely impaired⁶. Through ketogenesis, the liver metabolizes fatty acids to ketone bodies, such as β -hydroxybutyrate, acetone, and acetoacetate, to be used as an energy source during glucose shortage¹⁶⁶. Although the liver is the primary sites of ketone production, other tissues and cells, such as kidneys, astrocytes and intestinal crypts, can also perform ketogenesis^{167–169}. Recently, Zhang and colleagues have evidenced the crucial role in ketogenesis in CD8 T-cells memory development¹⁷⁰, suggesting that ketogenesis may be used in other cell types beyond liver. Furthermore, SGLT2 inhibitors are known to improve, glucose control and vascular repair and ketogenesis⁸⁴. The ketone bodies role in neutrophils is poorly investigated but a recent work suggest

that β -hydroxybutyrate reduces NLRP3 inflammasome activation in aged neutrophils during gout¹⁷¹.

These evidences prompted us to use β -hydroxybutyrate possibly as an alternative metabolic intermediate for diabetic mice to compensate the glucose-related metabolism. The ketone body consumption in T1D STZ mice during the treatment was confirmed by blood ketone measurements. Akin to spermidine, β -hydroxybutyrate alone is not sufficient for mobilization but it can restore partially mobilization.

Spermidine and β -hydroxybutyrate are likely two sides of the same coin: spermidine could be able to restore lipid droplet degradation through lipophagy, to provide free fatty acid for TCA cycle and the subsequently correct neutrophils differentiation¹¹⁹. On the other hand, we were also able to improve mobilization without targeting the autophagy pathway directly by providing β -hydroxybutyrate, which could be used without the autophagy mediation for the TCA cycle and subsequent oxidative phosphorylation¹⁷². We want in future study if the combination of spermidine and β -hydroxybutyrate during G-CSF treatment could have a synergistic effect,; while spermidine is able to induce autophagy, β -hydroxybutyrate could give an additional energy substrate, ameliorating both the metabolic and catabolic processes during diabetes and boosting the G-CSF treatment.

This project presents some limitations: due to the lack of a genetic model of autophagy inhibition, we cannot assess if spermidine is able to restore mobilization through autophagy modulation. To do this we are going take advantage of $Atg5^{flox/flox}Lyz2^{cre/cre}$ mouse model, which presents an autophagy defect in monocytes, macrophages and neutrophils. These mice were kindly donated by Prof. Hans Uwe Simon (University of Bern, Switzerland) and are now available and bred at the VIMM. By using this model, we will hope to provide a causal link the autophagy defect with impaired mobilization. Furthermore, it has been observed that spermidine induces lipolysis in HFD treated mice¹⁷³, thus evaluating the role of spermidine in diabetic lipid metabolism could be an interesting research direction. We also don't know yet if β -hydroxybutyrate is able to restore autophagy flux, so in future we want to use imaging flow cytometry to investigate its role within the autophagic pathway.

As a model of type 1 diabetes, we have used streptozotocin to induce hyperglycemia in mice. Streptozotocin is a chemical compound known to disrupt the pancreatic beta cells causing insulin deficiency¹²⁸. Mice treated with this drug show the same complications of an uncompensated patient with diabetes: polyuria, polydipsia, weight loss, hyperglycemia and hematopoietic

abnormalities, including mobilopathy⁸⁷. Despite this model is widely used for diabetes studies, some aspects should be considered during the experiments, such as the variability of diabetes severity between treated mice and the eventual regeneration of pancreatic beta cells¹⁷⁴. In this project these two aspects were at least in part balanced by using age/sex matched mice and by monitoring glycemia overtime, discarding the non-hyperglycemic mice. We acknowledge that weight loss due to lipodystrophy and muscle cachexia could represent potential biases as it could impinge on BM cell biology. However, treatments to constrain the severity of the model, such as moderate insulin injections or low-dose streptozotocin protocols, could not yield a sufficient degree of mobilopathy or BM remodelling.

Despite the result in reverting mobilopathy by modulating or bypassing autophagy, we still lack a mechanistic explanation, which will be subject of further investigation. To this aim, we want also to explore the possible role of lactate in linking impaired mobilization with autophagy in diabetes. Mature neutrophils show a metabolic shift from oxidative phosphorylation to glycolysis¹⁵⁸, which results in the production of lactate that is crucial for the HSCs mobilization^{175,176}. We could speculate that in the contest of diabetes the increased glucose flux might derange lactate production. Indeed, some evidences show the reduction in lactate production during diabetes^{177,178}. Whether spermidine and β -hydroxybutyrate-derived mobilization improvement could also affect the lactate production or modulation by improving glucose metabolism in neutrophils will be subject of investigation.

Finally, bulk RNAseq and single-cell RNAseq data analysis on human neutrophils confirmed that autophagy is modulated after G-CSF. In particular, we have observed that immature neutrophils shows a marked activation of a transcriptomic signature indicative of increased autophagy, compared to more mature neutrophils¹¹⁸. Furthermore, a recent study has assessed how G-CSF modify the systemic metabolomic profile in healthy humans. Free fatty acids were among the metabolites increased in serum after G-CSF¹⁷⁹, which could prompt the investigation for lipid metabolism of diabetic neutrophils as a potential mechanism to link autophagy with mobilization.

Beyond mobilization, diabetes, and specifically hyperglycemia, prompt neutrophils to undergo NETosis, encompassing massive nuclear remodeling culminating in the release of neutrophil extracellular traps (NETs), composed of sticky chromatin decorated with enzymes and other cellular proteins³⁶. NETosis aids the clearance of infectious agents, but an exaggerated release of NETs can damage tissues and propagate inflammation^{180,181}. Although the role of autophagy in the onset of NETosis is controversial^{182,183}, deregulation of NETosis and autophagy could be the touchstone of the profound remodeling characterizing the bone marrow in diabetes.

While diabetes is known to impair autophagy in several tissues in humans^{184,185}, the role of impaired autophagy in diabetic neutrophils is still an unexplored field. Once we can confirm the correlation between neutrophils' impaired autophagy and mobilopathy in human neutrophils, it would be intriguing to assess the effects of spermidine and β -hydroxybutyrate in patients with diabetes as these two molecules, which already shows anti-aging effects^{140,161,186,187}, are commonly used as food supplements. Beyond G-CSF, restoring mobilization in patients with diabetes might also revert other structural and functional alteration of the bone marrow such as the reduction of circulating levels of HSPCs and exacerbated myelopoiesis⁷⁴. Indeed, by replenish the correct HSPCs trafficking we may be able to recover endothelial dysfunction and CVD, reducing the detrimental effect of diabetes on vascular system.

5. BIBLIOGRAPHY

1. American Diabetes Association. Diagnosis and Classification of Diabetes Mellitus. *Diabetes Care* **37**, S81–S90 (2013).
2. Global report on diabetes: Executive Summary. <https://www.who.int/publications-detail-redirect/who-nmh-nvi-16.3>.
3. Knip, M. & Siljander, H. Autoimmune mechanisms in type 1 diabetes. *Autoimmun. Rev.* **7**, 550–557 (2008).
4. Narayan, K. M. V. *et al.* Diabetes: The Pandemic and Potential Solutions. in *Disease Control Priorities in Developing Countries* (eds. Jamison, D. T. *et al.*) (The International Bank for Reconstruction and Development / The World Bank, 2006).
5. Christ, A. & Latz, E. The Western lifestyle has lasting effects on metaflammation. *Nat. Rev. Immunol.* **19**, 267–268 (2019).
6. Seshasai, S. R. K. *et al.* Diabetes mellitus, fasting glucose, and risk of cause-specific death. *N. Engl. J. Med.* **364**, 829–841 (2011).
7. Fadini, G. P., Albiero, M., Bonora, B. M. & Avogaro, A. Angiogenic Abnormalities in Diabetes Mellitus: Mechanistic and Clinical Aspects. *J. Clin. Endocrinol. Metab.* **104**, 5431–5444 (2019).
8. Simó, R., Carrasco, E., García-Ramírez, M. & Hernández, C. Angiogenic and antiangiogenic factors in proliferative diabetic retinopathy. *Curr. Diabetes Rev.* **2**, 71–98 (2006).
9. Catrina, S.-B. & Zheng, X. Disturbed hypoxic responses as a pathogenic mechanism of diabetic foot ulcers. *Diabetes Metab. Res. Rev.* **32 Suppl 1**, 179–185 (2016).
10. Nakagawa, T., Kosugi, T., Haneda, M., Rivard, C. J. & Long, D. A. Abnormal angiogenesis in diabetic nephropathy. *Diabetes* **58**, 1471–1478 (2009).
11. Purushothaman, K.-R. *et al.* Inflammation, neovascularization and intra-plaque hemorrhage are associated with increased reparative collagen content: implication for plaque progression in diabetic atherosclerosis. *Vasc. Med. Lond. Engl.* **16**, 103–108 (2011).

12. Cameron, N. E., Eaton, S. E., Cotter, M. A. & Tesfaye, S. Vascular factors and metabolic interactions in the pathogenesis of diabetic neuropathy. *Diabetologia* **44**, 1973–1988 (2001).
13. DiPersio, J. F. Diabetic stem-cell ‘mobilopathy’. *N. Engl. J. Med.* **365**, 2536–2538 (2011).
14. Dealing with Diabetic Wounds: Causes, Symptoms, and Treatment.
<https://www.v3biomedical.com/post/dealing-with-diabetic-wounds-causes-symptoms-and-treatment>.
15. Nombela-Arrieta, C. & Manz, M. G. Quantification and three-dimensional microanatomical organization of the bone marrow. *Blood Adv.* **1**, 407–416 (2017).
16. Lucas, D. Structural organization of the bone marrow and its role in hematopoiesis. *Curr. Opin. Hematol.* **28**, 36–42 (2021).
17. Eliasson, P. & Jönsson, J.-I. The hematopoietic stem cell niche: Low in oxygen but a nice place to be. *J. Cell. Physiol.* **222**, 17–22 (2010).
18. Li, Z., Hardij, J., Bagchi, D. P., Scheller, E. L. & MacDougald, O. A. Development, regulation, metabolism and function of bone marrow adipose tissues. *Bone* **110**, 134–140 (2018).
19. Zanetti, C. & Krause, D. S. “Caught in the net”: the extracellular matrix of the bone marrow in normal hematopoiesis and leukemia. *Exp. Hematol.* **89**, 13–25 (2020).
20. Hynes, R. O. The extracellular matrix: Not just pretty fibrils. *Science* **326**, 1216–1219 (2009).
21. Verma, D. & Krause, D. S. Chapter Seven - Targeting the Bone Marrow Niche in Hematological Malignancies. in *Advances in Stem Cells and their Niches* (ed. Bonnet, D.) vol. 1 155–175 (Elsevier, 2017).
22. Hoffman, R. & Marcellino, B. K. Bone Marrow Microenvironment in Health and Disease. in *Encyclopedia of Bone Biology* (ed. Zaidi, M.) 1–11 (Academic Press, 2020). doi:10.1016/B978-0-12-801238-3.11195-X.
23. Fadini, G. P., Ferraro, F., Quaini, F., Asahara, T. & Madeddu, P. Concise Review: Diabetes, the Bone Marrow Niche, and Impaired Vascular Regeneration. *Stem Cells Transl. Med.* **3**, 949–957 (2014).

24. Lo Celso, C. *et al.* Live-animal tracking of individual haematopoietic stem/progenitor cells in their niche. *Nature* **457**, 92–96 (2009).
25. Taichman, R. S., Reilly, M. J. & Emerson, S. G. Human osteoblasts support human hematopoietic progenitor cells in vitro bone marrow cultures. *Blood* **87**, 518–524 (1996).
26. Sugiyama, T., Kohara, H., Noda, M. & Nagasawa, T. Maintenance of the hematopoietic stem cell pool by CXCL12-CXCR4 chemokine signaling in bone marrow stromal cell niches. *Immunity* **25**, 977–988 (2006).
27. Méndez-Ferrer, S. *et al.* Mesenchymal and haematopoietic stem cells form a unique bone marrow niche. *Nature* **466**, 829–834 (2010).
28. Lee, J. Y. & Hong, S.-H. Hematopoietic Stem Cells and Their Roles in Tissue Regeneration. *Int. J. Stem Cells* **13**, 1–12 (2019).
29. Cho, S. & Spangrude, G. J. Enrichment of functionally distinct mouse hematopoietic progenitor cell populations using CD62L. *J. Immunol. Baltim. Md 1950* **187**, 5203–5210 (2011).
30. Lennartsson, J. & Rönstrand, L. Stem cell factor receptor/c-Kit: From basic Science to clinical implications. *Physiol. Rev.* **92**, 1619–1649 (2012).
31. Weng, X., Maxwell-Warburton, S., Hasib, A., Ma, L. & Kang, L. The membrane receptor CD44: novel insights into metabolism. *Trends Endocrinol. Metab. TEM* **33**, 318–332 (2022).
32. Oostendorp, R. A. & Dörmer, P. VLA-4-mediated interactions between normal human hematopoietic progenitors and stromal cells. *Leuk. Lymphoma* **24**, 423–435 (1997).
33. Britton, C., Poznansky, M. C. & Reeves, P. Polyfunctionality of the CXCR4/CXCL12 axis in health and disease: Implications for therapeutic interventions in cancer and immune-mediated diseases. *FASEB J.* **35**, e21260 (2021).
34. Zhang, C. C. & Sadek, H. A. Hypoxia and Metabolic Properties of Hematopoietic Stem Cells. *Antioxid. Redox Signal.* **20**, 1891–1901 (2014).
35. Khaddour, K., Hana, C. K. & Mewawalla, P. Hematopoietic Stem Cell Transplantation. in *StatPearls* (StatPearls Publishing, 2023).

36. Mayadas, T. N., Cullere, X. & Lowell, C. A. The multifaceted functions of neutrophils. *Annu. Rev. Pathol.* **9**, 181–218 (2014).
37. Summers, C. *et al.* Neutrophil kinetics in health and disease. *Trends Immunol.* **31**, 318–324 (2010).
38. Tsioumpkou, M., Krijgsman, D., Leusen, J. H. W. & Olofsen, P. A. The Role of Cytokines in Neutrophil Development, Tissue Homing, Function and Plasticity in Health and Disease. *Cells* **12**, 1981 (2023).
39. Casanova-Acebes, M. *et al.* Rhythmic modulation of the hematopoietic niche through neutrophil clearance. *Cell* **153**, 1025–1035 (2013).
40. Basu, S., Hodgson, G., Katz, M. & Dunn, A. R. Evaluation of role of G-CSF in the production, survival, and release of neutrophils from bone marrow into circulation. *Blood* **100**, 854–861 (2002).
41. Dancey, J. T., Deubelbeiss, K. A., Harker, L. A. & Finch, C. A. Neutrophil kinetics in man. *J. Clin. Invest.* **58**, 705–715 (1976).
42. Cossío, I., Lucas, D. & Hidalgo, A. Neutrophils as regulators of the hematopoietic niche. *Blood* **133**, 2140–2148 (2019).
43. Ley, K. Integration of inflammatory signals by rolling neutrophils. *Immunol. Rev.* **186**, 8–18 (2002).
44. Kwak, H.-J. *et al.* Myeloid cell-derived reactive oxygen species externally regulate the proliferation of myeloid progenitors in emergency granulopoiesis. *Immunity* **42**, 159–171 (2015).
45. Bowers, E. *et al.* Granulocyte-derived TNF α promotes vascular and hematopoietic regeneration in the bone marrow. *Nat. Med.* **24**, 95–102 (2018).
46. Lapidot, T. & Petit, I. Current understanding of stem cell mobilization: the roles of chemokines, proteolytic enzymes, adhesion molecules, cytokines, and stromal cells. *Exp. Hematol.* **30**, 973–981 (2002).
47. Massberg, S. *et al.* Immunosurveillance by hematopoietic progenitor cells trafficking through blood, lymph, and peripheral tissues. *Cell* **131**, 994–1008 (2007).
48. Spiegel, A. *et al.* Catecholaminergic neurotransmitters regulate migration and repopulation of immature human CD34⁺ cells through Wnt signaling. *Nat. Immunol.* **8**, 1123–1131 (2007).

49. Cebon, J., Layton, J. E., Maher, D. & Morstyn, G. Endogenous haemopoietic growth factors in neutropenia and infection. *Br. J. Haematol.* **86**, 265–274 (1994).
50. CETEAN, S. *et al.* The importance of the granulocyte-colony stimulating factor in oncology. *Clujul Med.* **88**, 468–472 (2015).
51. Boettcher, S. *et al.* Endothelial cells translate pathogen signals into G-CSF-driven emergency granulopoiesis. *Blood* **124**, 1393–1403 (2014).
52. Betto, R. M. *et al.* Metabolic control of DNA methylation in naive pluripotent cells. *Nat. Genet.* **53**, 215–229 (2021).
53. Park, S. D. *et al.* A review of granulocyte colony-stimulating factor receptor signaling and regulation with implications for cancer. *Front. Oncol.* **12**, (2022).
54. Corey, S. J. *et al.* Granulocyte colony-stimulating factor receptor signaling involves the formation of a three-component complex with Lyn and Syk protein-tyrosine kinases. *Proc. Natl. Acad. Sci. U. S. A.* **91**, 4683–4687 (1994).
55. Katayama, Y. *et al.* Signals from the sympathetic nervous system regulate hematopoietic stem cell egress from bone marrow. *Cell* **124**, 407–421 (2006).
56. Dawn, B., Sanganalmath, S. K. & Bolli, R. G-CSF-Induced Mobilization of Bone Marrow Stem Cells and Cardiac Repair. in *Twenty Years of G-CSF* (eds. Molineux, G., Foote, M. & Arvedson, T.) 435–462 (Springer Basel, 2012). doi:10.1007/978-3-0348-0218-5_24.
57. Leveque-El Mouttie, L. *et al.* Autophagy is required for stem cell mobilization by G-CSF. *Blood* **125**, 2933–2936 (2015).
58. Lieschke, G. J. *et al.* Mice lacking granulocyte colony-stimulating factor have chronic neutropenia, granulocyte and macrophage progenitor cell deficiency, and impaired neutrophil mobilization. *Blood* **84**, 1737–1746 (1994).
59. Ioannis, K., Eralda, S., Egal, E. S. A. & Beswick, E. G-CSF in tumors: aggressiveness, tumor microenvironment and immune cell regulation. *Cytokine* **142**, 155479 (2021).

60. Duhrsen, U. *et al.* Effects of recombinant human granulocyte colony-stimulating factor on hematopoietic progenitor cells in cancer patients. *Blood* **72**, 2074–2081 (1988).
61. Bendall, L. J. & Bradstock, K. F. G-CSF: From granulopoietic stimulant to bone marrow stem cell mobilizing agent. *Cytokine Growth Factor Rev.* **25**, 355–367 (2014).
62. Donato, M. & Champlin, R. Granulocyte colony-stimulating factor-primed allogeneic bone marrow transplants: Capturing the advantages of blood stem cell transplants without increased risk of chronic graft-versus-host disease. *Biol. Blood Marrow Transplant.* **6**, 419–421 (2000).
63. Schmitz, N. *et al.* Randomised trial of filgrastim-mobilised peripheral blood progenitor cell transplantation versus autologous bone-marrow transplantation in lymphoma patients. *The Lancet* **347**, 353–357 (1996).
64. Trillet-Lenoir, V. *et al.* Recombinant granulocyte colony stimulating factor reduces the infectious complications of cytotoxic chemotherapy. *Eur. J. Cancer* **29**, 319–324 (1993).
65. Wuchter, P. *et al.* Poor Mobilization of Hematopoietic Stem Cells—Definitions, Incidence, Risk Factors, and Impact on Outcome of Autologous Transplantation. *Biol. Blood Marrow Transplant.* **16**, 490–499 (2010).
66. Ferraro, F. *et al.* Diabetes impairs hematopoietic stem cell mobilization by altering niche function. *Sci. Transl. Med.* **3**, 104ra101 (2011).
67. Albiero, M. *et al.* Diabetes Causes Bone Marrow Autonomic Neuropathy and Impairs Stem Cell Mobilization via Dysregulated p66Shc and Sirt1. *Diabetes* **63**, 1353–1365 (2014).
68. Ambrosi, T. H. *et al.* Adipocyte Accumulation in the Bone Marrow during Obesity and Aging Impairs Stem Cell-Based Hematopoietic and Bone Regeneration. *Cell Stem Cell* **20**, 771-784.e6 (2017).
69. Oikawa, A. *et al.* Diabetes mellitus induces bone marrow microangiopathy. *Arterioscler. Thromb. Vasc. Biol.* **30**, 498–508 (2010).
70. Fadini, G. P. & DiPersio, J. F. Diabetes mellitus as a poor mobilizer condition. *Blood Rev.* **32**, 184–191 (2018).

71. Fadini, G. P. *et al.* Diabetes impairs stem cell and proangiogenic cell mobilization in humans. *Diabetes Care* **36**, 943–949 (2013).
72. Nagareddy, P. R. *et al.* Hyperglycemia promotes myelopoiesis and impairs the resolution of atherosclerosis. *Cell Metab.* **17**, 695–708 (2013).
73. Ramsey, S. D. *et al.* Incidence, outcomes, and cost of foot ulcers in patients with diabetes. *Diabetes Care* **22**, 382–387 (1999).
74. Concise Review: Perspectives and Clinical Implications of Bone Marrow and Circulating Stem Cell Defects in Diabetes - Fadini - 2017 - STEM CELLS - Wiley Online Library.
<https://stemcellsjournals.onlinelibrary.wiley.com/doi/10.1002/stem.2445>.
75. Félétou, M. *The Endothelium: Part 1: Multiple Functions of the Endothelial Cells—Focus on Endothelium-Derived Vasoactive Mediators.* (Morgan & Claypool Life Sciences, 2011).
76. Cerutti, C. & Ridley, A. J. Endothelial cell-cell adhesion and signaling. *Exp. Cell Res.* **358**, 31–38 (2017).
77. Galley, H. F. & Webster, N. R. Physiology of the endothelium. *Br. J. Anaesth.* **93**, 105–113 (2004).
78. Madonna, R. & De Caterina, R. Cellular and molecular mechanisms of vascular injury in diabetes--part I: pathways of vascular disease in diabetes. *Vascul. Pharmacol.* **54**, 68–74 (2011).
79. Fadini, G. P. *et al.* Newly-diagnosed diabetes and admission hyperglycemia predict COVID-19 severity by aggravating respiratory deterioration. *Diabetes Res. Clin. Pract.* **168**, 108374 (2020).
80. Bonora, B. M. *et al.* Hyperglycemia, Reduced Hematopoietic Stem Cells, and Outcome of COVID-19. *Diabetes* **71**, 788–794 (2022).
81. Medina, R. J. *et al.* Endothelial Progenitors: A Consensus Statement on Nomenclature. *Stem Cells Transl. Med.* **6**, 1316–1320 (2017).
82. Fadini, G. P. *et al.* Diabetes impairs progenitor cell mobilisation after hindlimb ischaemia–reperfusion injury in rats. *Diabetologia* **49**, 3075–3084 (2006).
83. Fadini, G. P. *et al.* Circulating CD34+ cells, metabolic syndrome, and cardiovascular risk. *Eur. Heart J.* **27**, 2247–2255 (2006).

84. Albiero, M. *et al.* Inhibition of SGLT2 Rescues Bone Marrow Cell Traffic for Vascular Repair: Role of Glucose Control and Ketogenesis. *Diabetes* **70**, 1767–1779 (2021).
85. Albiero, M. *et al.* Bone Marrow Macrophages Contribute to Diabetic Stem Cell Mobilopathy by Producing Oncostatin M. *Diabetes* **64**, 2957–2968 (2015).
86. Rose, T. M. & Bruce, A. G. Oncostatin M is a member of a cytokine family that includes leukemia-inhibitory factor, granulocyte colony-stimulating factor, and interleukin 6. *Proc. Natl. Acad. Sci. U. S. A.* **88**, 8641–8645 (1991).
87. Albiero, M. *et al.* Diabetes-Associated Myelopoiesis Drives Stem Cell Mobilopathy Through an OSM-p66Shc Signaling Pathway. *Diabetes* **68**, 1303–1314 (2019).
88. Albiero, M., Bonora, B. M. & Fadini, G. P. Diabetes pharmacotherapy and circulating stem/progenitor cells. State of the art and evidence gaps. *Curr. Opin. Pharmacol.* **55**, 151–156 (2020).
89. Lucas, D. *et al.* Norepinephrine reuptake inhibition promotes mobilization in mice: potential impact to rescue low stem cell yields. *Blood* **119**, 3962–3965 (2012).
90. Shastri, A. *et al.* Stimulation of adrenergic activity by desipramine enhances hematopoietic stem and progenitor cell mobilization along with G-CSF in multiple myeloma: A pilot study. *Am. J. Hematol.* **92**, 1047–1051 (2017).
91. Zelniker, T. A. *et al.* SGLT2 inhibitors for primary and secondary prevention of cardiovascular and renal outcomes in type 2 diabetes: a systematic review and meta-analysis of cardiovascular outcome trials. *The Lancet* **393**, 31–39 (2019).
92. Nademanee, A. P. *et al.* Plerixafor Plus Granulocyte Colony-Stimulating Factor versus Placebo Plus Granulocyte Colony-Stimulating Factor for Mobilization of CD34+ Hematopoietic Stem Cells in Patients with Multiple Myeloma and Low Peripheral Blood CD34+ Cell Count: Results of a Subset Analysis of a Randomized Trial. *Biol. Blood Marrow Transplant.* **18**, 1564–1572 (2012).
93. Tepper, O. M. *et al.* Decreased Circulating Progenitor Cell Number and Failed Mechanisms of Stromal Cell-Derived Factor-1 α Mediated Bone Marrow Mobilization Impair Diabetic Tissue Repair. *Diabetes* **59**, 1974–1983 (2010).

94. Bonora, B. M. *et al.* Stem cell mobilization with plerixafor and healing of diabetic ischemic wounds: A phase IIa, randomized, double-blind, placebo-controlled trial. *Stem Cells Transl. Med.* **9**, 965–973 (2020).
95. Mizushima, N. & Komatsu, M. Autophagy: renovation of cells and tissues. *Cell* **147**, 728–741 (2011).
96. Yang, Z. & Klionsky, D. J. An Overview of the Molecular Mechanism of Autophagy. *Curr. Top. Microbiol. Immunol.* **335**, 1–32 (2009).
97. Agnello, M. *et al.* The Role of Autophagy and Apoptosis During Embryo Development. in *Cell Death - Autophagy, Apoptosis and Necrosis* (IntechOpen, 2015). doi:10.5772/61765.
98. An, B. The Research of Autophagy and Anti-Aging. in *Proceedings of the 2020 7th International Conference on Biomedical and Bioinformatics Engineering* 160–164 (Association for Computing Machinery, 2021). doi:10.1145/3444884.3444915.
99. Juste, Y. R. & Cuervo, A. M. Analysis of Chaperone-Mediated Autophagy. in *Autophagy: Methods and Protocols* (eds. Ktistakis, N. & Florey, O.) 703–727 (Springer, 2019). doi:10.1007/978-1-4939-8873-0_47.
100. Mijaljica, D., Prescott, M. & Devenish, R. J. Microautophagy in mammalian cells: revisiting a 40-year-old conundrum. *Autophagy* **7**, 673–682 (2011).
101. Mizushima, N. Autophagy: process and function. *Genes Dev.* **21**, 2861–2873 (2007).
102. Loos, B., du Toit, A. & Hofmeyr, J.-H. S. Defining and measuring autophagosome flux—concept and reality. *Autophagy* **10**, 2087–2096 (2014).
103. Parzych, K. R. & Klionsky, D. J. An Overview of Autophagy: Morphology, Mechanism, and Regulation. *Antioxid. Redox Signal.* **20**, 460–473 (2014).
104. Cheng, R. & Ma, J. Angiogenesis in Diabetes and Obesity. *Rev. Endocr. Metab. Disord.* **16**, 67–75 (2015).
105. Bhattacharya, D., Mukhopadhyay, M., Bhattacharyya, M. & Karmakar, P. Is autophagy associated with diabetes mellitus and its complications? A review. *EXCLI J.* **17Doc709** ISSN 1611-2156 (2018) doi:10.17179/EXCLI2018-1353.

106. Chen, Z. *et al.* The double-edged effect of autophagy in pancreatic beta cells and diabetes. *Autophagy* **7**, 12–16 (2011).
107. Muralidharan, C. & Linnemann, A. K. β -Cell autophagy in the pathogenesis of type 1 diabetes. *Am. J. Physiol.-Endocrinol. Metab.* **321**, E410–E416 (2021).
108. Han, Y.-P. *et al.* Autophagy and its therapeutic potential in diabetic nephropathy. *Front. Endocrinol.* **14**, (2023).
109. Liu, Y.-P., Shao, S.-J. & Guo, H.-D. Schwann cells apoptosis is induced by high glucose in diabetic peripheral neuropathy. *Life Sci.* **248**, 117459 (2020).
110. Ho, T. T. *et al.* Autophagy maintains the metabolism and function of young and old (hematopoietic) stem cells. *Nature* **543**, 205–210 (2017).
111. Salemi, S., Yousefi, S., Constantinescu, M. A., Fey, M. F. & Simon, H.-U. Autophagy is required for self-renewal and differentiation of adult human stem cells. *Cell Res.* **22**, 432–435 (2012).
112. Leveque, L., Le Texier, L., Lineburg, K. E., Hill, G. R. & MacDonald, K. P. Autophagy and haematopoietic stem cell transplantation. *Immunol. Cell Biol.* **93**, 43–50 (2015).
113. Mortensen, M. *et al.* The autophagy protein Atg7 is essential for hematopoietic stem cell maintenance. *J. Exp. Med.* **208**, 455–467 (2011).
114. Jung, H. E., Shim, Y. R., Oh, J. E., Oh, D. S. & Lee, H. K. The autophagy Protein Atg5 Plays a Crucial Role in the Maintenance and Reconstitution Ability of Hematopoietic Stem Cells. *Immune Netw.* **19**, e12 (2019).
115. Huang, J. *et al.* Impaired Autophagy in Adult Bone Marrow CD34+ Cells of Patients with Aplastic Anemia: Possible Pathogenic Significance. *PLOS ONE* **11**, e0149586 (2016).
116. Shrestha, S., Lee, J. M. & Hong, C.-W. Autophagy in neutrophils. *Korean J. Physiol. Pharmacol. Off. J. Korean Physiol. Soc. Korean Soc. Pharmacol.* **24**, 1–10 (2020).
117. Huang, Y. *et al.* Transcriptomic insights into temporal expression pattern of autophagy genes during monocytic and granulocytic differentiation. *Autophagy* **14**, 558–559 (2018).

118. Rožman, S. *et al.* The generation of neutrophils in the bone marrow is controlled by autophagy. *Cell Death Differ.* **22**, 445–456 (2015).
119. Riffelmacher, T. *et al.* Autophagy-Dependent Generation of Free Fatty Acids Is Critical for Normal Neutrophil Differentiation. *Immunity* **47**, 466-480.e5 (2017).
120. Levine, B., Mizushima, N. & Virgin, H. W. Autophagy in immunity and inflammation. *Nature* **469**, 323–335 (2011).
121. Li, X.-F. *et al.* Increased autophagy sustains the survival and pro-tumourigenic effects of neutrophils in human hepatocellular carcinoma. *J. Hepatol.* **62**, 131–139 (2015).
122. Jin, J. *et al.* Low Autophagy (ATG) Gene Expression Is Associated with an Immature AML Blast Cell Phenotype and Can Be Restored during AML Differentiation Therapy. *Oxid. Med. Cell. Longev.* **2018**, 1482795 (2018).
123. Park, S. Y. *et al.* Autophagy Primes Neutrophils for Neutrophil Extracellular Trap Formation during Sepsis. *Am. J. Respir. Crit. Care Med.* **196**, 577–589 (2017).
124. Kuwabara, W. M. T., Curi, R. & Alba-Loureiro, T. C. Autophagy Is Impaired in Neutrophils from Streptozotocin-Induced Diabetic Rats. *Front. Immunol.* **8**, 24 (2017).
125. Mizushima, N., Yamamoto, A., Matsui, M., Yoshimori, T. & Ohsumi, Y. In vivo analysis of autophagy in response to nutrient starvation using transgenic mice expressing a fluorescent autophagosome marker. *Mol. Biol. Cell* **15**, 1101–1111 (2004).
126. Mizushima, N. Chapter 2 Methods for Monitoring Autophagy Using GFP-LC3 Transgenic Mice. in *Methods in Enzymology* vol. 452 13–23 (Elsevier, 2009).
127. Chromosomal mapping of the GFP-LC3 transgene in GFP-LC3 mice.
<https://www.tandfonline.com/doi/epdf/10.4161/auto.4846?needAccess=true&role=button>
doi:10.4161/auto.4846.
128. Streptozotocin - an overview | ScienceDirect Topics.
<https://www.sciencedirect.com/topics/biochemistry-genetics-and-molecular-biology/streptozotocin>.

129. Montaldo, E. *et al.* Cellular and transcriptional dynamics of human neutrophils at steady state and upon stress. *Nat. Immunol.* **23**, 1470–1483 (2022).
130. Martinelli, S. *et al.* Induction of genes mediating interferon-dependent extracellular trap formation during neutrophil differentiation. *J. Biol. Chem.* **279**, 44123–44132 (2004).
131. Mazher, M., Moqidem, Y. A., Zidan, M., Sayed, A. A. & Abdellatif, A. Autophagic reprogramming of bone marrow–derived macrophages. *Immunol. Res.* **71**, 229–246 (2023).
132. MacDonald, K. P. A. *et al.* Modification of T cell responses by stem cell mobilization requires direct signaling of the T cell by G-CSF and IL-10. *J. Immunol. Baltim. Md 1950* **192**, 3180–3189 (2014).
133. Garneau, N. L., Wilusz, J. & Wilusz, C. J. The highways and byways of mRNA decay. *Nat. Rev. Mol. Cell Biol.* **8**, 113–126 (2007).
134. Moss Bendtsen, K., Jensen, M. H., Krishna, S. & Semsey, S. The role of mRNA and protein stability in the function of coupled positive and negative feedback systems in eukaryotic cells. *Sci. Rep.* **5**, 13910 (2015).
135. Corbett, A. H. Post-transcriptional Regulation of Gene Expression and Human Disease. *Curr. Opin. Cell Biol.* **52**, 96–104 (2018).
136. Ye, X., Zhou, X.-J. & Zhang, H. Exploring the Role of Autophagy-Related Gene 5 (ATG5) Yields Important Insights Into Autophagy in Autoimmune/Autoinflammatory Diseases. *Front. Immunol.* **9**, (2018).
137. Vargas, J. N. S., Hamasaki, M., Kawabata, T., Youle, R. J. & Yoshimori, T. The mechanisms and roles of selective autophagy in mammals. *Nat. Rev. Mol. Cell Biol.* **24**, 167–185 (2023).
138. Mauthe, M. *et al.* Chloroquine inhibits autophagic flux by decreasing autophagosome-lysosome fusion. *Autophagy* **14**, 1435–1455 (2018).
139. Evrard, M. *et al.* Developmental Analysis of Bone Marrow Neutrophils Reveals Populations Specialized in Expansion, Trafficking, and Effector Functions. *Immunity* **48**, 364–379.e8 (2018).
140. Madeo, F., Bauer, M. A., Carmona-Gutierrez, D. & Kroemer, G. Spermidine: a physiological autophagy inducer acting as an anti-aging vitamin in humans? *Autophagy* **15**, 165–168 (2019).

141. Zou, D. *et al.* A comprehensive review of spermidine: Safety, health effects, absorption and metabolism, food materials evaluation, physical and chemical processing, and bioprocessing. *Compr. Rev. Food Sci. Food Saf.* **21**, 2820–2842 (2022).
142. Ketogenesis - an overview | ScienceDirect Topics. <https://www.sciencedirect.com/topics/medicine-and-dentistry/ketogenesis>.
143. Cannoodt, R., Saelens, W. & Saeys, Y. Computational methods for trajectory inference from single-cell transcriptomics. *Eur. J. Immunol.* **46**, 2496–2506 (2016).
144. Semerad, C. L., Liu, F., Gregory, A. D., Stumpf, K. & Link, D. C. G-CSF is an essential regulator of neutrophil trafficking from the bone marrow to the blood. *Immunity* **17**, 413–423 (2002).
145. Collier, J. J., Suomi, F., Oláhová, M., McWilliams, T. G. & Taylor, R. W. Emerging roles of ATG7 in human health and disease. *EMBO Mol. Med.* **13**, e14824 (2021).
146. Schneider, M., Fohr, B., Weiss, M., Hsiu, H. & Joos, T. G-CSF is an endothelial survival factor in LPS-induced inflammatory conditions. *Crit. Care* **10**, P89 (2006).
147. Garratt, L. W. Current Understanding of the Neutrophil Transcriptome in Health and Disease. *Cells* **10**, 2406 (2021).
148. Wong, J. J.-L. *et al.* Orchestrated intron retention regulates normal granulocyte differentiation. *Cell* **154**, 583–595 (2013).
149. Laboratory, P. N. N. Lost in translation: Gene expression changes don't always alter protein levels. <https://phys.org/news/2013-10-lost-gene-dont-protein.html>.
150. Ma, Q. *et al.* Transcriptional and Post-Transcriptional Regulation of Autophagy. *Cells* **11**, 441 (2022).
151. Orphanides, G. & Reinberg, D. A Unified Theory of Gene Expression. *Cell* **108**, 439–451 (2002).
152. Yu, Z.-Q. *et al.* Dual roles of Atg8-PE deconjugation by Atg4 in autophagy. *Autophagy* **8**, 883–892 (2012).
153. Nakatogawa, H., Ishii, J., Asai, E. & Ohsumi, Y. Atg4 recycles inappropriately lipidated Atg8 to promote autophagosome biogenesis. *Autophagy* **8**, 177–186 (2012).

154. Zhang, S., Yazaki, E., Sakamoto, H., Yamamoto, H. & Mizushima, N. Evolutionary diversification of the autophagy-related ubiquitin-like conjugation systems. *Autophagy* **18**, 2969–2984.
155. Mizushima, N. *et al.* Dissection of Autophagosome Formation Using Apg5-Deficient Mouse Embryonic Stem Cells. *J. Cell Biol.* **152**, 657–668 (2001).
156. Noda, T., Fujita, N. & Yoshimori, T. The late stages of autophagy: how does the end begin? *Cell Death Differ.* **16**, 984–990 (2009).
157. Klionsky, D. J. *et al.* Guidelines for the use and interpretation of assays for monitoring autophagy (4th edition)1. *Autophagy* **17**, 1–382 (2021).
158. Jeon, J.-H., Hong, C.-W., Kim, E. Y. & Lee, J. M. Current Understanding on the Metabolism of Neutrophils. *Immune Netw.* **20**, e46 (2020).
159. Schwarz, C. *et al.* Safety and tolerability of spermidine supplementation in mice and older adults with subjective cognitive decline. *Aging* **10**, 19–33 (2018).
160. Pekar, T. *et al.* The positive effect of spermidine in older adults suffering from dementia. *Wien. Klin. Wochenschr.* **133**, 484–491 (2021).
161. Kiechl, S. *et al.* Higher spermidine intake is linked to lower mortality: a prospective population-based study. *Am. J. Clin. Nutr.* **108**, 371–380 (2018).
162. Figure 1. Spermidine oral administration does not alter mouse feed... *ResearchGate*
https://www.researchgate.net/figure/Spermidine-oral-administration-does-not-alter-mouse-feed-intake-and-body-weight-gain_fig1_340770539.
163. Yang, Q. *et al.* Spermidine alleviates experimental autoimmune encephalomyelitis through inducing inhibitory macrophages. *Cell Death Differ.* **23**, 1850–1861 (2016).
164. Jeong, J.-W. *et al.* Spermidine Protects against Oxidative Stress in Inflammation Models Using Macrophages and Zebrafish. *Biomol. Ther.* **26**, 146–156 (2018).
165. Wang, J. *et al.* Spermidine alleviates cardiac aging by improving mitochondrial biogenesis and function. *Aging* **12**, 650–671 (2020).

166. Laffel, L. Ketone bodies: a review of physiology, pathophysiology and application of monitoring to diabetes. *Diabetes Metab. Res. Rev.* **15**, 412–426 (1999).
167. Auestad, N., Korsak, R. A., Morrow, J. W. & Edmond, J. Fatty Acid Oxidation and Ketogenesis by Astrocytes in Primary Culture. *J. Neurochem.* **56**, 1376–1386 (1991).
168. Cheng, C.-W. *et al.* Ketone Body Signaling Mediates Intestinal Stem Cell Homeostasis and Adaptation to Diet. *Cell* **178**, 1115–1131.e15 (2019).
169. Yi, W., Sylvester, E., Lian, J. & Deng, C. Kidney plays an important role in ketogenesis induced by risperidone and voluntary exercise in juvenile female rats. *Psychiatry Res.* **305**, 114196 (2021).
170. Zhang, H. *et al.* Ketogenesis-generated β -hydroxybutyrate is an epigenetic regulator of CD8⁺ T-cell memory development. *Nat. Cell Biol.* **22**, 18–25 (2020).
171. Goldberg, E. L. *et al.* β -hydroxybutyrate deactivates neutrophil NLRP3 inflammasome to relieve gout flares. *Cell Rep.* **18**, 2077–2087 (2017).
172. Masino, S. A. & Rho, J. M. Mechanisms of Ketogenic Diet Action. in *Jasper's Basic Mechanisms of the Epilepsies* (eds. Noebels, J. L., Avoli, M., Rogawski, M. A., Olsen, R. W. & Delgado-Escueta, A. V.) (National Center for Biotechnology Information (US), 2012).
173. Liao, C.-Y. *et al.* The Autophagy Inducer Spermidine Protects Against Metabolic Dysfunction During Overnutrition. *J. Gerontol. A. Biol. Sci. Med. Sci.* **76**, 1714–1725 (2021).
174. Furman, B. L. Streptozotocin-Induced Diabetic Models in Mice and Rats. *Curr. Protoc.* **1**, e78 (2021).
175. Ordonez-Moreno, L.-A. *et al.* Lactate-a new player in G-CSF-induced mobilization of hematopoietic stem/progenitor cells. *Leukemia* **37**, 1757–1761 (2023).
176. Khatib-Massalha, E. *et al.* Lactate released by inflammatory bone marrow neutrophils induces their mobilization via endothelial GPR81 signaling. *Nat. Commun.* **11**, 3547 (2020).
177. DULKADİROĞLU, E., ÖZDEN, H. & DEMİRCİ, H. The evaluation of intracellular energy metabolism in prediabetic patients and patients newly diagnosed with type 2 diabetes mellitus. *Turk. J. Med. Sci.* **51**, 238–245 (2021).

178. Alba-Loureiro, T. C., Hirabara, S. M., Mendonça, J. R., Curi, R. & Pithon-Curi, T. C. Diabetes causes marked changes in function and metabolism of rat neutrophils. *J. Endocrinol.* **188**, 295–303 (2006).
179. Hatfield, K. J., Melve, G. K. & Bruserud, Ø. Granulocyte colony-stimulating factor alters the systemic metabolomic profile in healthy donors. *Metabolomics* **13**, 2 (2017).
180. Fadini, G. P. *et al.* NETosis Delays Diabetic Wound Healing in Mice and Humans. *Diabetes* **65**, 1061–1071 (2016).
181. Fadini, G. P. *et al.* A perspective on NETosis in diabetes and cardiometabolic disorders. *Nutr. Metab. Cardiovasc. Dis. NMCD* **26**, 1–8 (2016).
182. Germic, N., Stojkov, D., Oberson, K., Yousefi, S. & Simon, H.-U. Neither eosinophils nor neutrophils require ATG5-dependent autophagy for extracellular DNA trap formation. *Immunology* **152**, 517–525 (2017).
183. Xu, F. *et al.* Aging-related Atg5 defect impairs neutrophil extracellular traps formation. *Immunology* **151**, 417–432 (2017).
184. Henriksen, T. I. *et al.* Dysregulated autophagy in muscle precursor cells from humans with type 2 diabetes. *Sci. Rep.* **9**, 8169 (2019).
185. Mei, Y., Thompson, M. D., Cohen, R. A. & Tong, X. Autophagy and oxidative stress in cardiovascular diseases. *Biochim. Biophys. Acta* **1852**, 243–251 (2015).
186. Steichen, P., Gruber, K., Hippe, B. & Haslberger, A. Spermidine content of selected dietary supplements: potential for improvement? *Funct. Foods Health Dis.* **13**, 258 (2023).
187. Wang, L., Chen, P. & Xiao, W. β -hydroxybutyrate as an Anti-Aging Metabolite. *Nutrients* **13**, 3420 (2021).

